Environmental
Studies
Research
Fund

201

Biodegradation of Naturally and Chemically Dispersed Crude Oils and Scotian Shelf Condensate from Atlantic Canada

Biodégradation de pétroles bruts et de condensats de la plateforme néo-écossaise naturellement ou chimiquement dispersés du Canada Atlantique

Canada

October 2015

Biodegradation of Naturally and Chemically Dispersed Crude Oils and Scotian Shelf Condensate from Atlantic Canada

---

Biodégradation de pétroles bruts et de condensats de la plateforme néo-écossaise naturellement ou chimiquement dispersés du Canada Atlantique

Prepared For

Environmental Studies Research Funds Program

Submitted by
National Research Council Canada
(NRC)
And
Fisheries and Oceans Canada
Centre for Offshore Oil, Gas and Energy Research
(COOGER)

1 October, 2015

Executive Summary

The biodegradation of crude oils and gas condensate off eastern Canada in the event of a spill could be an important natural component of an area risk assessment and a spill response strategy. The purpose of this study was to evaluate the natural attenuation potential for hydrocarbons in near surface seawater from eastern Canada in the areas of crude oil and natural gas production facilities. Seawater samples, collected in the summer and winter to evaluate possible seasonal variations, were subjected to a variety of microbiological, chemical and genomic analyses, to determine hydrocarbon degradation rates, the microbial populations performing the degradation and the activities involved, and the impact of dispersants on the degradation rates.

Respirometric analysis demonstrated that the inclusion of oil alone and with dispersant resulted in good oxygen consumption at all three sites (Hibernia, Terra Nova and Sable (Thebaud)) both in summer and winter. In contrast, seawater alone or with just dispersant did not elicit any statistically significant oxygen consumption. Further aspects of these results are discussed in more detail in the appropriate section of this report.

Crude oil from Hibernia and Terra Nova were degraded effectively under both summer (13 °C) and winter (6-7 °C) temperature conditions, with the rates being 2 to 3 times higher in the summer. The presence of dispersant had a slight positive impact on the degradation rate of alkanes in the summer, but less so for polycyclic aromatic hydrocarbons (PAHs) and their Alkylated derivatives (Alk-PAHs). In contrast, dispersant had a greater impact on alkane degradation in the winter, but again, the impact on PAHs and Alk-PAHs degradation was low. The degradation of gas condensate in seawater from Sable (Thebaud), was very rapid in the summer, but was much slower in the winter. During the summer, degradation of all chemical fractions was very rapid and dispersant did not have much impact on this rate. Surprisingly, there was generally poor degradation in the winter and dispersant may have had a detrimental effect on the rate and half-life of substrate degradation. There are other factors at play in the degradation rates in summer and winter, these being related to nutrient availability in the water and other oceanographic factors that come into play. It is clear that the locations of the different sampling sites (Hibernia and Terra Nova being distant from Thebaud) are influenced by different factors including temperature, ocean currents, and different nutrient contents, especially at different times of the year. Considering the properties of the hydrocarbon substrates used in this study (resins and asphaltenes made up less than 10% of these substrates) and the observed degradation rates for the three fractions monitored, we observed total degradation of nearly 90% of the hydrocarbons in these substrates.

The microbial community structures (metagenomic profile), from the three sites, were examined prior to and following incubation with oil alone or with dispersant. The presence of the oil alone caused considerable shifts in the community structure with known hydrocarbon degrading genera (many from the *Gammaproteobacteria*), becoming predominant after only a few days and persisting for the entire incubation period (42 days), although there were differences in the population members between the short and longer incubation times. The inclusion of dispersant with the oil resulted in similar, but distinctive shifts in the microbial community structure. With the dispersant, other *Gammaproteobacteria* became dominant, especially during the early stages of the incubation period,

and again later in the incubation other hydrocarbon degrading bacterial genera became dominant. The three sites behaved differently from each other and seasonal effects were apparent (e.g. summer verses winter). In all cases, *Alcanivorax* became a dominant community component at the end of the incubation period, highlighting the importance of this genus in natural oil degradation in the marine environment.

Comparative metagenomic and metatranscriptomic dynamics of the microbial population was evaluated by looking at the frequency of metabolic genes (e.g. combined metabolic pathways; metagenomics profile) and by targeting specific key genes involved in hydrocarbon degradation (e.g. alkane monooxygenases, cytochrome P450 oxygenases, ring hydroxylases/dioxygenases) or other cellular processes (nitrogen metabolism; metatranscriptomic profile). Increased frequency (e.g. increased expression/activity) of overall metabolism was observed with several key orders of bacteria, notably the *Alteromonadales, Oceanospirillales, Rhodobacterales,* and *Pseudomonadales*, all of which are rich in hydrocarbon degrading bacteria, in the presence of oil. The targeted key hydrocarbon degradation genes were also up-regulated under these conditions, especially in genera such as *Marinobacter (Alteromonadales)* and *Alcanivorax (Oceanospirillales),* which were producing numerous variants of each of these target enzymes. The increased expression was observed at all the sites, when the microbial population was exposed to oil with dispersant, in both the summer and the winter, although up-regulation was considerably less in the winter. In addition to the increased expression of hydrocarbon degradation genes and overall metabolism in these key orders of bacteria, it was also noted that nitrogen metabolism was increased. This is expected for these organisms, because in order to incorporate carbon from the hydrocarbons into their cellular macromolecules, nitrogen would also be required. This confirms that the actively metabolizing bacteria were degrading the hydrocarbons.

Overall the results demonstrate that the indigenous microbial populations in the marine environment in the areas of the Hibernia, Terra Nova and Thebaud facilities possess hydrocarbon-degrading bacteria that respond positively to exposure to oil under ambient temperature conditions in the summer (13°C) and winter (6-7°C). Their population densities are typically quite low to non-detectable prior to oil exposure, but they did become dominant components of the total bacterial population when oil was present. This is possibly not entirely surprising, since some members of these bacterial groups are known obligate hydrocarbon degraders, meaning that the only substrates they can use are hydrocarbons. Under conditions where the substrates are not present these bacteria undergo modifications to conserve energy, such as dormancy. Under appropriate conditions when substrate is present and other conditions are favourable, they respond rapidly. The exposure to oil resulted in increased numbers and activity of known degrader genera of bacteria in addition to the increased expression of their hydrocarbon degradation genes. Crude oil and gas condensate were rapidly degraded under summer conditions, but more slowly under winter conditions, with the alkane fraction being the most rapidly degraded. The presence of dispersant did have a positive impact on the degradation kinetics for the alkane fraction, and especially in the winter. There were some indications that dispersant had a slight negative impact on hydrocarbon degradation but this appeared to affect primarily the aromatic substrates, and was not consistently observed throughout the study. Of

importance to note, dispersant did not have a negative impact on alkane degradation in the summer or winter at any of the study sites.

Sommaire

Dans l'éventualité d'un déversement, la biodégradation de pétroles bruts et de condensat de gaz au large de l'est du Canada pourrait représenter une importante composante naturelle de l'évaluation des risques dans la zone et d'une stratégie d'intervention en cas de déversement. L'étude avait pour objectif d'évaluer le potentiel d'atténuation naturelle dans le cas d'hydrocarbures dans l'eau de mer près de la surface de l'est du Canada à proximité d'installations de production de pétrole brut et de gaz naturel. Des échantillons d'eau de mer, prélevés en été et en hiver en vue d'évaluer les variations saisonnières possibles, ont fait l'objet de diverses analyses microbiologiques, chimiques et génomiques afin de déterminer les taux de dégradation d'hydrocarbures, les populations microbiennes effectuant la dégradation et les activités connexes ainsi que l'incidence d'agents dispersants sur les taux de dégradation.

Selon l'analyse respirométrique, l'inclusion de pétrole uniquement et avec un agent dispersant a eu pour résultat une bonne consommation d'oxygène dans l'ensemble des trois sites, soit les plateformes Hibernia, Terra Nova et Thebaud (l'île de Sable), tant en été qu'en hiver. Par contre, l'eau de mer seule ou avec seulement un agent dispersant n'a pas eu pour résultat une consommation d'oxygène statistiquement significative. D'autres éléments des résultats de cette analyse sont traités en plus amples détails dans la section pertinente du présent rapport.

La dégradation du pétrole brut des sites Hibernia et Terra Nova a été efficace dans des conditions tant estivales (13 °C) qu'hivernales (6 à 7 °C), les taux de dégradation étant de deux à trois fois plus élevés en été. La présence d'un agent dispersant a eu une légère incidence positive sur le taux de dégradation d'alcanes en été, mais une incidence moindre pour ce qui est des hydrocarbures aromatiques polycycliques (HAP) et leurs homologues alkylés. Ceci étant dit, l'incidence d'un agent dispersant était plus forte sur la dégradation d'alcanes en hiver, mais encore une fois, l'incidence sur les HAP et leurs homologues alkylés était faible. La dégradation de condensat de gaz dans l'eau de mer du site Thebaud (l'île de Sable) était très rapide en été, mais beaucoup plus lente en hiver. Pendant l'été, la dégradation de toutes les fractions chimiques était très rapide et l'agent dispersant n'a pas eu beaucoup d'effet à cet égard. Curieusement, la dégradation en hiver était faible en général et il se peut que l'agent dispersant ait eu un effet nuisible sur le taux et la demi-vie de dégradation du substrat. Dans les taux de dégradation en été et en hiver, d'autres facteurs océanographiques et relatifs à la disponibilité d'éléments nutritifs entrent en jeu. Il est évident que les lieux des différents sites d'échantillonnage (les sites Hibernia et Terra Nova étant éloignés de celui de Thebaud) sont touchés par des facteurs différents, notamment la température, les courants océaniques et la teneur en éléments nutritifs et surtout, à des moments différents de l'année. Compte tenu des propriétés des substrats d'hydrocarbures utilisés dans le cadre de cette étude (des résines et des asphaltènes représentaient moins de 10 % de ces substrats) et des taux de dégradations observés pour les trois fractions contrôlées, nous avons observé une dégradation totale de presque 90 % des hydrocarbures dans ces substrats.

Les structures des communautés microbiennes (le profil métagénomique) des trois sites ont été examinées avant et après l'incubation avec du pétrole uniquement ou avec un agent dispersant. La présence de pétrole uniquement a causé des changements considérables dans la structure des

communautés, les genres connus pour la dégradation d'hydrocarbures (dont bon nombre de *Gammaprotéobacteria*) devenant prédominants après quelques jours seulement et persistant pendant la période entière d'incubation (42 jours), quoique des différences soient remarquées dans les membres des populations selon qu'il s'agissait d'une incubation de courte ou de plus longue durée. L'inclusion d'un agent dispersant avec le pétrole a eu pour résultat des changements semblables, mais distincts, dans la structure des communautés microbiennes. Avec l'agent dispersant, d'autres *Gammaprotéobacteria* sont devenues dominantes, surtout dans les premières étapes de la période d'incubation, et encore une fois plus tard, alors que d'autres genres de bactéries dégradant les hydrocarbures sont devenues dominantes. Des différences dans les trois sites ont été observées tout comme des effets saisonniers (c.-à-d. en saison estivale ou hivernale). Dans tous les cas, à la fin de la période d'incubation, la bactérie *Alcanivorax* est devenue une composante dominante de la communauté, ce qui souligne l'importance du genre dans la dégradation naturelle de pétrole en milieu marin.

La dynamique métagénomique et métatranscriptomique comparée de la population microbienne a été évaluée en examinant la fréquence de gênes métaboliques (p. ex., les voies métaboliques combinées, le profil métagénomique) et en ciblant des gênes clés particulières jouant un rôle dans la dégradation d'hydrocarbures (p. ex., monooxygénases d'alcanes, oxygénases de cytochrome P450, hydroxylases/dioxygénases à noyau) ou d'autres processus cellulaires (métabolisme azoté; profil métatranscriptomique). Une fréquence accrue (c.-à-d. expression ou activité accrue) de métabolisme global a été observée dans plusieurs ordres principaux de bactéries, notamment *Alteromonadales, Oceanospirillales, Rhodobacterales* et *Pseudomonadales*, dont tous sont riches en bactéries dégradant les hydrocarbures en présence de pétrole. De plus, les gênes clés ciblées de dégradation d'hydrocarbures ont été surexprimées dans de telles conditions, surtout dans des genres tels que *Marinobacter (Alteromonadales)* et *Alcanivorax (Oceanospirillales),* qui produisaient de nombreuses variantes de chacun de ces enzymes cibles. L'expression accrue a été observée dans tous les sites alors que la population microbienne a été exposée au pétrole avec un agent dispersant, en été comme en hiver, quoique la surexpression soit considérablement moindre en hiver. En plus de l'expression accrue des gênes de dégradation d'hydrocarbures et du métabolisme global dans ces genres clés de bactéries, il a également été remarqué que le métabolisme azoté s'est accru. Cela est attendu chez ces organismes puisqu'afin d'intégrer le carbone des hydrocarbures dans leurs macromolécules cellulaires, il faut également de l'azote. Ainsi, nous avons pu confirmer que les bactéries dégradaient les hydrocarbures en les métabolisant activement.

Globalement, les résultats montrent que les populations microbiennes indigènes dans le milieu marin à proximité des installations aux sites Hibernia, Terra Nova et Thebaud renferment des bactéries dégradant les hydrocarbures qui répondent de façon positive à l'exposition au pétrole à des températures ambiantes en été (13 °C) et en hiver (6 à 7 °C). Normalement, avant une exposition au pétrole, ces populations sont assez faibles ou négligeables, mais en présence de pétrole, elles deviennent des composantes dominantes de la population bactérienne totale. Les résultats ne sont peut-être pas tout à fait étonnants puisque certains membres de ces populations bactériennes sont connus pour dégrader forcément les hydrocarbures puisque ceux-ci constituent les seuls substrats qui

leur sont utiles. Lorsque de tels substrats sont absents, ils subissent des modifications, notamment en entrant dans un état de dormance, pour conserver de l'énergie. Dans des conditions appropriées, alors que le substrat est présent et d'autres conditions sont favorables, ils répondent rapidement. L'exposition au pétrole a donné lieu à la croissance du nombre et de l'activité des genres de bactéries connus pour dégrader les hydrocarbures et à l'expression plus élevée de leurs gênes de dégradation des hydrocarbures. La dégradation de pétrole brut et de condensat de gaz a été rapide dans des conditions estivales. Par contre, elle a été moins rapide dans des conditions hivernales, et la dégradation la plus rapide a eu lieu dans la fraction d'alcane. La présence d'un agent dispersant a quand même eu une incidence positive sur la cinétique de dégradation de la fraction d'alcane, et ce, surtout en hiver. Certains indicateurs suggèrent que l'incidence de l'agent dispersant était légèrement négative sur la dégradation d'hydrocarbures, mais apparemment surtout de substrats aromatiques, et cette incidence n'a pas été observée systématiquement au cours de l'étude. Il est important de souligner que dans aucun site d'étude l'agent dispersant n'a eu d'incidence négative sur la dégradation d'alcanes, en hiver ou en été.

Table of Contents

List of Tables in Body of the Report

List of Figures in Body of Report

List of Appendices

List of Tables in the Appendices

List of Figures in the Appendices

Project Team

National Research Council Canada

Charles Greer

Nathalie Fortin

Etienne Yergeau

Julien Tremblay

Miria Elias

Fisheries and Oceans Canada

Pêches et Océans Canada

Fisheries and Oceans Canada

Thomas King

Susan Cobanli

Brian Robinson

Gary Wohlgeschaffen

Jennifer Mason

Scott Ryan

Peter Thamer

Claire McIntyre

Allison Thomas

Brianna Vaughan

1.0 Introduction

In the context of the recent Deepwater Horizon MC252 oil spill in the Gulf of Mexico, there is now scientific consensus that microorganisms (e.g. hydrocarbon degrading bacteria) may have played a major role in the removal of the contaminant hydrocarbons from the ecosystem (American Academy of Microbiology, 2011)

Currently, Newfoundland and Labrador is home to three active offshore oil projects: Hibernia, Terra Nova and White Rose. All three facilities produce a medium density; low viscosity crude oil with API gravities in the range of 30 to 34°. Crude oil is known to contain a very complex mixture of more than 17,000 compounds that can be grouped into four main classes: the saturated and aromatic hydrocarbons, the more polar non-hydrocarbons, the resins and the asphaltenes. Recent studies have identified bacteria from more than 79 genera that are able to degrade hydrocarbons, and several of these including *Alcanivorax*, *Cycloclasticus*, *Oleiphilus*, *Oleispira*, *Thalassolituus* and some members of the genus *Planomicrobium*, use hydrocarbons almost exclusively as carbon sources (Prince 2010, Prince et al. 2010).

Condensate, recovered off the coast of Nova Scotia with an API gravity of approximately 39.9° (SL Ross, 2015), is largely comprised of chemical compounds ranging from C_6 to C_9 (aliphatic hydrocarbons), single ring aromatics, (BTEX) and 2 to 3 ring polycyclic aromatic hydrocarbons and their alkylated homologs. As many components within condensate are considered to be highly water-soluble and/or rapidly evaporate upon their release into the environment, it was deemed that they would have a short residence time in the water column, ranging from several hours to a few days in the event of an accidental spill. However, the impacts of a condensate spill may have been underestimated on the basis of physical-chemical parameters alone. For example, while its half-life in the environment may be short, the BTEX components within condensate are considered acutely toxic. Indeed, limited studies following an accidental spill of condensate off the coast of Nova Scotia in 1984 showed no tainting of commercial fish species. However, concerns remain over the potential effects associated with prolonged environmental exposure, such as that which may result from a subsurface blowout event, as we have limited knowledge about the physical behaviour, toxicity, and subsequent environmental persistence of highly weathered condensate.

In light of known natural seepages of oil and gas in the oceans worldwide, widespread observations of indigenous microorganisms with hydrocarbon degradation pathways is not unexpected. Indeed recent preliminary metagenomic studies in the Gulf of Mexico on the subsurface oil plume (1100 m depth, 5^{o}C) have demonstrated rapid responses by the microbial community to the complex mixture of substrates in the oil that may also include chemical oil dispersants (Hazen et al., 2010). Knowledge on the rates and extent of oil degradation are essential for the assessment of habitat recovery.

The interpretation of these recent results on oil biodegradation potential must be assessed within

regions of concern due to factors, such as the limitation of oil biodegradation by available inorganic nutrients such as nitrogen and phosphorus, as well as the bioavailability of the hydrocarbon substrate itself. However, while nutrient limitation has been used as an argument for low oil biodegradation rates, at the concentrations oil is typically found in the water column after dispersion, high oil biodegradation rates have been shown to exist (Lee et al., 2011). This concept of natural oil degradation accounting for effective removal of oil from accidental spills was recently acknowledged by the American Academy of Microbiology (2011).

As primary producers at the base of the food web, an alteration in microbial productivity will influence the abundance of organisms at higher trophic levels. Following any pollution event, it is important to be able to comprehensively evaluate the effects on the ecosystem and to determine whether recovery is occurring naturally or as a consequence of some form of intervention. Microorganisms are ideal test organisms for environmental assessment, as they respond rapidly to their surrounding environment and are responsible for primary ecosystem processes including carbon fixation, nutrient regeneration, biotransformation and degradation of contaminants. During oil spill response operations in the marine environment, the application of countermeasures, such as the addition of chemical oil dispersants may alter the productivity of indigenous microorganisms, their community structure and function, including oil degradation.

Until recently, the ecological significance that microorganisms have on the degradation of hydrocarbons in the marine environment is not fully understood due to limitations in biotechnology analytical procedures. This study applied the most recent advances in metagenomic and metatranscriptomic analyses to evaluate the natural microbial community response following hypothetical spills of condensate on the Scotian Shelf and crude oil offshore Newfoundland and Labrador. The study monitored biodegradation of physically and chemically dispersed condensate and crude oils by conducting microcosm studies using seawater freshly procured from the Scotian Shelf and Grand Banks, respectively. This information obtained will form a valuable part of any strategy to assess the risks and develop effective countermeasures for addressing potential petroleum spills offshore of eastern Canada.

2.0 Field Studies

Seawater samples, from locations in the vicinity of oil and natural gas production platforms offshore Newfoundland and Labrador and Nova Scotia, were collected from the sea surface (3-5 m depth), using a Seabird Niskin rosette frame (24-10 L bottles) cast from a Canadian Coast Guard research vessel in the summer and late fall/winter of 2013 (Station locations, e.g. latitudes and longitudes are found in Appendix 1, Tables 1-1 and 1-2). There is concern about storage time before commencing microbial analysis, as decomposition to free most inorganic micronutrients occurs within two weeks of storage, and major changes in micronutrient concentrations due to bacterial metabolism can occur within one day (Crompton 2006; Cappello et al., 2007). Therefore, microcosm studies were initiated, onboard the ship, as soon as seawater was procured from the reference sites. This ensured that results would be representative of the samples at the time of collection.

2.1 Summer Sampling Mission

A dedicated oceanographic mission to the Grand Banks and Scotian Shelf region on board Canadian Coast Guard Ship *Hudson* from July 10th to 19th, 2013 (HUD2013-023) was conducted to collect representative seawater samples and initiate microcosm experiments at the three locations. For offshore Newfoundland and Labrador, sampling was conducted at 5 km south of the Hibernia Gravity Base Structure (GBS) and 5 km south of the Terra Nova Floating Production Storage and Offloading vessel (FPSO), subsequently referred to as Hibernia and Terra Nova, respectively. For offshore Nova Scotia, sampling was conducted 5 km south-east of the Thebaud (Sable) Processing Platform. Table 1 provides the three sampling locations where the microcosm experiments were initiated with freshly collected seawater, maintained at ambient surface temperature and monitored throughout the mission. The entire experiment continued onboard until the ship returned to the Bedford Institute of Oceanography (BIO, Dartmouth, Nova Scotia), where incubations were continued with completion after a total incubation time of 42 days.

Table 1: Sampling Locations for Summer Microcosm Experiments

Date	Location	Description	Latitude North	Longitude West	Depth (m)	Incubation Temperature °C Avg/SD
12-Jul-13	Hibernia	South–5 km	46.707	-48.785	2	12.8 ± 0.7
13-Jul-13	Terra Nova	South–5 km	46.431	-48.480	3	12.9 ± 0.4
17-Jul-13	Thebaud (Sable)	South-East–5km	43.858	-60.157	4	12.9 ± 0.4

2.1.1 Water Collection for Microcosms

All seawater samples were collected using a Seabird rosette frame containing 24-10 L Niskin bottles that held Seabird conductivity, temperature, and depth (CTD) sensors (SBE911plus), a Chelsea AquaTracka Mk3 fluorometer, and a Seabird E43 oxygen sensor. The fluorometer was set to 430 nm excitation and 685 nm emission wavelengths for phytoplankton chlorophyll-a determination and was calibrated with various concentrations of chlorophyll-a dissolved in pure water and the zero offset was determined in the laboratory using purified water from a reverse osmosis/ion exchange column. For the microcosms, freshly collected seawater from a depth of 3 m (surface) was dispensed directly into acid-washed (1 M HCl) Nalgene® jerricans that were rinsed three times with sample water. A total volume of 20 L of seawater was required for the set-up of each experiment; therefore, the contents of two of the surface jerricans were blended into one acid-cleaned 20 L jerrican. This blended sample was used for preparing the flask microcosms.

2.1.2 Water Collection for Genomics Studies and Oceanographic Survey

To evaluate baseline conditions in the reference areas, an oceanographic survey was conducted involving CTD profiles and the collection of water samples at various depths for the analysis of nutrients, salinity, temperature, oxygen, chlorophyll, bacterial enumeration and genomics. Samples were also collected for baseline hydrocarbons (e.g. BTEX, saturates and polycyclic aromatics and their alkylated homologs) in the water column. In addition, water samples were filtered to capture bacteria for genomic analyses to characterize the indigenous microbial population and their ability to degrade hydrocarbons.

For the Hibernia and Terra Nova locations where the depth ranged from approximately 80-100 m, samples were collected from five depths (surface, 10, 25, 50 and 5 m from bottom). For the Thebaud location where the depth ranged from approximately 15-50 m, only three depths were sampled (surface, 10 and 5 m from bottom).

At each sampling station, four Niskin bottles were fired at each depth. Water for genomics filtration (2 L) was collected in 10 L acid-washed jerricans from three of the Niskins, while all other samples were collected from the remaining Niskin bottle. Subsamples for BTEX, alkanes and PAHs, nutrients and chlorophyll were collected directly from the Niskin bottle and transferred into the appropriate sampling container. Bacterial enumeration samples were sub-sampled from the chlorophyll sample. Appendix 1 provides detailed sampling methods for nutrients, salinity, BTEX, PAH and aliphatic hydrocarbons and Appendix 2 provides detailed sampling methods for chlorophyll analyses and bacterial enumeration.

Station locations for this survey were selected based on prevailing monthly mean surface currents for the region using a Canadian East Coast Ocean Model (CECOM) (http://www.bio.gc.ca/science/research-recherche/ocean/forecasts-previsions/model-en.php). The model agrees well with observations in October 2007, but the agreement was not known in July 2013, since observations in that month were not available (H. Niu and Y. Wu, personal communication, May 22, 2013). The general trend of currents for this region was a north-west to south-east direction for the Grand Banks and a less organized prevailing direction in proximity to Sable Island (Fig. 1).

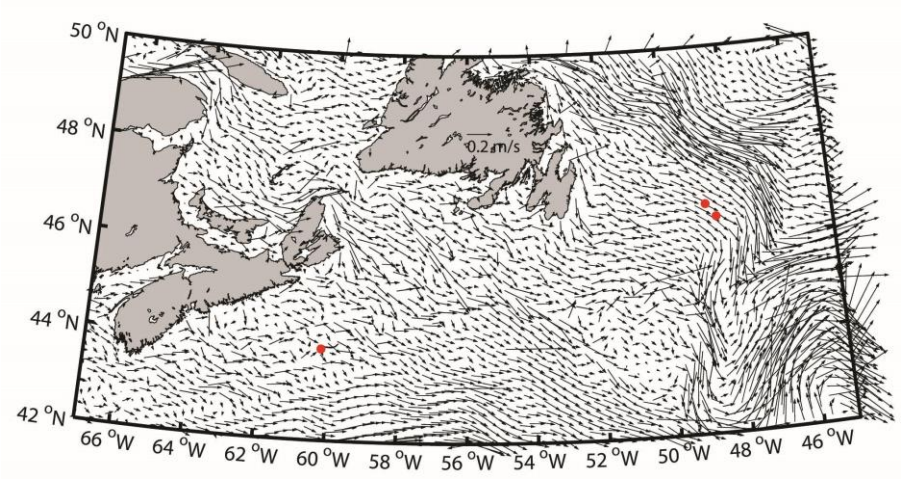

Figure 1: Prevailing monthly mean surface currents for the Grand Banks and Sable Regions (Y. Wu, Bedford Institute of Oceanography). Red dots identify the sampling locations.

Figures 2 and 3 provide the locations of stations sampled for the microcosm experiments, genomics filtration and oceanographic survey.

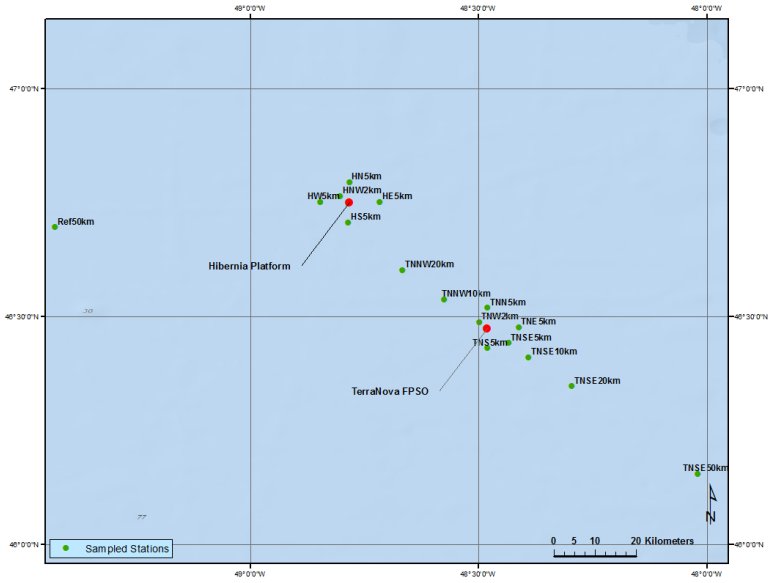

Figure 2: Summer sampling locations in the Grand Banks Region (Hibernia and Terra Nova), offshore Newfoundland and Labrador.

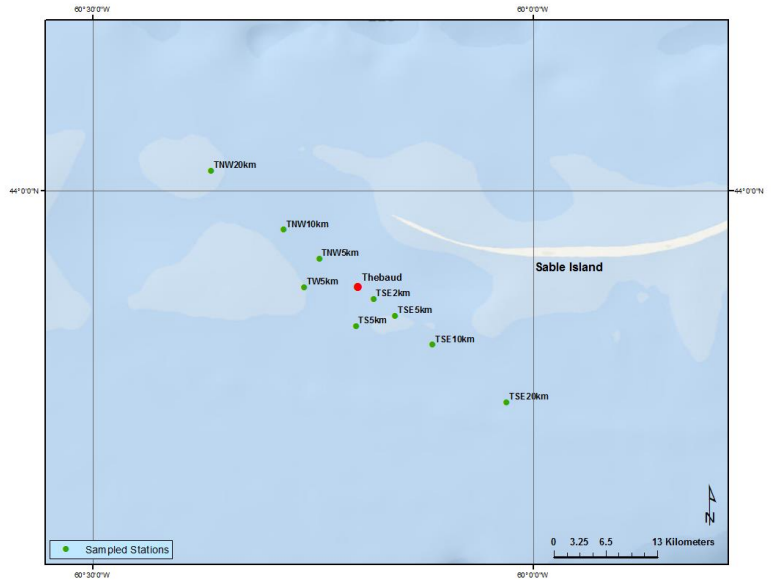

Figure 3: Sampling location near Sable Island (Thebaud) offshore Nova Scotia. Both summer and winter microcosm studies were conducted using water from the TSE 5km location.

2.2 Winter Sampling Mission

Additional sea-time on *CCGS Hudson* was provided in November 2013 by DFO-Newfoundland as part of their yearly Atlantic Zone Monitoring Program (AZMP) mission (HUD2013-042, from November 14th to December 10th, 2013). The main purpose of the sampling mission was to evaluate biodegradation rates of the oils and condensate in winter temperatures and collect water samples for genomics analyses. At Thebaud, water sampling, for the winter microcosm station, was in the same location as the summer study while the *Hudson* was transiting from BIO to St. John's NL. At Terra Nova and Hibernia, water sampling, for winter microcosms, was conducted at two stations to the north on the Flemish Cap sampling line of the AZMP monitoring mission, as these locations were the closest locations possible during that mission (Table 2, Figure 3).

Table 2: Sampling Locations for Winter Microcosm Experiments

Date	Location	Description	Latitude North	Longitude West	Depth (m)	Incubation Temperature °C Avg ± SD
15-Nov-13	Thebaud	South-East - 5 km	47.000	-48.471	3	6.8 ± 1.2
25-Nov-13	Terra Nova	North – 60 km	47.000	-48.288	5	5.9 ± 0.7
25-Nov-13	Hibernia	North - 36 km	43.858	-60.157	5	5.9 ± 0.7

Figure 4: Winter sampling locations in the Grand Banks Region (Hibernia and Terra Nova) offshore Newfoundland and Labrador.

2.2.1 Water Collection for Microcosms

For the Thebaud station, a portable Seabird SBE 25 plus CTD that included an SBE43 oxygen sensor was deployed from a hydrowire to collect water column data. Seawater was collected from multiple casts

(seven x 5 L) of Niskin bottles also deployed from a hydrowire to a depth of 3 – 5 m. Immediately after collection, the contents of the Niskin bottles were blended into 3 x 10 L jerricans and approximately 1/3 of the water from each of these jerricans was blended into 1 x 20 L jerrican. At Hibernia and Terra Nova, water samples were collected using a Seabird SBE9 CTD rosette frame that included an SBE43 oxygen sensor, WET Labs ECO-AFL fluorometer and 5 L Niskin bottles. For both locations, ten bottles were fired at the surface (5 m) and the contents from three Niskins were blended into a 20 L jerrican.

3.0 Microcosm Experimental Design

For both series of experiments (summer and winter) the core experimental design to evaluate the biodegradation of reference oils and condensate is outlined in Table 3. All experimental treatments were conducted in triplicate. One concentration of oil and condensate was used to assess biodegradation kinetics, since the losses in hydrocarbon concentrations are expected to follow a logarithmic based function. Once the ship returned to shore, the remaining active microcosms were moved onshore while maintaining incubation at ambient seawater temperature (recorded at the surface depth at the time of sampling) until the flasks were sacrificed at the desired end time points.

Table 3: Microcosm treatments for chemistry, genomics and respirometry for each location for both summer and winter missions.

Chemistry: July and November 2013							
Time (Days)	**Unfiltered Seawater + Bushnell Haas Nutrients**				**Filtered (0.22µM) Seawater + Bushnell Haas Nutrients**		Total
	Oil/Condensate	**Oil/Condensate**	**-**	**-**	**Oil/Condensate**	**Oil/Condensate**	
	-	**+Dispersant**	**+Dispersant**	**-**	**-**	**Dispersant**	
0	3	3		3	3	3	15
3	3	3			3	3	12
10	3	3			3	3	12
15	3	3			3	3	12
28	3	3			3	3	12
42	3	3			3	3	12
						TOTAL	75
Genomics/Respirometry: July 2013							**Total**
5	3	3					6
42	2 -3	3	3	3		2	13-14
						TOTAL	19-20
Genomics/Respirometry: November 2013							**Total**
7	6	3					9
42	3	3	3	3		3	15
						TOTAL	24

3.1 Microcosms

To avoid contamination, all equipment and materials were sterilized prior to transport to the research vessel. All glassware (baffle flasks, graduated cylinders, syringes, filtration bases and funnels) and plastic-ware (pipette tips, graduated cylinders, transfer bottles) were wrapped with aluminum foil and autoclaved at 121° C for 15-30 minutes. New Teflon-lined flask caps were rinsed with 95% ethanol, air-

dried in a laminar flow cabinet and wrapped with aluminum foil. Nutrient media (Bushnell Haas broth) to sustain extended microbial activity was prepared according to the manufacturer's directions and sterilized at 121° C for 15 minutes.

Since microbial populations change upon storage (some become dormant while others can become more active) the experiments were commenced immediately after the seawater was procured. Freshly collected seawater (100 mL) was dispensed directly into a 150 mL Wheaton® trypsinizing flask (Wheaton # 355394, borosilicate glass, with deep fluted sides for enhanced agitation) and capped. Time = 0 chemistry flasks were prepared in pre-cleaned certified amber bottles (250 mL). Bushnell Haas nutrients (2 mL), and weathered oils, condensate and premixed dispersant (Corexit 9500) with oil or condensate were added to each flask/bottle. The flasks were incubated at the ambient surface seawater temperature, at the time of collection, and continually mixed on Thermo Max Q 2000 orbital shaker tables at 150 rpm.

3.2 Test Materials

3.2.1 Oils and Condensate

Representative samples of Hibernia and Terra Nova crude oil (20 L) were provided to DFO's Centre for Offshore Oil, Gas and Energy Research (COOGER) labs by *Hibernia Management Development Corporation* (May 16, 2013) and *Suncor* (June 17, 2013), and *ExxonMobil* provided a 20 L sample of Scotian Shelf Condensate from the Goldboro gas plant in Guysborough County, Nova Scotia on May 15, 2013. All samples were collected directly by the company staff. To simulate the physical changes (evaporation) that occur within the first 24 hours of an accidental spill at sea, the oils and condensate were artificially weathered prior to use. A sample of each oil/condensate was weathered for 24 hours by purging with a gentle stream of nitrogen and recording the change in mass to determine the percentage (%) weathered. The physical property measurements of the weathered oil and condensate products are presented in Table 4. In addition, the Sable condensate was spiked with the conservative biomarker 17α-21β hopane as it did not have a high enough natural concentration to normalize the biodegradable saturate and aromatic fractions of the product. The final % weathered after 24 hours for Hibernia, Terra Nova and for Sable condensate and their physical properties are presented in Table 4. Sub-samples of the two oils and condensate were chemically characterized after weathering. The chemical compositions (saturates and aromatics) of the weathered products, used to prepare the microcosms, are presented in Table 3-1, Appendix 3. In addition, the percentage composition (e.g. saturates, aromatics, resins and asphaltenes) of the oils and condensate are presented in Table 5.

Table 4: Physical properties of the weathered oils and condensate used in the study.

	Amount Weathered %	Viscosity (centistokes)		Density (g/mL)	
		15°C	40°C	15°C	40°C
Hibernia Crude Oil	10.0	48.7	10.7	0.874	0.856
Terra Nova Crude Oil	8.9	49.5	11.8	0.877	0.858

Scotian Shelf Condensate	45.2	0.8	0.6	0.784	0.764

Table 5: Properties of crude oil and gas condensate used in this study (based on EC oil properties database)

	Hibernia	Terra Nova	Condensate
	%	%	%
Saturates	79	61	88
Aromatics	15	31	11
Resins and Asphaltenes	7	8	1

3.2.2 Dispersant

COREXIT®EC9500A (Nalco Energy Services) was used for both the oil and condensate studies. COREXIT®EC9500A was selected based on its availability, the fact that there is readily accessible data pertaining to it in the literature, and its long history of use in response to spill emergencies. The *Energy Safety and Security Act*, which received royal assent on February 26, 2015, aims to strengthen the safety and security of offshore oil production through improved oil spill prevention, response, accountability and transparency. The Act amends the *Canada-Nova Scotia Offshore Petroleum Resources Accord Implementation Act*, the *Canada–Newfoundland Atlantic Accord Implementation Act* and the *Canada Oil and Gas Operations Act* (COGOA) to allow for the use of spill treating agents (STAs) in the offshore under specific conditions. Subsequent to this, it was announced in the Canadian Gazette Part I (http://gazette.gc.ca/rp-pr/p1/2015/2015-07-04/pdf/g1-14927.pdf) on July 4, 2015, that "Canada is committed to the moderation of its offshore oil and gas regime by implementing a world class regulatory system and strengthening environmental protection. The regulations support the initiative by establishing a list of spill treating agents (STA) acceptable for use in the event of a spill from an offshore oil facility."

According to the US Environmental Protection Agency, a treatment rate of about 2 to 10 U.S. gallons per acre, or a dispersant-to-oil ratio (DOR) of 1:50 to 1:10 is recommended. This rate varies depending on water temperature and salinity, thickness of the oil slick, the type of oil, and degree of weathering (http://www2.epa.gov/emergency-response/corexitr-ec9500a). The oils and condensate in this study have low viscosities therefore a DOR of 1:25 was chosen. COREXIT®EC9500A (0.5 mL) was premixed with 10 mL of oil or condensate in a glass scintillation vial. For the genomics and respirometry microcosms with only dispersant added, the dispersant was prepared by adding 100µL COREXIT®EC9500A to a sterile 50 mL Falcon tube containing 10 mL of raw seawater. After thorough mixing, 75 µL of the seawater/dispersant mixture was added directly to the microcosm flask with 100 mL seawater and Bushnell Haas using an Eppendorf pipette. The oil-dispersant mixture was prepared at a dispersant-to-oil ratio (DOR) of 1:25, which is the recommended dosage to be applied to an oil spill in the marine environment.

3.3 Bushnell Haas Broth Preparation

Nutrients and trace elements were added to the microcosms to support microbial growth in a closed system. Difco™ Bushnell Haas marine salts broth (Difco, Becton Dickinson and Company) contained the trace elements magnesium sulfate, calcium chloride and ferric chloride that are necessary for bacterial growth and sources of nitrogen and phosphorus. The solution was prepared by adding 3.27 g per liter of deionized distilled water. A single batch of 4 L of the solution was prepared, which required heating the mixture with frequent agitation until it reached boiling, which was maintained for one minute. Aliquots of ~ 500 – 600 mL of the broth were dispensed into 1 L amber glass bottles each containing a small magnetic stir bar, capped and autoclaved at 121 °C for 15 minutes. After cooling, the bottles of broth were stored at 4 °C until the day of the experiment. On the day of the experiment, the bottle of broth, fitted with a sterilized bottle top dispenser (Calibrex 520, 10 mL) was placed on a magnetic stirring plate and was stirred constantly, to ensure a homogeneous solution, while dispensing 2 mL of nutrients into each microcosm flask.

3.4 Experimental Set-up

3.4.1 Chemistry Microcosms

For each location, triplicate treatments of oil/condensate with and without COREXIT®EC9500A were prepared in microcosm (baffled) flasks. Treatments were prepared by adding seawater (100 mL) to each microcosm using a sterile 100 mL glass graduated cylinder. Bushnell Haas media (2 mL) was dispensed into each microcosm to provide sufficient nutrients for the biodegradation. Condensate, oil or condensate/oil + dispersant premix was added (11.5 µL for both oils and 12.8 µL condensate to obtain exactly 100 ppm per microcosm) by using a sterilized Hamilton glass syringe. The syringe needle tip was wiped clean with a Kimwipe® between applications. All microcosm flasks were immediately capped with ethanol rinsed Teflon lined caps. One triplicate set of microcosms was immediately sacrificed (at T = 0) by adding 10 mL dichloromethane (DCM) (pesticide grade distilled in glass, Caledon, Georgetown, Ontario, Canada). All remaining microcosms were placed on a Thermo Max Q 2000 orbital shaker and mixed at 150 rpm, incubated at ambient seawater temperature inside a refrigerated container (reefer) on the deck of the ship and sacrificed at the specified time points (T = 3, 10, 15, 28 and 42 days). The temperature within the reefer was monitored hourly throughout the study with an Oakion Temp 340 data logging thermometer with the probe placed inside a baffle flask containing 100 mL of seawater.

3.4.2 Sterile Controls

Sterile seawater was prepared by passing seawater through a Millipore Express Plus® 0.22 µM Stericup assembly. Aliquots of the weathered oils and condensate were placed in 100 mL serum bottles and sealed with butyl septa and aluminum caps. The headspace in each serum bottle was replaced with nitrogen. The bottles were autoclaved at 121 °C for 15 minutes. Sub-samples of the two oils and condensate and oil/condensate dispersant mixture were chemically characterized before and after

autoclaving to ensure that the chemical composition of the hydrocarbons was not affected by the sterilization process.

To account for the effects of physical and chemical processes (e.g. oxidation, evaporation, etc.) on the biodegradation rates, a series of sterile control microcosms were prepared identical to the non-sterile microcosms with the exception of adding sterile seawater and oil/condensate or oil/condensate/dispersant mix. These sterile control microcosms were run concurrently with and under the same experimental conditions as the oil and condensate biodegradation microcosm studies, and sacrificed in triplicate at the same time points (t = 0, 3, 10, 15, 28 and 42 days) for chemical analysis.

4.0 Sample Processing and Hydrocarbon Analysis

4.1 Sample Extraction

Upon return to the BIO laboratories, water samples from the microcosms were processed using liquid-liquid extraction (modified version of EPA Method 3510C). Further details can be found in Cole et al., 2007; King et al. 2015. Briefly, the water samples were transferred into a 250 mL separatory funnel, and a surrogate recovery standard was added containing Phenanthrene-D_{10}, Pyrene-D_{10}, Benzo[*a*]Pyrene-D_{12}, Benzo[*b*]Fluoranthene-D_{12}, Dibenz[*a*,*h*]Anthracene-D_{14}; deuterated alkanes Dodecane-D_{26}, Heptadecane-D_{36}, *n*-Tetracosane-D_{50}, *n*-Dotricontane-D_{66}, and 5β-Cholestane (Cambridge Isotope Laboratories, Inc. Canada). Each sample was extracted three times, each with 10 mL dichloromethane (DCM). The 30 mL DCM extracts were combined and concentrated to 1 mL using a Turbo Vap II concentrator (Zymark, Hopkinton, MA, USA) then quantitatively transferred to a 15 mL graduated centrifuge tube (with hexane rinses) and further concentrated to 1 mL using a nitrogen evaporator (Organomation Associates Inc., Berlin, MA, USA). Extracts were stored in 15 mL graduated centrifuge tubes. Subsequently, the extracts were purified using a Solid-Phase extraction (VWR-Canlab, Mont-Royal, Québec, Canada, cat no. BJ9400) column packed with silica gel (activated at 200 °C for 17 hours and deactivated in 5% w/v HPLC grade water; Whatman Laboratory Division, Clifton, NJ, USA, 60A 70-230 mesh ASTM for HPLC, cat no. 4791-010) using a modified version of EPA Method 3630C. The column was washed with hexane (Caledon, Georgetown, Ontario, Canada, distilled in glass) and the sample was applied as a 1 mL extract and PAHs and saturates were eluted with 10 mL hexane:dichloromethane (4:1 v/v).

4.2 GC-MS Analysis

Purified extracts of water from the microcosms were analyzed using high resolution gas chromatography (Agilent 6890 GC) coupled to an Agilent 5973N mass selective detector (Wilmington, DE, USA) operated in the selective ion monitoring mode using the following GC (MDN-5S column 30 m × 0.25 mm id 0.25 µm film thickness, Supelco Canada) conditions: cool on-column injection with oven track mode (tracks 3 °C higher than the oven temperature program); 80 °C hold 2 min; ramp at 4 °C/min to 280 °C; hold 10 min.

Quantification criteria for PAH included retention time matching, i.e. within ± 0.010 min of the retention time of the standard, and comparing the relative abundance of the qualifying ion(s) (±10%),

the molecular ion, and one or more qualifier ions in the mass spectrum of the compound with the commercial standard. Seven levels of PAH standards were used to calibrate the system. The auto-quant software allowed for easy interpretation and quantification of analytes present in samples. The Chemstation software allowed for custom reporting. The sample information collected by the Chemstation can be transferred through the use of custom reports into Microsoft Excel format. The calibration curve was updated with each batch of samples analyzed. The auto-quant software was used to interpret and quantify analytes detected in the extracts.

All processed data were compared to established limits in order to pass quality control. These limits have been set at ± 30% of the true value compared to experimental values. If results fell outside the limits they were repeated. The same was true for reference materials used to track analytical quality.

4.3 Chemometric Analysis

17α(H), 21β(H)-hopane was used as a conservative biomarker to monitor the bioremediation effectiveness of crude oils and condensates (Prince et al. 1994; Venosa et al. 1997). This complex molecule is resistant to microbial attack and, therefore serves as an excellent internal conserved marker in crude oil, since it is not expected to degrade over the 42 day duration of the study. The kinetics of biodegradation should follow 1st order logic; therefore, the rate law of the analyte is expressed as (dC/dt)t, and the rate law of hopane is expressed as (dH/dt)t,c and the biodegradation rate of the analyte (-kC) are related by the following equation:

$$\left(\frac{dC}{dt}\right)_t = \frac{C}{H}\left(\frac{dH}{dt}\right)_t = -kC \quad (1)$$

where C is the concentration of an analyte, H is the concentration of hopane, and k is the first-order biodegradation rate constant for an analyte. Using the definition of the derivative of a quotient, eq. 1 can be rewritten as

$$\frac{d\left(\frac{C}{H}\right)}{dt} = -k\left(\frac{C}{H}\right) \quad (2)$$

Integrating eq. 2 yields the following first-order relationship:

$$\left(\frac{C}{H}\right) = \left(\frac{C}{H}\right)_0 e^{-kt} \quad (3)$$

where (C/H) is the time-varying hopane-normalized concentration of an analyte, and $(C/H)_0$ is the value of that quantity at time 0. Further to this, if the natural log is applied to both sides of the equation and it is rearranged to follow the typical format of y=mx+b (equation of a line) the following is generated:

$$ln\left(\frac{C}{H}\right) = ln\left(\frac{C}{H}\right)_0 - kt \quad (4)$$

where $ln(C/H)_0$ is the y-intercept and $-k$ is the slope of the line or the biodegradation rate constant. Regression analysis will be used to determine if the 1st order plots are statistically significant and that the analyte degradation is strictly due to biological processes.

In addition, the half-life ($t_{\frac{1}{2}}$) can be determined by modifying equation (4) to produce the following expression:

$$-kt_{\frac{1}{2}} = ln\left(\left(\frac{C}{H}\right)_0 \div 2 \Big/ \left(\frac{C}{H}\right)_0\right) = -\ln 2 \quad (5)$$

$$t_{\frac{1}{2}} = ln2/k \quad (6)$$

The percent biodegradation can be calculated as follows:

$$Percent\ Biodegradation = \left[1 - \frac{\left(\frac{C}{H}\right)_t}{\left(\frac{C}{H}\right)_0}\right] x100 \quad (7)$$

5.0 Microbiology

5.1 Respirometry Flasks

Microcosm flasks to measure changes in microbial respiration over time (expressed as the change in the percentage of oxygen in the headspace of the microcosms), were prepared identically to the genomics and chemical flasks; however, were fitted with a non-invasive oxygen sensor button to measure the partial pressure of both dissolved and gaseous oxygen within the flask as part of a fibre optic oxygen transmitter system (PreSens Precision Sensing GmbH, Germany). Light emitted from an LED probe attached to the oxygen transmitter (Microx OXY-4) summer and Fibox 4 for winter) and data logger excited the sensor buttons to emit fluorescence. Oxygen in the headspace of the flask quenched the fluorescence signal and the degree of quenching correlated to the partial pressure of oxygen. Measurements were compensated for temperature, pressure and salinity. Two sensor buttons (PSt3, detection limit 15 ppb dissolved oxygen, 0-100%) were affixed with silicone glue to the inside of a clean baffle flask prior to autoclaving, one near the bottom of the flask and a second near the neck of the flask to measure the change in oxygen in the headspace of the flask. The winter mission flasks contained only one sensor spot located in the neck of the flask.

To determine if the sensors were measuring a response, a positive control was prepared by adding raw seawater, Bushnell Haas and sugar (several grams) to a flask and was monitored along with the treatment flasks.

Once the microcosm flasks were prepared, they were moved to the reefer and placed in the shakers. After a temperature equilibrium period of approximately one hour, the percent oxygen in the

headspace was measured by holding the probe to the side of the flask adjacent to the sensor button. Readings were conducted daily while at sea and every 3 – 4 days while on shore. The Fibox meter was calibrated daily prior to measurements using a sealed serum bottle purged with nitrogen (0% control) and an open serum bottle for 100% control.

On Day = 42, a final respiration reading was taken for each flask. The triplicate treatments were filtered (<10 psi) onto a Millipore® 0.22 µM GPWP04700 filter held in a fritted glass base and 250 mL funnel that had both been autoclaved. The flasks were rinsed (1 x 5 mL) with a 0.22 µM filtered and autoclaved solution of 30 g/L NaCl in deionized distilled water. The funnels were rinsed with 1 x 5 mL of the NaCl solution. The filter was removed and placed in a sterile 50 mL Falcon tube, flash frozen with liquid nitrogen and stored in a -80 °C freezer until shipped on dry ice to National Research Council (NRC) in Montreal, Québec for further analyses.

5.2 Genomics Microcosms

Microcosm flasks to measure microbial respiration and genomics were established concurrently with the chemical microcosms that measured changes in hydrocarbon chemistry. Genomics microcosm flasks were prepared identically to the chemical flasks by adding 100 mL of either raw or 0.22 µM filtered seawater to a baffle flask, 2 mL of Bushnell Haas media, and finally adding the oil/condensate or oil/condensate + dispersant mix. The genomics had an additional treatment of raw seawater + Bushnell Haas + dispersant alone to determine the effects of the dispersant on the microbial population.

For T = 0 collection of genomic material for total nucleic acid extraction, initial seawater samples (2 L) were filtered (< 10 psi) onto Millipore® 0.22 µM GPWP04700 filters held in a sterilized fritted glass base and 250 mL funnel. The filter was placed in a 50 mL sterile Falcon tube, immediately flash frozen by submersion in liquid nitrogen and stored in a -20 °C freezer on board the ship prior to being transferred to a -80 °C freezer upon return to BIO. The samples were shipped to NRC in Montreal on dry ice for metagenomic and metatranscriptomic analyses.

The genomics flasks were sacrificed at T = 5 and T = 42 days for the summer study and T = 7 and T = 42 days for the winter study by filtering (≤10 psi) the contents of each flask through a 0.22µM filter (as described above). Each microcosm flask was rinsed with 1 x 5 mL of 0.22 µM filtered seawater and the filter funnel was rinsed with 3 x 5 mL of filtered seawater. The filter was collected as above. The filter funnels and bases were rinsed with DCM after use to remove residual hydrocarbons and sterilized at sea by soaking in a 6% sodium hypochlorite (bleach) solution for 15 minutes, followed by soaking in two successive washes of autoclaved deionized distilled water for ten minutes each.

5.2.1 Nucleic Acid Extraction

Total nucleic acids were recovered using a modified version of the hexadecyl trimethyl ammonium bromide (CTAB) method of Ausubel et al. (2002). The modifications were as follows: the incubation time for the TE/Lysozyme treatment was reduced substantially from one hour to 15 minutes and the temperature for this step was increased from 37 °C to 56 °C. The CTAB/NaCl incubation was followed by

phenol/chloroform/isoamyl alcohol (25:24:1) then a chloroform/isoamyl alcohol extraction steps. Nucleic acids were precipitated overnight at -20 °C with isopropanol and glycogen (Roche, Mississauga, ON). DNA was quantified using Quant-iT PicoGreen assay (Invitrogen, Life Technologies) and 1 ng of gDNA was used as a template to construct the sequencing library, using the Illumina Nextera XT library preparation protocol following the manufacturer's instructions. However, the "Library Normalization" step was omitted and normalization was instead performed by pooling equal amounts of libraries after Quant-iT PicoGreen quantification. The quality of the pooled library was assessed (http://support.illumina.com/sequencing/sequencing_kits/nextera_xt_dna_kit/documentation.html) using an Agilent 2100 Bioanalyzer with a High Sensitivity DNA Kit.

5.2.2 Sequence Analysis

Total RNA was quantified using Quant-iT RiboGreen assay (Invitrogen, Life Technologies). Ribosomal RNAs were removed and library preparation was performed using ScriptSeq Complete Kit Bacteria Low-Input Library Prep protocol according to the manufacturer's (Epicentre) instructions starting with 100ng total RNA. Normalization was performed by pooling equal amounts of libraries after Quant-iT PicoGreen quantification. The quality of the pooled library was assessed (http://support.illumina.com/sequencing/sequencing_kits/scriptseq-complete-bacteria/documentation.html) using an Agilent 2100 Bioanalyzer with a High Sensitivity DNA Kit.

5.2.2.1 Shotgun metagenomics data processing

Sequencing adapters were removed from each read (Trimmomatic v0.32) to generate quality controlled (QC) reads. Each QC-passed read from each sample was assembled into a large metagenome assembly using Ray software v2.3.1. Gene prediction on obtained contigs (overlapping DNA segments) was performed by calling genes (ORF, start codon, stop codon) on each assembled contig using MetageneMark v1.0. Genes were annotated in the following way: 1) RPSBLAST (v.2.2.30+) against COG database, and 2) against KOG database; 3) HMMSCAN (v.3.1b1) against PFAM-A database, and against 4) TIGRFAM database; 5) BLASTP (v2.2.30+) against KEGG database, and 6) BLASTN (v2.2.30+) against NCBI`s nucleotide (nt) database. Mapping (BWA mem v0.7.10) of QC-passed reads against contigs and called gene sequences were done as follows: Raw reads were mapped against contigs to assess quality of metagenome assembly. Raw reads were also mapped against called genes to obtain abundance measures of each gene. Alignment files in bam format were sorted by read coordinates using samtools v1.1. According to the supplied experimental design, Differential DNA Abundance (DDA) was computed (edgeR v3.10.2) for each design. Genes having a false discovery rate (FDR) value ≤ "fdr" and logFC ≤ "logfc" are considered to be differentially abundant. PcoAs and heatmaps were generated for each experimental design. Tables containing DDA genes were included in the report archive. The taxonomic summary was performed using a combination of in-house scripts and Qiime v.1.8.0.

5.2.2.2 Shotgun metatranscriptomics data processing.

Sequencing adapters were removed from each read (Trimmomatic v0.32). Mapping (BWA mem v0.7.10) of the QC-passed reads against contigs and called gene sequences generated during the

metagenomics data processing steps was generated as follows: Raw reads were mapped against contigs to assess quality of metagenome assembly. Raw reads were also mapped against called genes to obtain abundance measures of each gene. Alignment files in bam format were sorted by read coordinates using samtools v1.1. According to the supplied experimental design, Differential DNA Abundance (DDA) was computed (edgeR v3.10.2) for each design. Genes having a FDR value ≤ ", fdr," and logFC ≤ ", logfc, " were considered to be differentially abundant. PCoAs and heatmaps were generated for each experimental design. Tables containing DDA genes were included in the report archive. A taxonomic summary was performed using a combination of in-house scripts and QIIME v.1.8.0.

6.0 Results

6.1 Baseline Data

Baseline data for all reference areas including; CTD profiles (salinity, temperature, oxygen, pressure, fluorescence), nutrients and salinity, organics (BTEX, PAHs, and Alkylated PAHs), chlorophyll and phaeopigments, bacterial enumeration and genomics, and further details on the methodologies are presented in the Appendices.

Salinity values, measured from collected water samples, were typically greater than 30 psu, which is normal for marine waters (Tables 1-6 to 1-8, Appendix 1). These reading were consistent with the salinometer readings taken *in situ* by the SeaBird SBE9 (Tables 1-3 to 1-5, Appendix 1). Other *in situ* measurements such as; oxygen, temperature, and fluorescence are at background levels for all three sites.

In all cases, the water samples that were analysed had negligible values for organics (e.g. BTEX, saturates, PAHs, and Alk-PAHs) and extremely low concentrations (ppb range) of other important nutrients, such as nitrate, ammonia and phosphate (Appendix 1).

Bacterial enumeration data for the summer mission showed comparable, but highly variable population densities for Hibernia and Terra Nova (Fig. 2-1, Appendix 2). The population densities were higher at the surface, ranging from 4 to 6 x 10^5 cells/mL, and decreased with depth to 2 to 4 x 10^5 cells/mL. Thebaud (Sable) bacterial densities showed the same pattern (decreasing with depth), but were generally twice as high as those observed at Hibernia and Terra Nova. These population densities are quite typical in terms of quantities and distribution with depth.

Chlorophyll and phaeopigment concentrations in samples collected at various depths for all three sites are showed in Tables 2-1 to 2-3, Appendix 2. These readings are also consistent with background levels reported by others (Zhai et al., 2011; Li and Harrison, 2014; Li, 2014).

6.2 Respirometry

The respirometry results for the microcosms, from each of the three sites for the summer and winter samples, are presented in Figures 5 to 8. The raw respirometric data are presented in tabular form in

Appendix 4 (Tables 4-1 to 4-6). For the summer mission, sensor buttons were placed on both the bottom and side of the flasks. Only the side (headspace) readings data were used. A reading was taken for each flask after approximately 10 seconds or once the readings were stable. The % saturation reading of each of the three replicate treatments was averaged (n = 3). Two of the condensate + dispersant microcosms (Sable summer) were found to have loose caps on Day = 2. Readings in these two flasks changed very little over the course of the experiment, therefore it was suspected that there may have been a problem with the loose caps and these two replicates were dropped (Figure 7a). The positive control showed that the sensors were measuring headspace oxygen (Figure 8).

For the winter mission, sensor buttons were placed only on the side of each flask to measure headspace oxygen saturation. Three readings were recorded for each microcosm flask. The three measurements from each of the three replicate treatments were averaged (n = 9) (Tables 4 and 5 and Figure 5a and 5b provide the respirometry results from Hibernia summer and winter). The experiments and reefer were removed from the *Hudson* on the morning of December 12. Respirometry measurements were taken after the reefer was re-established on the jetty (Day = 17 for Hibernia and Terra Nova) and (Day 27 for Sable). There was a power failure to the GFI plug on the jetty that powered the shakers at some point of December 13 (approximately) due to inclement weather, so the flasks were not shaking for approximately 72 hours. We do not expect this to have a significant bearing on the final results as every experiment had appropriate controls that would have been affected similarly. The reefer unit was not affected and was still maintaining temperature. On Day = 35 (winter experiment), all the Sable flasks were opened for 30 minutes to refresh the headspace due to some readings below 12% oxygen (See Figure 7b). This was done as a precautionary measure to ensure that internal oxygen concentrations in the flasks did not become too low.

At the Hibernia site, respirometric activity was expected to be generally high in the summer in the microcosms that contained oil alone or with dispersant, but surprisingly, the activity was slightly higher or comparable in the winter (Fig. 5). It is possible that other nutrients were present in the winter water that elicited a higher respiration response. Dispersant alone did not elicit a significant response when compared to seawater alone. Filtered seawater did show respirometric activity comparable to the oil alone or with dispersant. This was subsequently shown to be attributable to an inability to adequately sterilize the oil substrate in addition to the presence of ultramicrobacteria in the filtrate, likely more prevalent during the winter sampling. The ultramicrobacteria were largely composed of *Pelagibacter*, identified by performing sequencing on filtrate samples, which have been shown to have oil degradation capabilities (Prince et al. 2010).

Terra Nova showed almost identical results to Hibernia, with respirometric activity being slightly higher in the winter with oil alone or with dispersant (Fig. 6). Again, the filtered seawater controls showed significant respiration.

Thebaud (Sable) samples also had high respirometric activity at both times of the year, but in the summer there was a more significant difference between the oil alone or with dispersant and the filtered seawater control (Fig. 7). In the winter sampling this difference was not evident.

In all the sampling sites, negligible respiration was detected with seawater alone or seawater with dispersant alone and no statistically significant differences were noted between these two conditions. In a subsequent experiment, using seawater from 30 nautical miles off Nova Scotia, it was clearly determined that the respiration observed in the control flasks was due to unsterilized oil substrate (Fig. 9). The oil was autoclaved on two separate occasions to sterilize it, but that was clearly not sufficient. We were concerned about using too rigorous conditions, since this could have altered the oil substrates resulting in an inadequate control. It should also be emphasized that the observed respiration did not correlate with oil degradation as the chemical analysis did not show significant differences between the starting concentration and the final concentration of alkanes, PAHs or Alk-PAHs following incubation. This has to be considered in future experiments where sterile (negative) controls are required. Due to the nature of this study, which also incorporated chemical and genomic analyses, we had other means at our disposal to interpret these control data, so they did not jeopardize the outcome of these experiments.

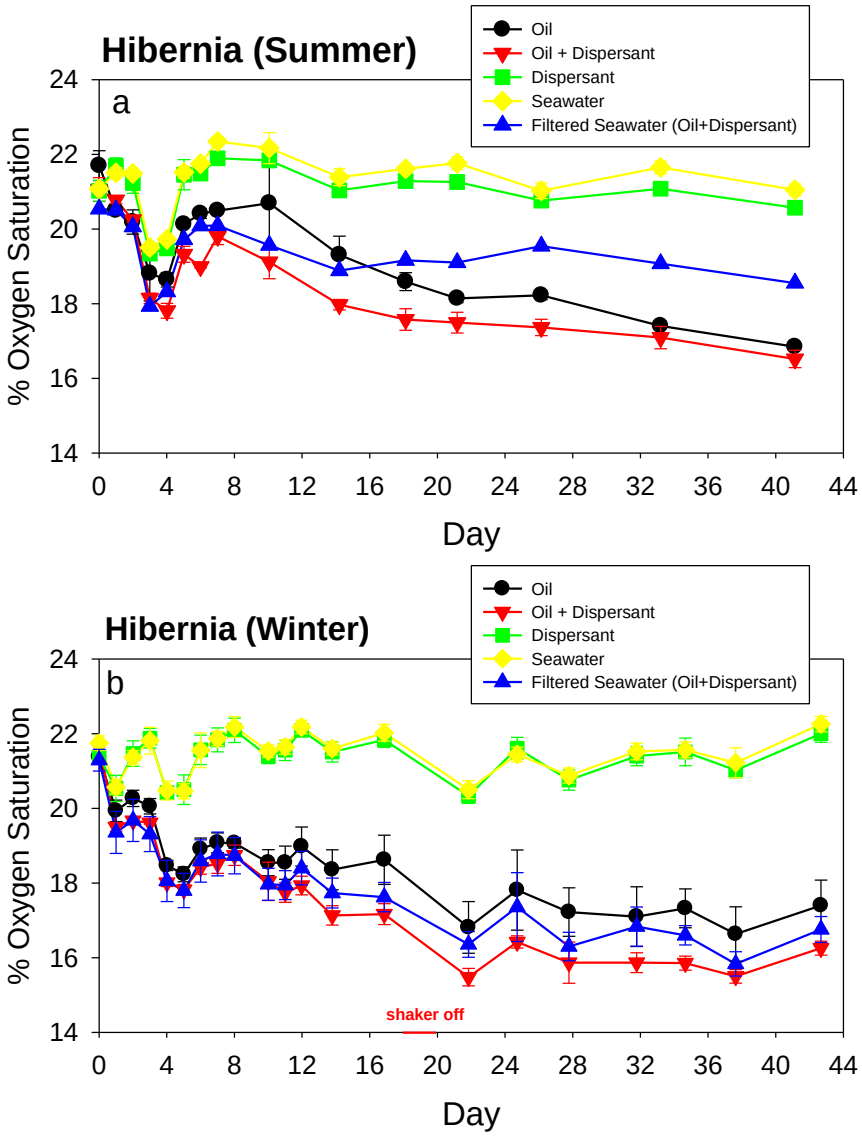

Figure 5: Microcosm respirometry results for Hibernia summer (a) and winter (b). Treatments are as shown in figure legends.

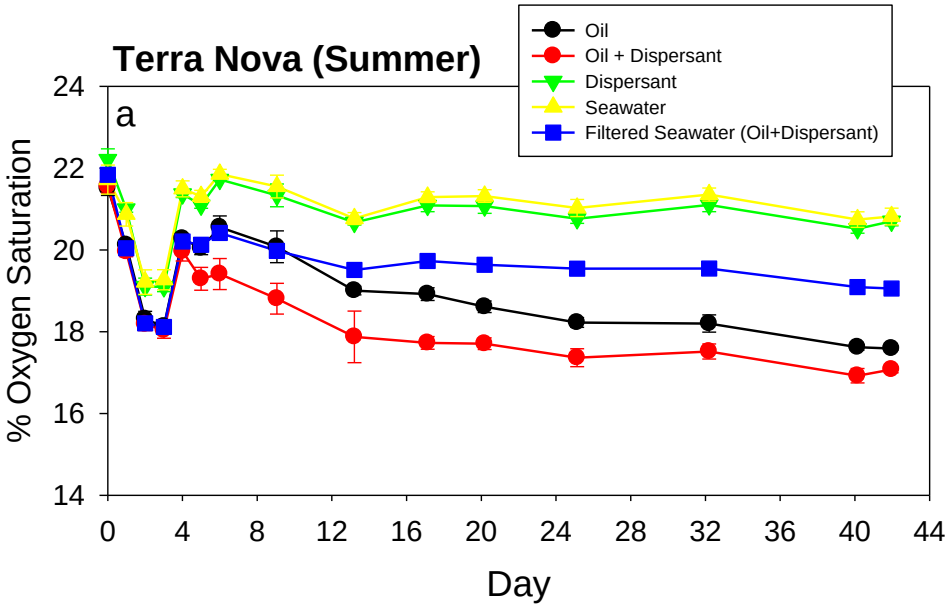

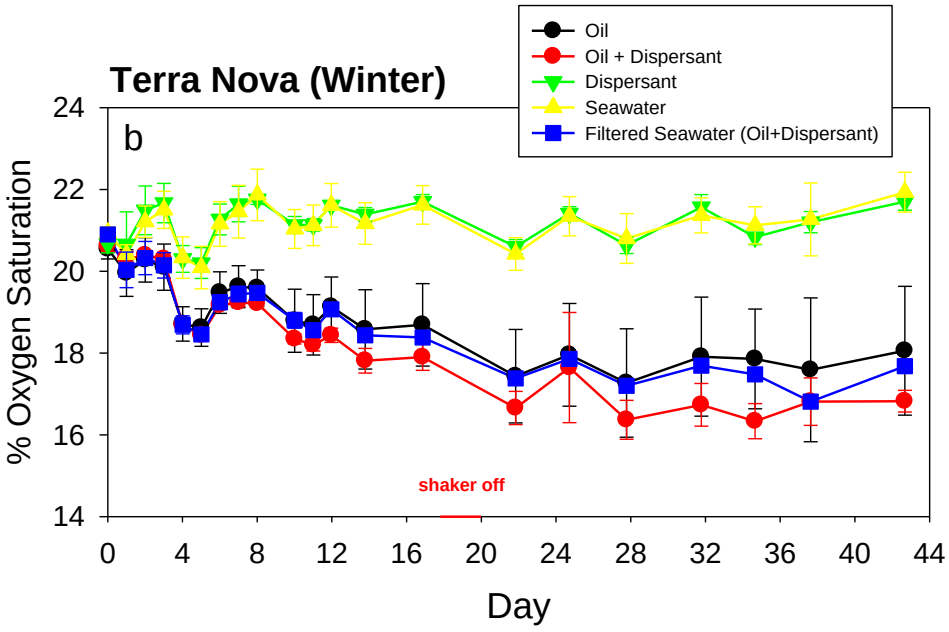

Figure 6: Microcosm respirometry results for Terra Nova summer (a) and winter (b). Treatments are as shown in the figure legends.

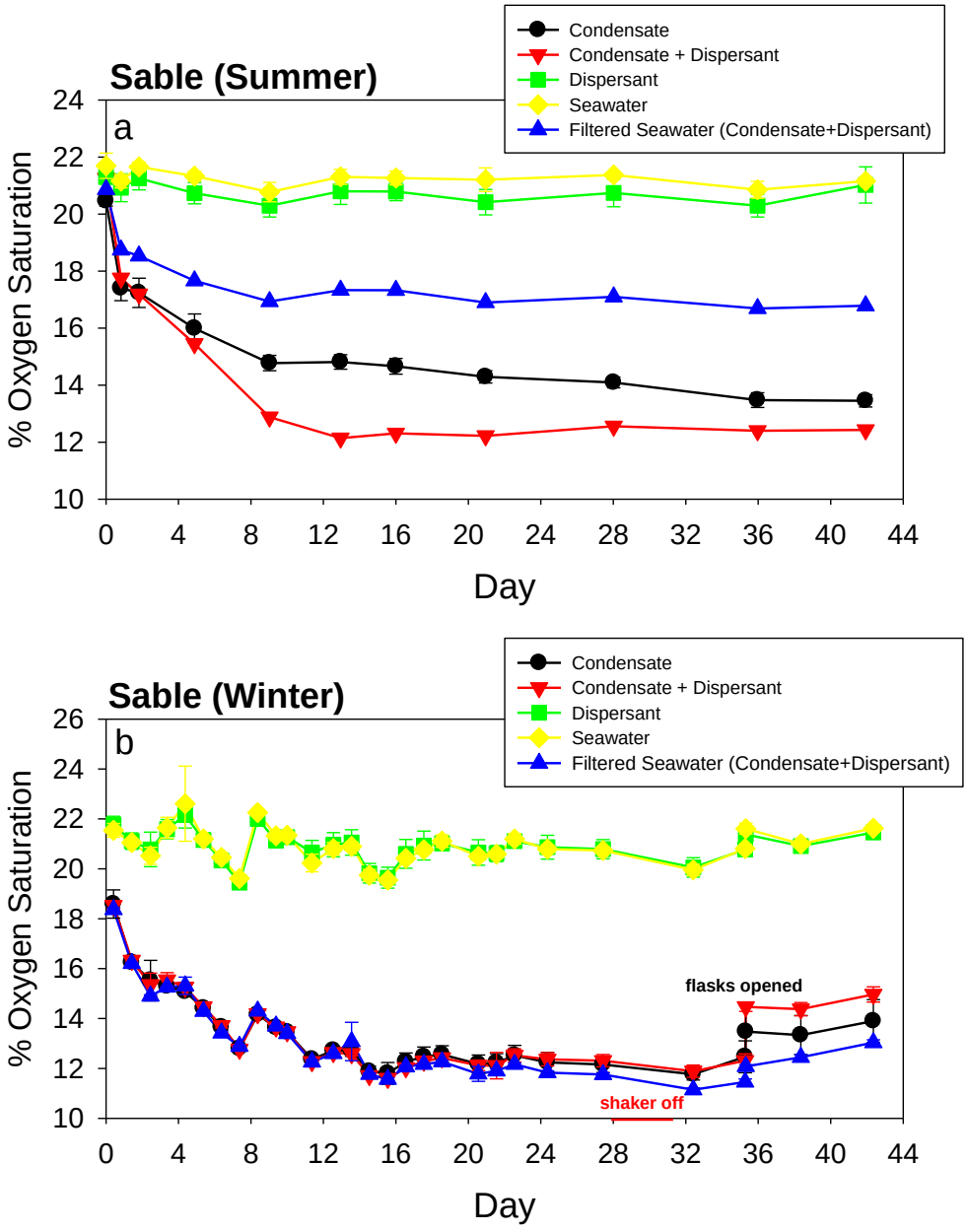

Figure 7: Microcosm respirometry results for Sable (Thebaud) summer (a) and winter (b). Treatments are as shown in the figure legends.

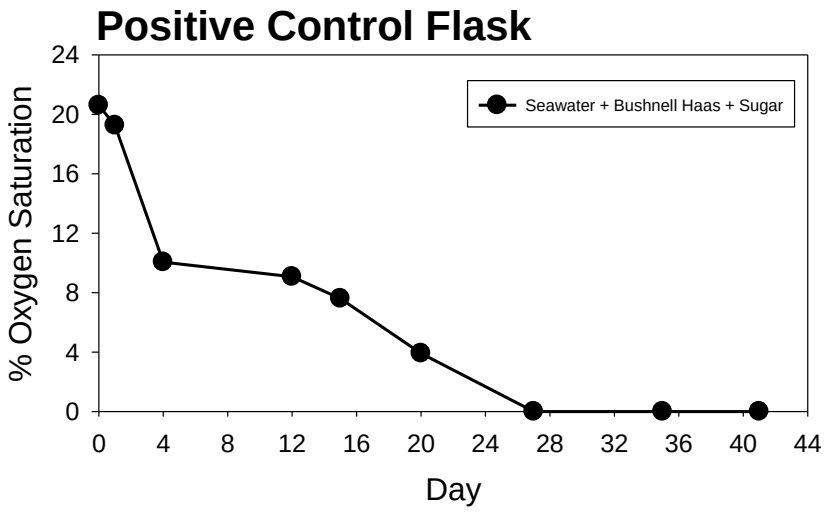

Figure 8: Positive control respirometry flask showing oxygen consumption in the presence of sugar as substrate.

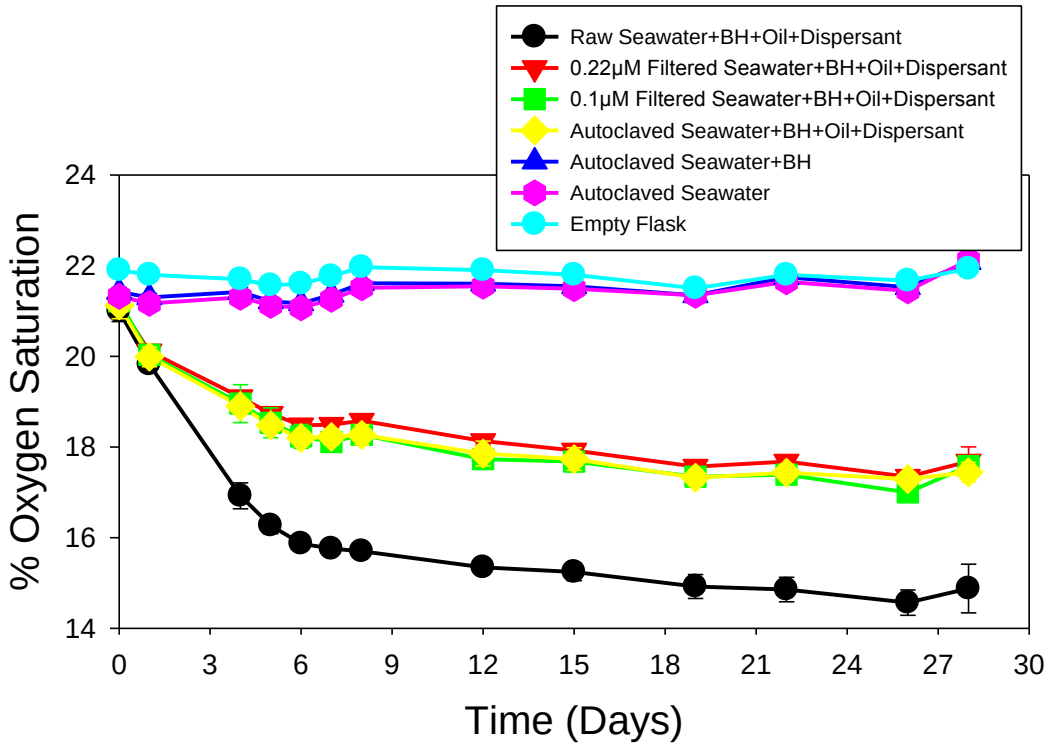

Figure 9: Control experiment using seawater from offshore Nova Scotia to examine various methods of sterilization. Note that respiration was observed using autoclaved seawater containing nutrients and oil/dispersant. No respiration was observed where there was no oil/dispersant substrate.

6.3 Chemistry Results

6.3.1 Microcosms

Microcosm flasks were sacrificed throughout the incubation period and analyzed for residual hydrocarbons, including alkanes, polycyclic aromatic hydrocarbons (PAHs) and Alkylated PAHs. Figures 10 to 12 show bar graphs of the sum of alkanes, Alkylated PAHs, and PAHs for summer and winter microcosms from Hibernia, Terra Nova and Sable (Thebaud), respectively.

The degradation of hydrocarbons (Hibernia crude oil) with Hibernia seawater was quite rapid in the summer, but considerably slower in the winter (Fig. 10). The alkane and PAH fractions were degraded almost completely within two weeks in the summer, whereas the Alkylated PAHs were degraded more slowly. The presence of dispersant accelerated the alkane degradation rate, whereas the initial rates for PAHs and Alkylated PAHs degradation were slightly reduced. Degradation was also observed with filtered seawater, but not nearly to the same extent, and dispersant did not seem to enhance this degradation. In contrast, degradation in the winter was considerably slower and not as extensive, and alkane degradation, in particular, was highly enhanced by the presence of dispersant. The degradation of PAHs and Alkylated PAHs in the winter was much slower and although the results showed some variability, a clear effect of dispersant was not evident. The difference in degradation rates between the summer and winter are likely due, at least in part, to temperature, but other factors dictated by oceanographic conditions (for example, nutrient availability) or differences in degrader microbial populations are also likely to have contributed. The line graph of oil component biodegradation is presented as Figure 5-1 in Appendix 5.

The degradation of hydrocarbons (Terra Nova crude oil) with Terra Nova seawater was very similar to what was observed with Hibernia (Fig. 11). There were clear differences between the degradation rates in the summer and winter and of the effects of dispersant on alkane degradation especially in the winter, which can be clearly seen in Figure 5-2 in Appendix 5. The degradation of PAHs and Alkylated PAHs were also quite high in the summer and much slower in the winter. With these latter two substrates, there did not appear to be a significant difference between with and without dispersant.

The degradation of hydrocarbons (gas condensate) with Sable (Thebaud) seawater was very rapid in the summer and very slow in the winter (Fig. 12). In this case, there was a much more pronounced difference between the summer and winter rates. All fractions (alkanes, PAHs and Alkylated PAHs) were almost completely degraded within 10 days in the summer. The degradation was so rapid in the summer that an effect of dispersant was not evident and in the winter, the rates were quite low and variable with and without dispersant, so no clear effect of dispersant was evident, except at the final sampling point, when dispersant presence appeared to have had a negative impact on degradation. The graphical data illustrating gas condensate biodegradation is presented as Figure 5-3 in Appendix 5.

6.3.2 Chemometric Analysis

The degradation rates in both summer and winter for each of the three sites (Hibernia, Terra Nova and Thebaud), in addition to the half-lives of the different components (alkanes, PAHs and Alkylated PAHs)

are summarized in Table 6. These analyses provide an overview of the overall degradation rates that could be expected in situ for the different hydrocarbon components. Degradation rates were typically higher in the summer than in the winter for all hydrocarbon components at all three sites.

Table 6: Chemometric analysis of crude oil and gas condensate biodegradation. Data are presented rates of alkane, PAH and alkylated PAH degradation kinetics for each location, for summer and winter samplings, with and without dispersant.

		Hibernia NO Dispersant Summer					Hibernia Dispersant Summer				
	-k	r2	t1/2	% Biodegradation (42 d)		-k	r2	t1/2	% Biodegradation (42 d)	
			(Days)	Avg	SD			(Days)	Avg	SD
alkanes	0.0981	0.95	7.1	98.06	0.39	0.0943	0.68	7.4	98.13	0.43
Alkyl-PAHs	0.0359	0.76	19.3	80.02	3.75	0.0324	0.85	21.4	73.08	3.80
PAHs	0.0719	0.76	9.6	95.81	0.40	0.0877	0.89	7.9	96.87	0.34
		Hibernia NO Dispersant Winter					Hibernia Dispersant Winter				
	-k	r2	t1/2	% Biodegradation (42 d)		-k	r2	t1/2	% Biodegradation (42 d)	
			(Days)	Avg	SD			(Days)	Avg	SD
alkanes	0.0137	0.61	50.6	39.11	11.62	0.0403	0.83	17.2	77.23	2.43
Alkyl-PAHs	0.0189	0.61	36.7	41.67	17.53	0.0141	0.61	49.2	52.33	5.02
PAHs	0.0382	0.73	18.1	71.09	6.03	0.0456	0.67	15.2	90.37	1.46
		Terra Nova NO Dispersant Summer					Terra Nova Dispersant Summer				
	-k	r2	t1/2	% Biodegradation (42 d)		-k	r2	t1/2	% Biodegradation (42 d)	
			(Days)	Avg	SD			(Days)	Avg	SD
alkanes	0.0838	0.95	8.3	96.14	1.92	0.085	0.74	8.2	97.14	2.17
Alkyl-PAHs	0.0451	0.83	15.4	82.85	5.30	0.0491	0.83	14.1	85.70	1.47
PAHs	0.0740	0.81	9.4	94.90	1.55	0.0965	0.83	7.2	97.75	1.34
		Terra Nova NO Dispersant Winter					Terra Nova Dispersant Winter				
	-k	r2	t1/2	% Biodegradation (42 d)		-k	r2	t1/2	% Biodegradation (42 d)	
			(Days)	Avg	SD			(Days)	Avg	SD
alkanes	0.0124	0.56	55.9	31.10	13.28	0.0529	0.93	13.1	87.38	1.45
Alkyl-PAHs	0.0145	0.57	47.8	48.47	10.73	0.0081	0.60	85.6	28.88	7.73
PAHs	0.0333	0.70	20.8	76.97	3.66	0.0401	0.85	17.3	80.71	4.08
		Sable NO Dispersant Summer					Sable Dispersant Summer				
	-k	r2	t1/2	% Biodegradation (42 d)		-k	r2	t1/2	% Biodegradation (42 d)	
			(Days)	Avg	SD			(Days)	Avg	SD
alkanes	0.0890	0.51	7.8	99.48	0.15	0.1044	0.45	6.64	99.67	0.28
Alkyl-PAHs	0.0997	0.56	7.0	98.79	0.42	0.1066	0.48	6.50	99.38	0.19
PAHs	0.0936	0.48	7.4	98.60	2.10	0.1073	0.84	6.46	99.39	0.78
		Sable NO Dispersant Winter					Sable Dispersant Winter				
	-k	r2	t1/2	% Biodegradation (42 d)		-k	r2	t1/2	% Biodegradation (42 d)	
			(Days)	Avg	SD			(Days)	Avg	SD
alkanes	0.0200	0.62	34.7	64.00	14.05	0.0089	0.43	77.9	32.22	23.77
Alkyl-PAHs	0.0101	0.42	68.6	45.69	4.98	0.0021	0.08	330.1	8.79	10.87
PAHs	0.0073	0.30	95.0	38.43	4.91	0.0032	0.11	216.6	13.62	9.48

k = reaction rate constant

r^2 = (correlation coefficient)^2

$t_{1/2}$ = half-life

Note: Day = 28 data from the Sable Winter Dispersant treatment for alkylated PAHs and PAHs were considered to be anomalous and therefore excluded.

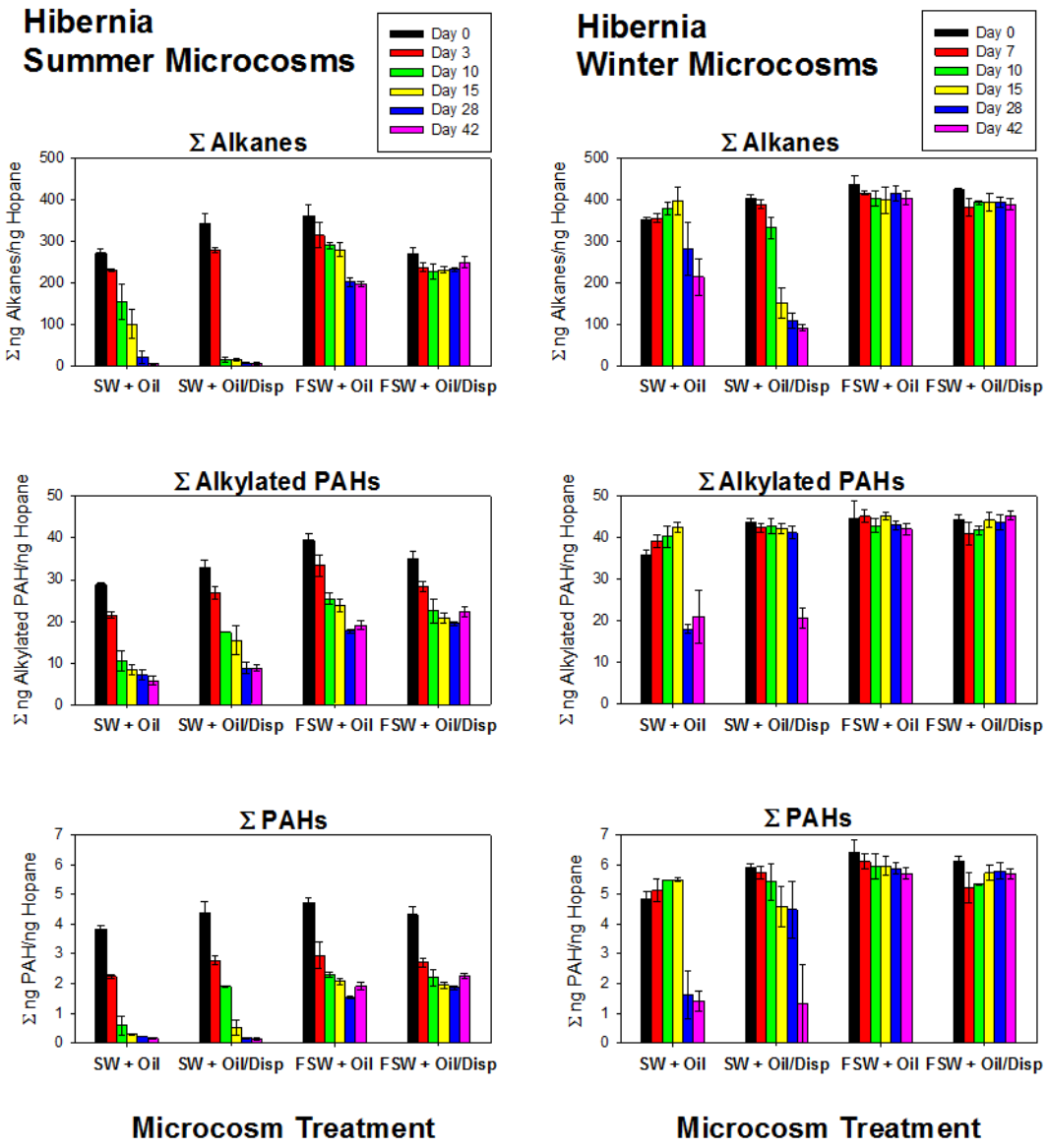

Figure 10: Residual hydrocarbon concentrations (alkanes, PAHs, and Alkylated PAHs) in Hibernia summer and winter microcosms. Treatments are seawater plus oil (SW +Oil), seawater plus oil with dispersant (SW + Oil/Disp), filtered seawater plus oil (FW + Oil), and filtered seawater plus oil with dispersant (FSW + Oil/Disp). All microcosms received Bushnell Haas nutrients. Time of sacrificing is shown by colored bars.

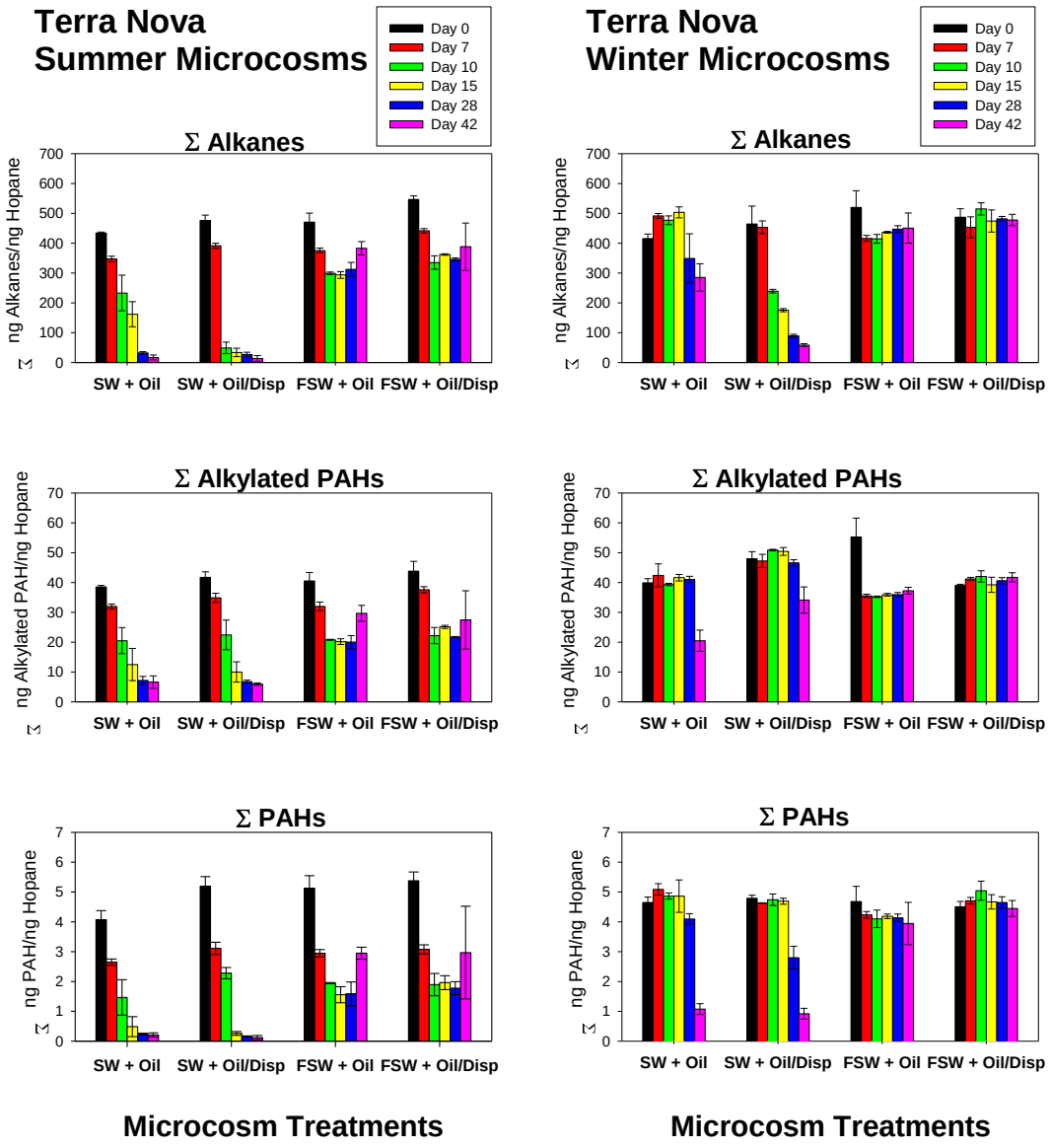

Figure 11: Residual hydrocarbon concentrations (alkanes, alkylated PAHs and PAHs) in Terra Nova summer and winter microcosms. Treatments are seawater plus oil (SW + Oil), seawater plus oil with dispersant (SW + Oil/Disp), filtered seawater plus oil (FSW + Oil) and filtered seawater + plus oil with dispersant (FSW + Oil/Disp). All microcosms received Bushnell Haas nutrients. Time of sacrificing is shown by colored bars.

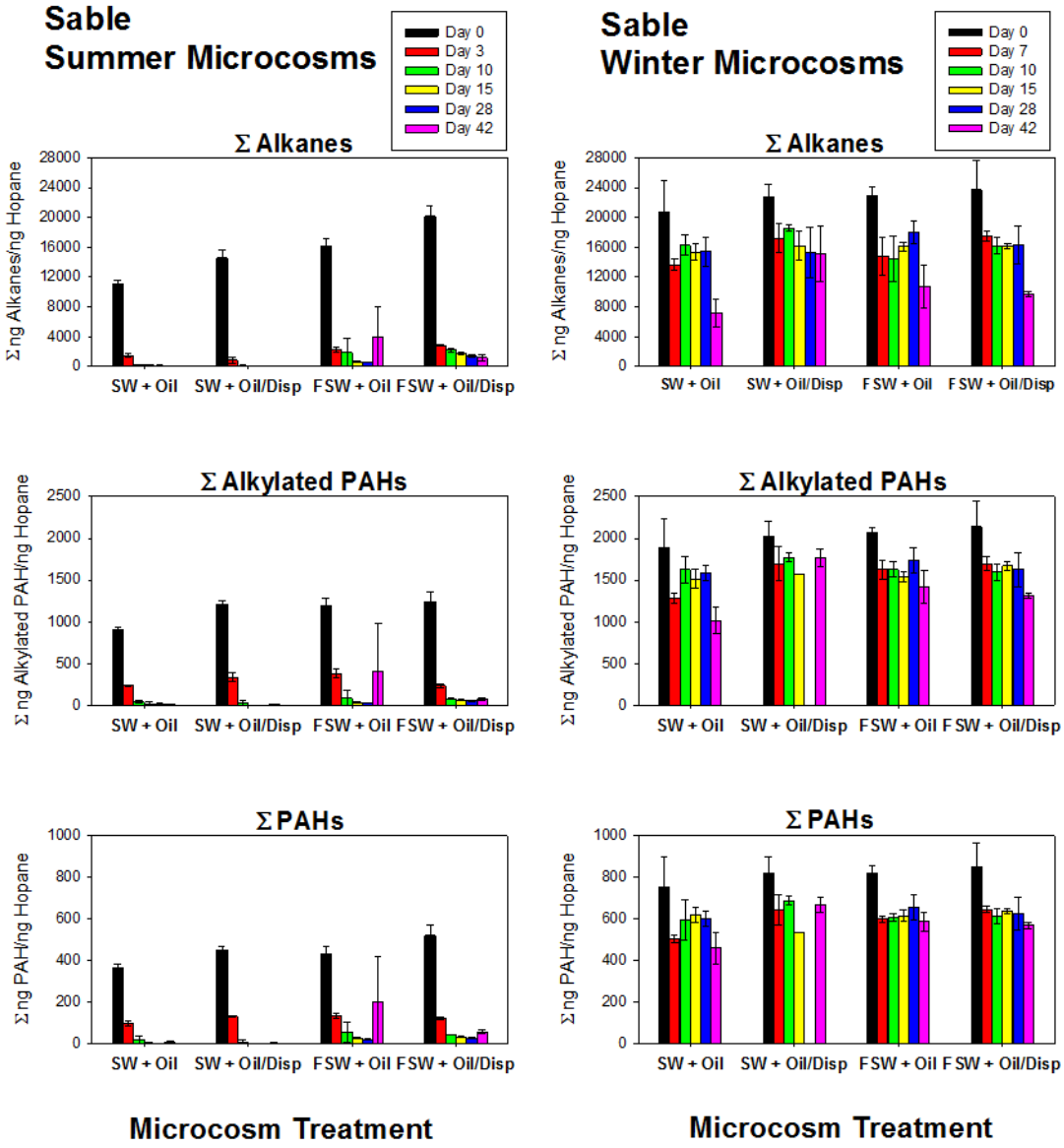

Figure 12: **Residual hydrocarbon concentrations (alkanes, alkylated PAHs and PAHs) in Sable (Thebaud) summer and winter microcosms. Treatments are seawater plus oil (SW + Oil), seawater plus oil with dispersant (SW + Oil/Disp), filtered seawater plus oil (FSW + Oil) and filtered seawater + plus oil with dispersant (FSW + Oil/Disp). All microcosms received Bushnell Haas nutrients. Time of sacrificing is shown by colored bars.**

Alkanes were degraded faster and more thoroughly at all three sites in comparison to PAHs and Alkylated PAHs. The positive effect of dispersant application was noted during the winter degradation studies for the alkanes, whereas no clear or consistent impacts were identified with PAH and Alkylated PAH degradation rates.

At the Hibernia location, there was a positive effect of dispersant on the alkane degradation rate in the summer, but in the winter both the rate and half-life were significantly improved (*p-value* <0.05; Two-Factor ANOVA) by the presence of dispersant. The effect of dispersant on PAH and Alkylated PAH degradation was less obvious with a slight improvement in degradation rate in the summer, but a potential negative effect in the winter (Table 6 and Figure 5.1, Appendix 5).

Similar results to Hibernia were observed at Terra Nova, with the alkane degradation rate increased slightly in the summer but much more markedly in the winter by the presence of the dispersant. There was little difference in PAH and Alkylated PAH degradation rates in the summer with or without dispersant and in the winter the rates of degradation were much lower with or without dispersant, with little clear advantage for the presence of dispersant, but with a potential negative impact on Alkylated PAH degradation rates and half-lives. (Table 6 and Figure 5.2, Appendix 5).

At Thebaud (Sable), degradation rates in the summer were very rapid and dispersant did not have a clear impact on the process, with short half-lives and high degradation percentages for all hydrocarbon components. When examining the winter results, the data for 28 days was a clear anomaly (e.g. showed very little biodegradation, which was not a consistent trend with the other time points for the same treatment and most likely due to a problem with the PAH internal standard used in quantification) and therefore eliminated. The degradation rates of all substrates was much slower in the winter and no significant differences in rates between with and without dispersant was obvious until the final sampling point, when it appeared that dispersant might have had a negative impact on degradation (Table 6 and Figure 5.3, Appendix 5).

Overall the results suggest that especially in winter, dispersant had a positive effect on hydrocarbon degradation, most notably with the alkane fraction. In the summer, conditions appeared to be more conducive to degradation such that degradation rates of the three hydrocarbon fractions were not largely affected by the presence of dispersant. In particular, at the Thebaud site, possibly due to the lower molecular weight of the substrates (gas condensate) and hence their bioavailability, degradation rates in the summer were very fast and not impacted by the presence of dispersant. In contrast to a recently published study (Kleindienst et al., 2015) that suggested that dispersants had a negative impact on the hydrocarbon-degrading activity of indigenous bacteria, we did not see a clear negative impact of dispersant, especially on alkane degrading bacterial activity at any of the three study sites.

6.4 Metagenomic Analysis

6.4.1 Bacterial Population Dynamics

Total community DNA, extracted from the filters (used to filter the initial seawater or the microcosm water following treatment) was analyzed using shotgun metagenomic sequencing.

The list of sample identities that were analyzed along with their origin, treatment and harvest time is presented in Appendix 6. A list of the samples that were sequenced, along with their sequencing statistics, is presented in Appendix 7.

This was performed on the initial water samples collected from each of the three sites (Hibernia, Terra Nova and Sable (Thebaud)) for both the summer and winter missions, in addition to microcosm treated samples for each site at both times. The metagenomic analysis provided a detailed characterization of the microbial community structure in the water initially and following exposure to oil with and without dispersant under ambient seawater temperatures. This analysis enabled us to determine how the different treatments affected the community structure. An initial study was conducted using the sequencing of 16S RNA gene amplicons (prokaryotic taxonomic target gene) from the three sites in comparison with metagenomic sequencing (Fig. 13). The results were similar for both analyses, showing a dominance of *Gammaproteobacteria*, *Alphaproteobacteria* and *Flavobacteria* (*Bacteroidetes*) in all the samples, but the metagenomic sequencing revealed a greater taxonomic depth, allowing us to identify more of the lower abundance taxa.

The microbial community structure in the initial seawater at each sampling location is presented in the top left panel in each of the following three figures (Figs. 14-16). The initial samples had a very diverse microbial population with little in the way of dominant phyla, as shown by the low percentage of reads in the major phyla detected, and many representative organisms detected at very low densities. The middle vertical panels show the microbial community structures in seawater incubated with nutrients (BH) and oil for 5 (summer), 7 (winter) and 42 days (summer and winter). The right vertical panels show seawater incubated with nutrients and oil plus dispersant for the same time periods.

At the shorter incubation times (5 and 7 days, summer and winter, respectively) in Hibernia seawater microcosms, the genus *Thalassolituus* becomes dominant only in the presence of dispersant, and then after 42 days is almost undetectable (Fig. 14). The hydrocarbon degrader genera *Colwellia, Alcanivorax* and *Pseudoalteromonas* are also dominant organisms early, and *Alcanivorax* dominated the community structure after 42 days in the presence of oil alone or with dispersant.

In the Terra Nova microcosms, in the summer (5 days) *Glaciecola* and *Alteromonas* were dominant genera, unlike Hibernia in oil alone and oil with dispersant (Fig. 15). The other oil degrading genera were also present (*Colwellia*, *Pseudoalteromonas* and *Alcanivorax*) and again, after 42 days incubation, *Alcanivorax* became the dominant genus in both treatments.

In the Thebaud seawater, after 5 days of incubation (summer) *Thalassolituus* and *Alteromonas* were present, with the former being a very dominant genus in the presence of dispersant (Fig. 16). After 42

days of incubation, *Alcanivorax* was a dominant genus, as well as *Cycloclasticus*, a well-known aromatic hydrocarbon degrader (Kasai et al. 2002).

There was a clear succession of bacterial genera during the incubations with *Colwellia*, *Pseudoalteromonas, Thalassolituus* and *Alteromonas* seen early, and replaced almost entirely by *Alcanivorax* later in the incubation.

6.4.2 Comparative Metabolic Dynamics

In-depth comparative metagenomic analysis was conducted on the samples listed in Appendices 6 and 7. The initial focus was to examine overall metabolic pathway gene frequency, an indication of the overall activity increase of general metabolic pathways associated with increased gene abundance. This general analysis provided information on which microorganisms were responding to the oil and dispersant, in particular. The heatmaps presented in Figures 17-20 show a comparison of gene abundance at the time the water was collected (time = 0) and after 5 days (summer) or 7 days (winter) incubation of the water in the presence of oil and dispersant. It was clear from the results (Fig. 17) that members of the orders *Alteromonadales, Oceanospirillales, Rhodobacterales* and *Pseudomonadales* were the most responsive to the oil and dispersant in the summer at the Hibernia site. These four orders are rich in known hydrocarbon degrading bacteria, and in fact, the order *Oceanospirillales* became the dominant bacterial order in the Gulf of Mexico shortly after the Deepwater Horizon accident (Dubinsky et al. 2013; Hazen et al. 2010; Mason et al. 2012; Redmond and Valentine 2012; Yang et al. 2014).

A more comprehensive analysis of the individual sites (Hibernia, Terra Nova and Thebaud) in the summer and winter is shown in Figures 18-20. In these cases, the data have been trimmed to show only the highest gene frequency differences and again it can be noted that at all sites, it is the *Alteromonadales* and *Oceanospirillales* that are demonstrating the greatest gene frequencies increases, both under summer and winter conditions, with the overall gene frequencies being higher in the summer than in the winter.

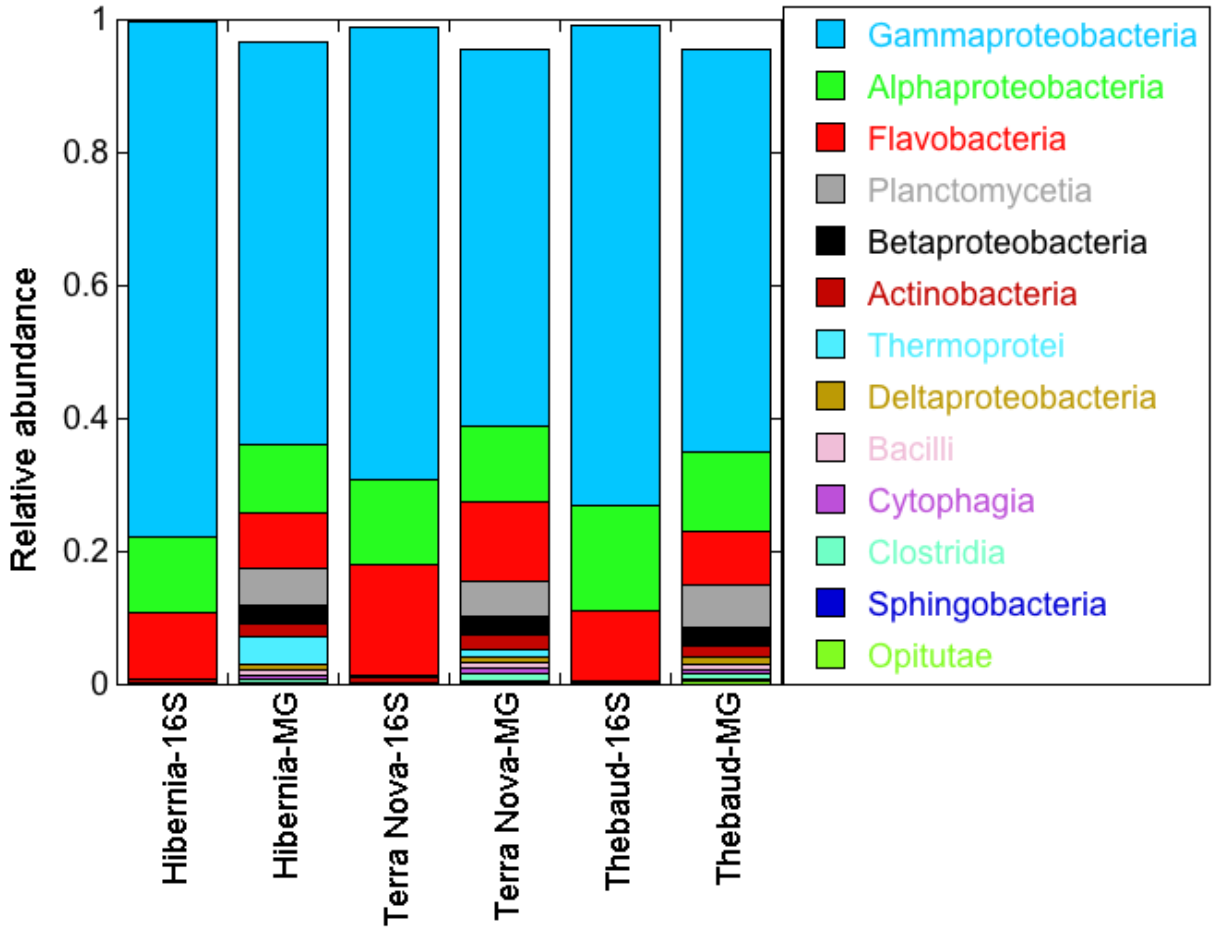

Figure 13: Initial comparative analysis evaluating the sequencing of 16S rRNA gene amplicons (16S) in comparison to shotgun metagenomics (MG) for the initial seawater from the 3 sampling locations, Hibernia, Terra Nova and Thebaud (Sable).

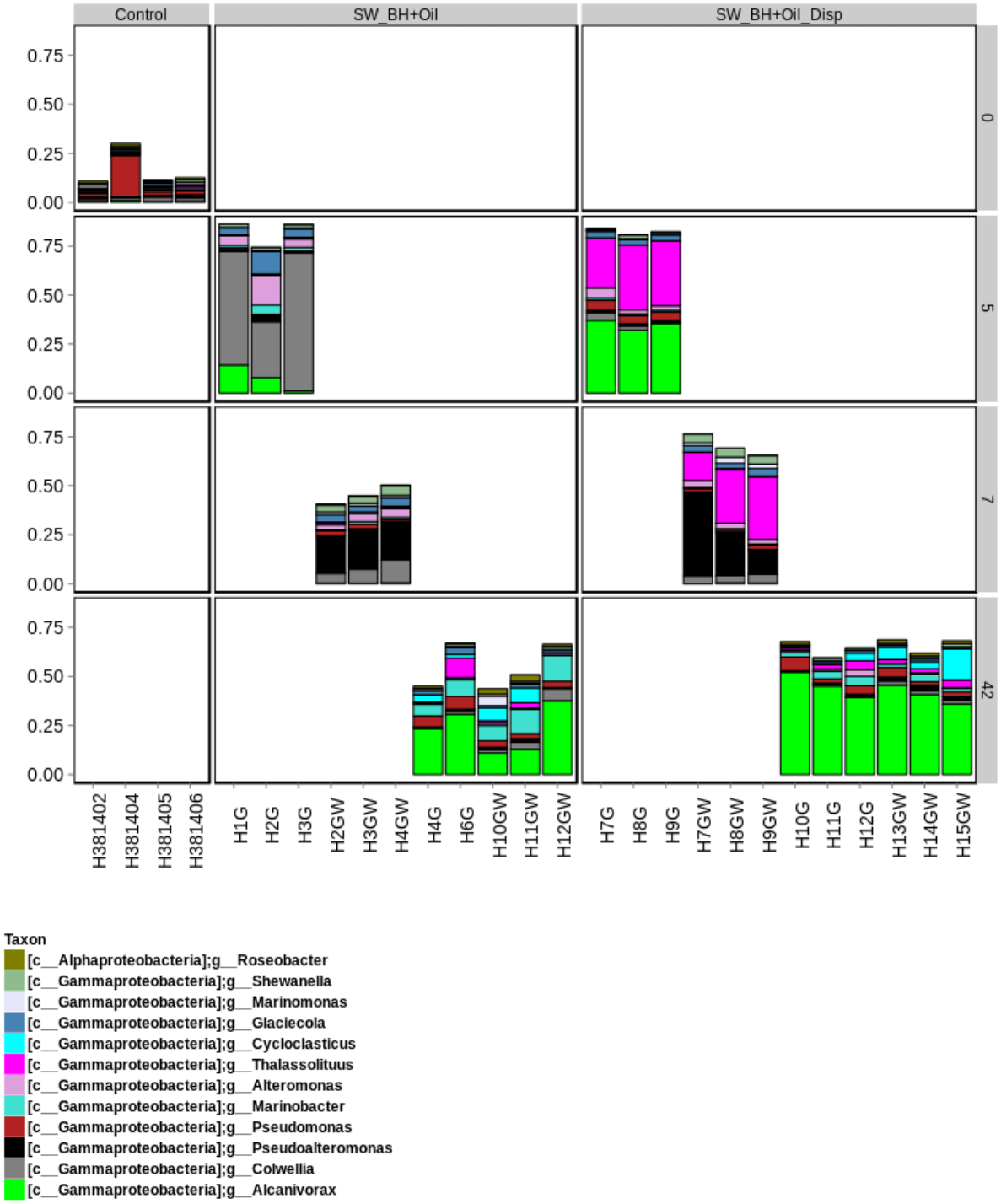

Figure 14: Shotgun metagenomic analysis of the major taxa in the microbial community from Hibernia in summer or winter (suffix 'W' on sample identification on x-axis) in the initial seawater (control - top left panel) followed by changes in the community composition following microcosm treatment with oil (middle vertical panels) or oil with dispersant (right vertical panels). The time of sacrificing (days) of the microcosms in presented on the y-axis (right).

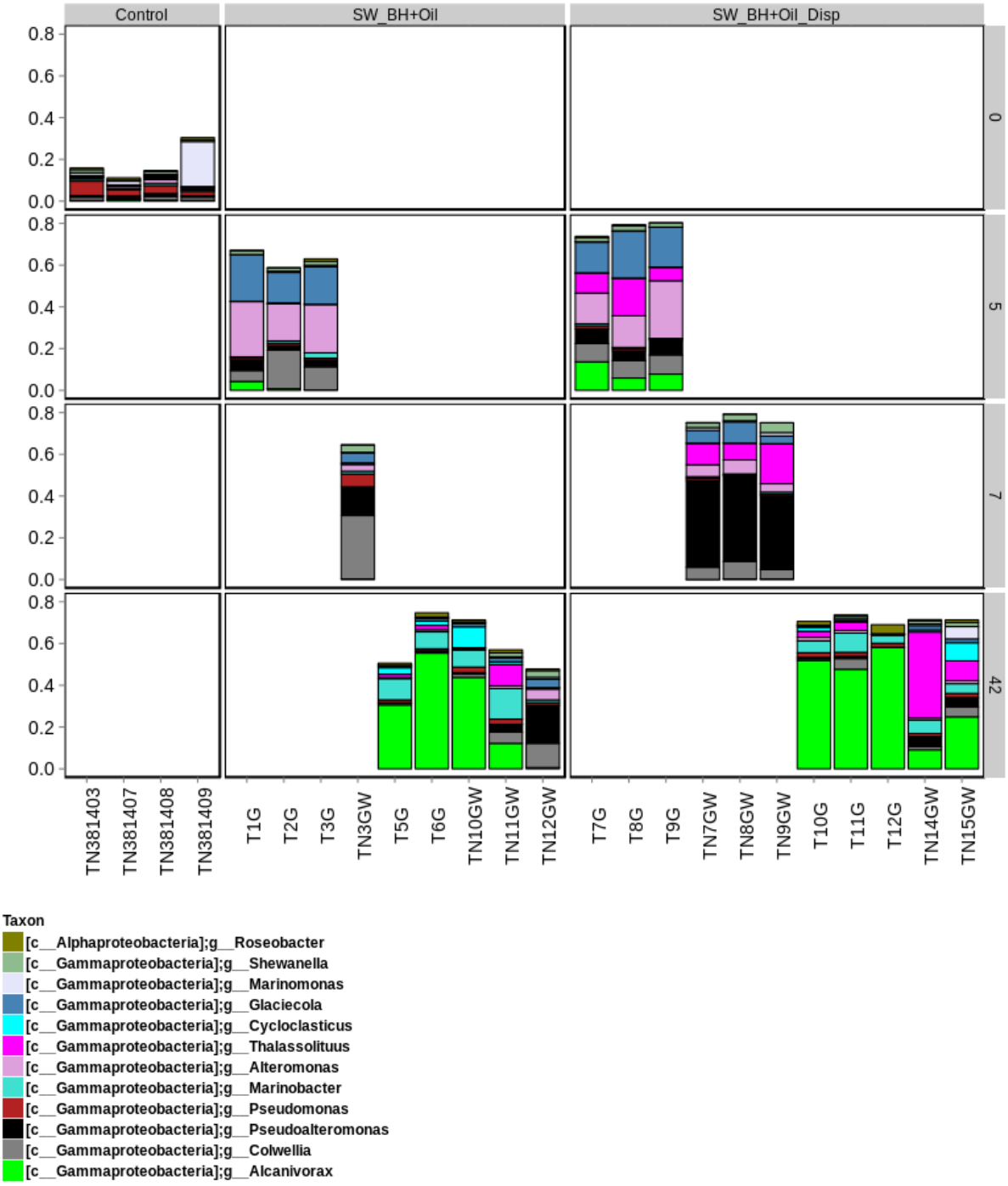

Figure 15: Shotgun metagenomic analysis of the major taxa in the microbial community from Terra Nova in summer or winter (suffix 'W' on sample identification on x-axis) in the initial seawater (control - top left panel) followed by changes in the community composition following microcosm treatment with oil (middle vertical panels) or oil with dispersant (right vertical panels). The time of sacrificing (days) of the microcosms in presented on the y-axis (right).

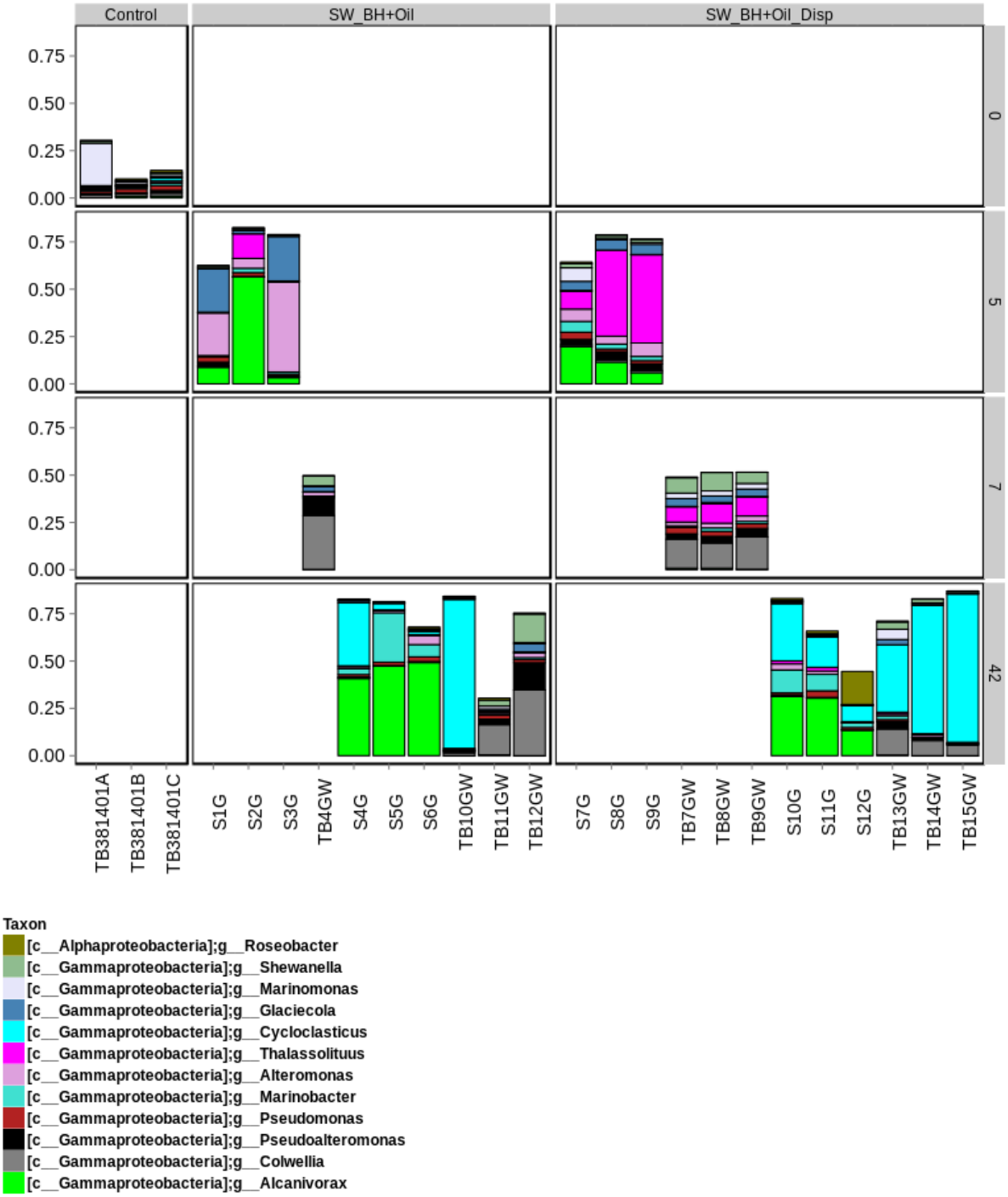

Figure 16: Shotgun metagenomic analysis of the major taxa in the microbial community from Thebaud (Sable) in summer or winter (suffix 'W' on sample identification on x-axis) in the initial seawater (control - top left panel) followed by changes in the community composition following microcosm treatment with oil (middle vertical panels) or oil with dispersant (right vertical panels). The time of sacrificing (days) of the microcosms in presented on the y-axis (right).

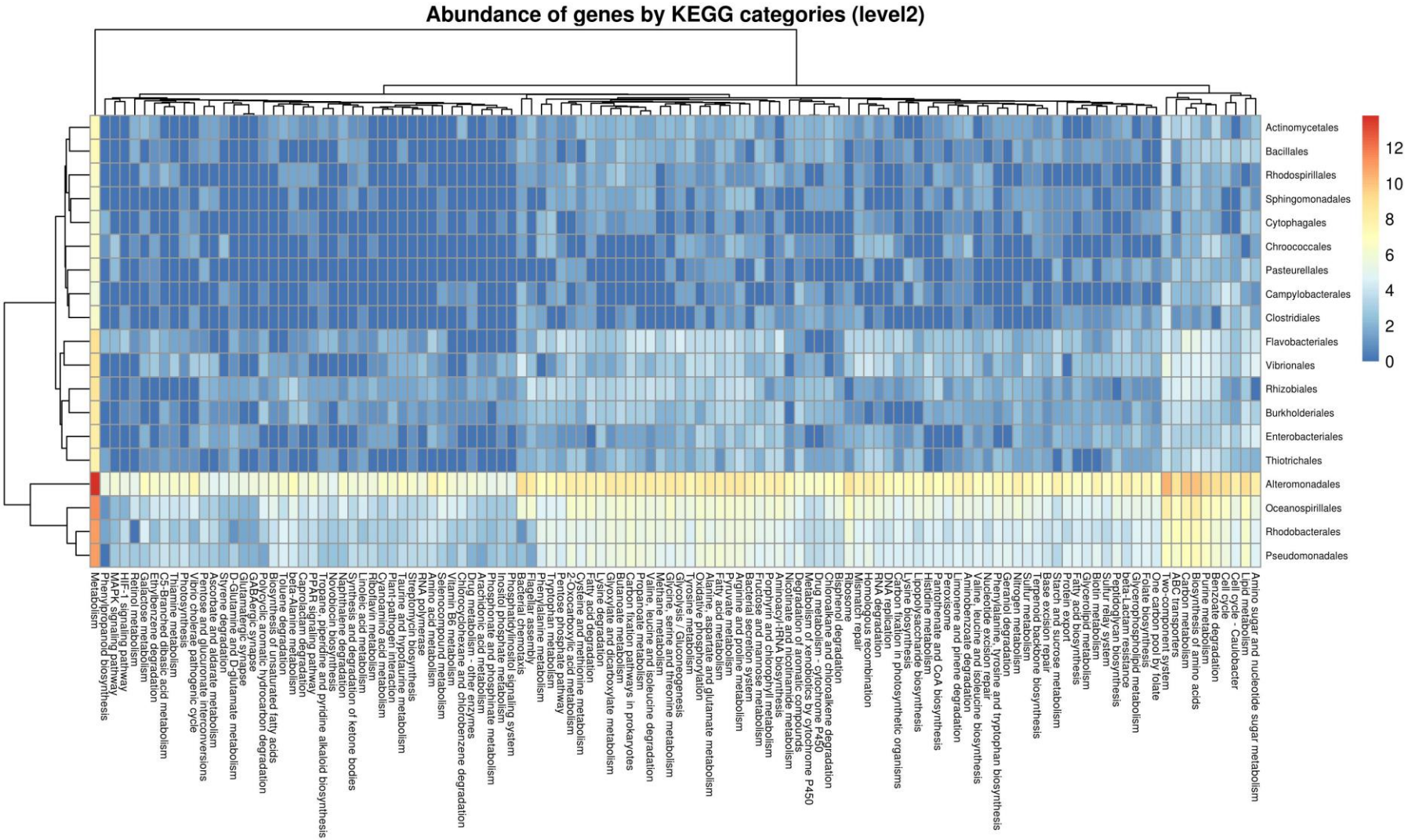

Figure 17: Comparative metagenomic analysis of microbial community dynamics from Hibernia summer samples. Results show the occurrence (log_2 transformed) of the frequency of metabolic genes by KEGG pathways, binned by Order and comparing 5 days of microcosm incubation with oil and dispersant against time zero. Results have been trimmed to the pathways showing the greatest increases in gene frequency (log fold-change ≥ 1.5).

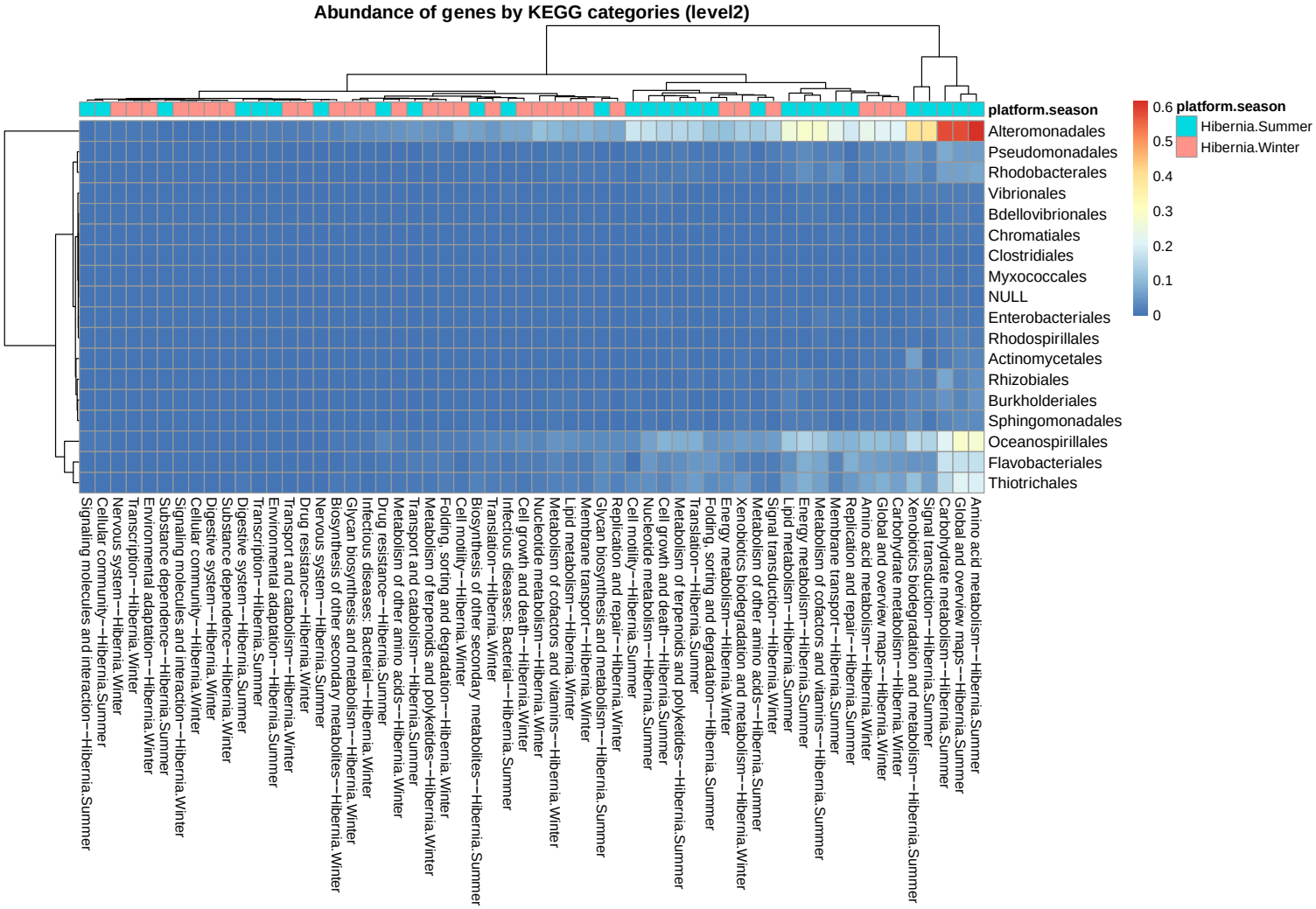

Figure 18: Comparative metagenomic analysis of microbial community dynamics from Hibernia summer and winter samples. Results show the occurrence (log_2 transformed) of the frequency of metabolic genes by KEGG pathways, binned by Order and comparing 5 days (summer) or 7 days (winter) of microcosm incubation with oil and dispersant against time zero. Results have been trimmed to the pathways showing the greatest increases in gene frequency (log fold-change ≥ 4).

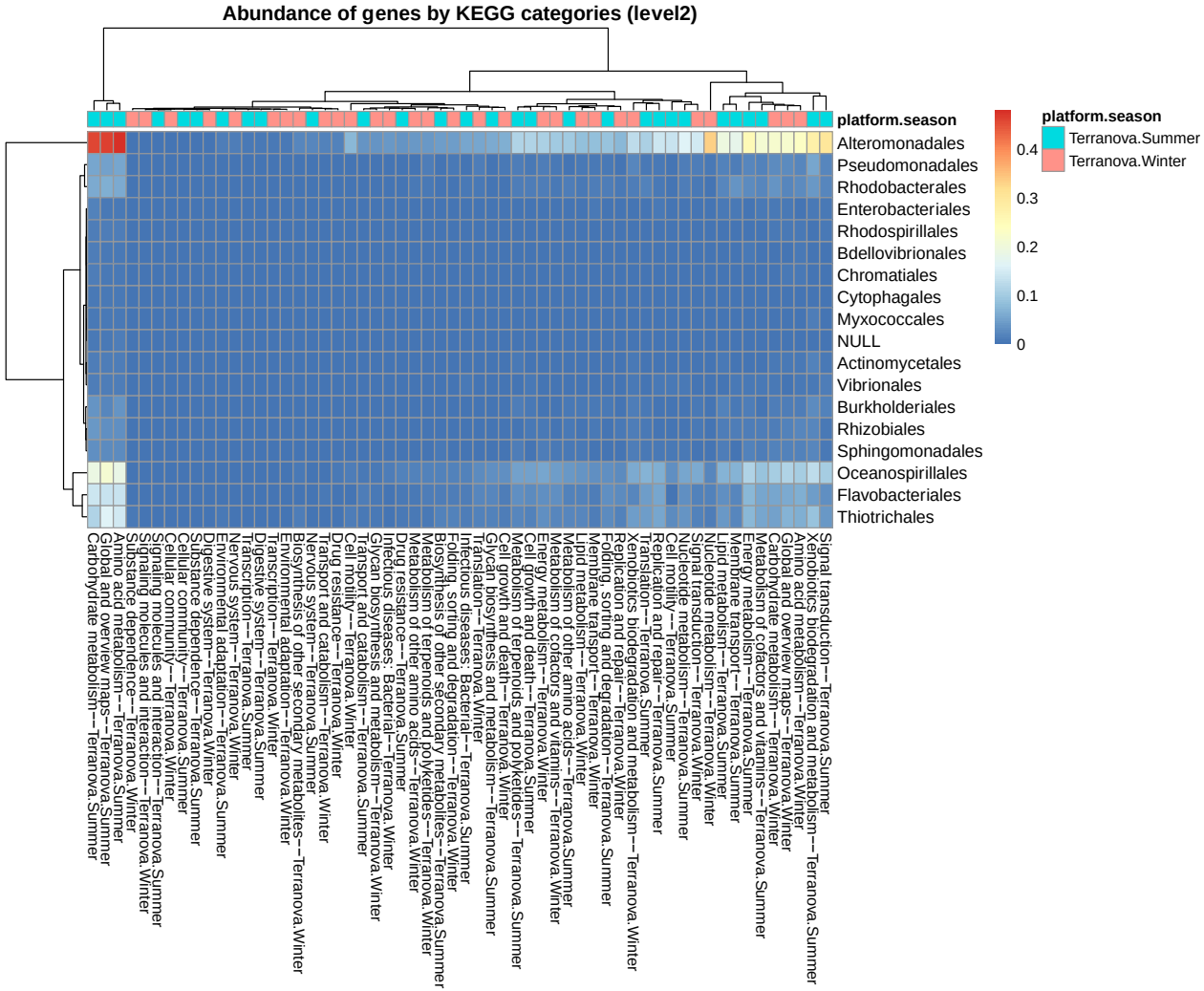

Figure 19: Comparative metagenomic analysis of microbial community dynamics from Terra Nova summer and winter samples. Results show the occurrence (log_2 transformed) of the frequency of metabolic genes by KEGG pathways, binned by Order and comparing 5 days (summer) or 7 days (winter) of microcosm incubation with oil and dispersant against time zero. Results have been trimmed to the pathways showing the greatest increases in gene frequency. (log fold-change ≥ 4).

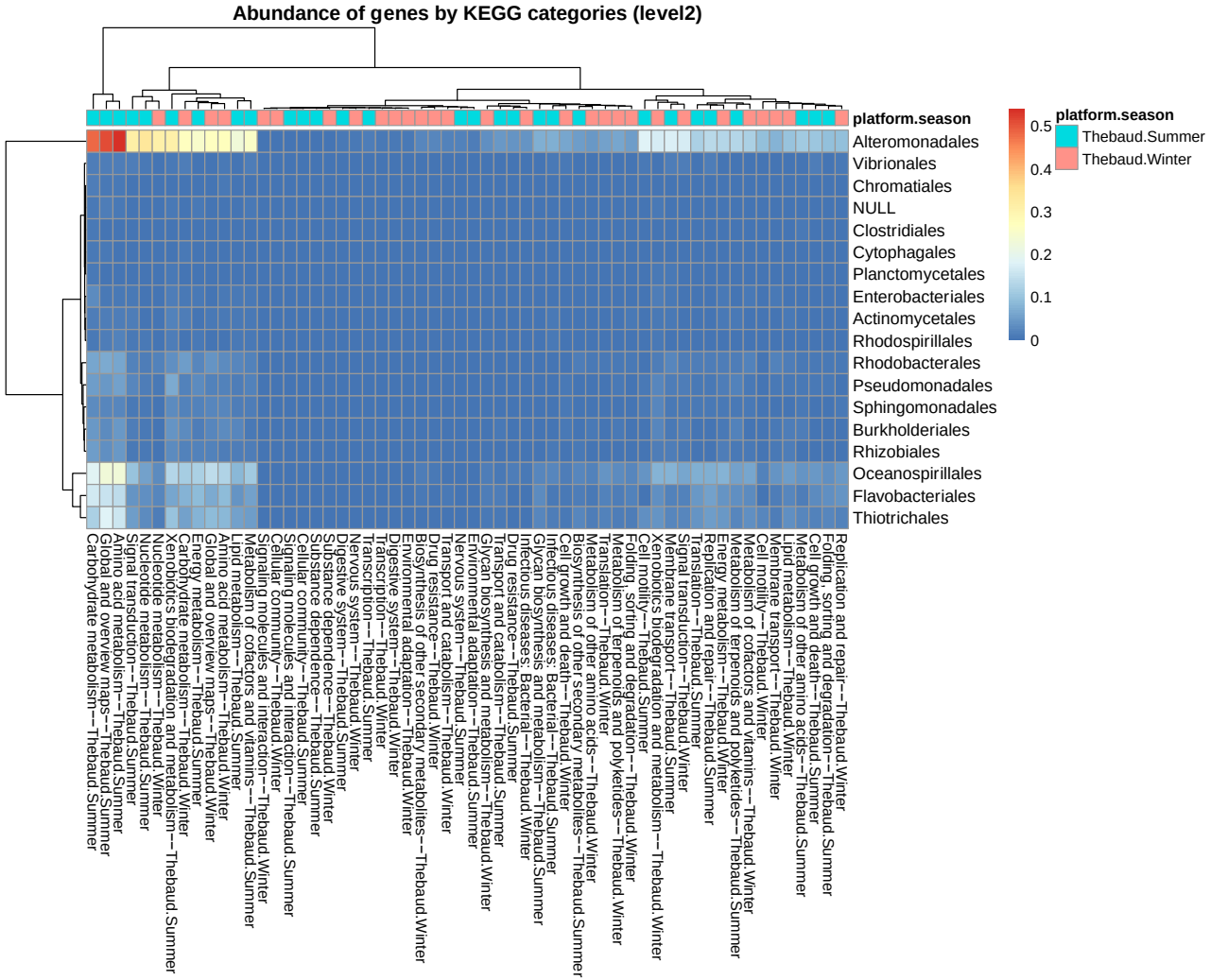

Figure 20: Comparative metagenomic analysis of microbial community dynamics from Thebaud (Sable) summer and winter samples. Results show the occurrence (log_2 transformed) of the frequency of metabolic genes by KEGG pathways, binned by Order and comparing 5 days (summer) or 7 days (winter) of microcosm incubation with gas condensate and dispersant against time zero. Results have been trimmed to the pathways showing the greatest increases in gene frequency (log fold-change ≥ 4).

6.5 Metatranscriptomic Analysis

6.5.1 Hydrocarbon Metabolism

Metatranscriptomic analysis of alkane 1-monooxygenase genes, key genes in the initial degradation of alkanes, for all three locations in both summer and winter for the different treatments demonstrated a strong up-regulation of the gene in the presence of oil alone or with dispersant (Fig. 21). The higher expression levels of these genes were particularly strong in the summer but certain bacteria were also quite active in the winter. Most of the up-regulated genes were associated with the genera *Marinobacter* and *Alcanivorax* of the *Alteromonadales* and *Oceanospirillales* orders, respectively. This correlates well with the observed higher activity levels of these two orders in the whole metabolic profile data, and shows a strong relationship between these particular bacteria and the oil degradation that was observed at these sites, as has been observed in other recent studies (Brakstad et al. 2015). The results indicate that these two bacterial genera are largely responsible for the degradation of the alkane hydrocarbon fraction in all the sites offshore of eastern Canada.

More detailed results of the alkane-1-monooxygenase expression at each location (Hibernia, Terra Nova or Thebaud) are presented in Figures 8-1 to 8-3 in Appendix 8. In these results only the most highly expressed representatives are shown, thereby limiting the analysis to only the most important alkane degraders present at each location. The results emphasize that *Marinobacter* and *Alcanivorax* are clearly the most important alkane degraders at all three locations both in the summer and the winter.

In addition to alkane degradation, genes for aromatic hydrocarbon degradation were also targeted for analysis. These included naphthalene dioxygenase, the first enzyme in the naphthalene degradation pathway, a key/central polycyclic aromatic hydrocarbon. Also, cytochrome P450, which is involved in the degradation of both alkane and aromatic hydrocarbons, in addition to the ring hydroxylases/dioxygenases, which are also key genes in polycyclic aromatic hydrocarbon degradation, were targeted for detailed analysis.

There were numerous up-regulated naphthalene dioxygenase genes identified at all three sampling sites (Fig. 22). The most dominant of these genes were represented by *Alcanivorax*, *Thalassolituus*, *Cycloclasticus, Alteromonas* and *Marinobacter* and gene variants were present mainly in the summer at the three sites, but occasional presence of the *Alcanivorax* genes was noted in the winter primarily at the Hibernia site. A more detailed analysis of the most highly expressed naphthalene dioxygenase genes at each sampling site is presented in Figs. 8-4 to 8-6 in Appendix 8.

Analysis of the cytochrome P450 genes from each of the sites showed that *Cycloclasticus* produced by far the most dominant form of this gene both in the summer and winter (Fig. 23). Versions of this gene produced by other bacteria were also detected, but these tended to be more sporadic across all the sites and seasons. A more detailed analysis of the most up-regulated cytochrome P450 genes, presented for each individual site (Hibernia, Terra Nova and Thebaud) is presented in Figs. 8-7 to 8-9 in Appendix 8.

The last category of aromatic hydrocarbon degrading genes examined was the ring-hydroxylases/dioxygenases. The up-regulated versions of this gene was dominated by *Alcanivorax*,

however, the most up-regulated version was produced by a *Streptomyces* (Fig. 24). The *Streptomyces* were present at all three locations and in both the summer and winter and this gene was up-regulated under a variety of incubation conditions, but most significantly in the presence of oil with or without dispersant. *Streptomyces* are known to produce a variety of important enzymes, including those that can modify aromatic compounds. Again, a more detailed analysis of the most up-regulated ring hydroxylase/dioxygenases from each of the individual sites is presented in Figs. 8-10 to 8-12 in Appendix 8.

6.5.2 Nitrogen Metabolism

In order for bacteria to metabolize and grow using hydrocarbons as a carbon source they also require other key nutrients, such as nitrogen. Nitrogen is part of many cellular macromolecules such as the nucleic acids and proteins, without which life would not be possible. When bacteria are degrading hydrocarbons, a supply of nitrogen is necessary, which could come from a variety of organic or inorganic sources. Nitrate and ammonia are the most easily accessible forms of inorganic nitrogen although some bacteria do possess the ability to use atmospheric nitrogen (nitrogen-fixation).

In this study, we examined the metatranscriptomic dataset for genes that are involved in nitrogen metabolism to determine if the same bacteria that were up-regulating their hydrocarbon degradation pathway genes were also up-regulating their nitrogen metabolism pathways (Fig. 25). The same genera that were expressing their hydrocarbon degradation genes more highly in the presence of oil with and without dispersant, such as *Alcanivorax*, *Marinobacter* and *Cycloclasticus,* were also up-regulated for nitrogen metabolism genes.

These results, combined with the overall metabolism and hydrocarbon degradation profiles observed at all three sites indicate that species of *Alcanivorax*, *Marinobacter* and *Cycloclasticus* are the key hydrocarbon degraders in the marine offshore environment of eastern Canada, and that they are present and active at different times of the year. Knowing that these specific bacteria are the key players in oil degradation in this marine environment provides further clues into what types of conditions might be used to enhance their in situ oil degrading activity.

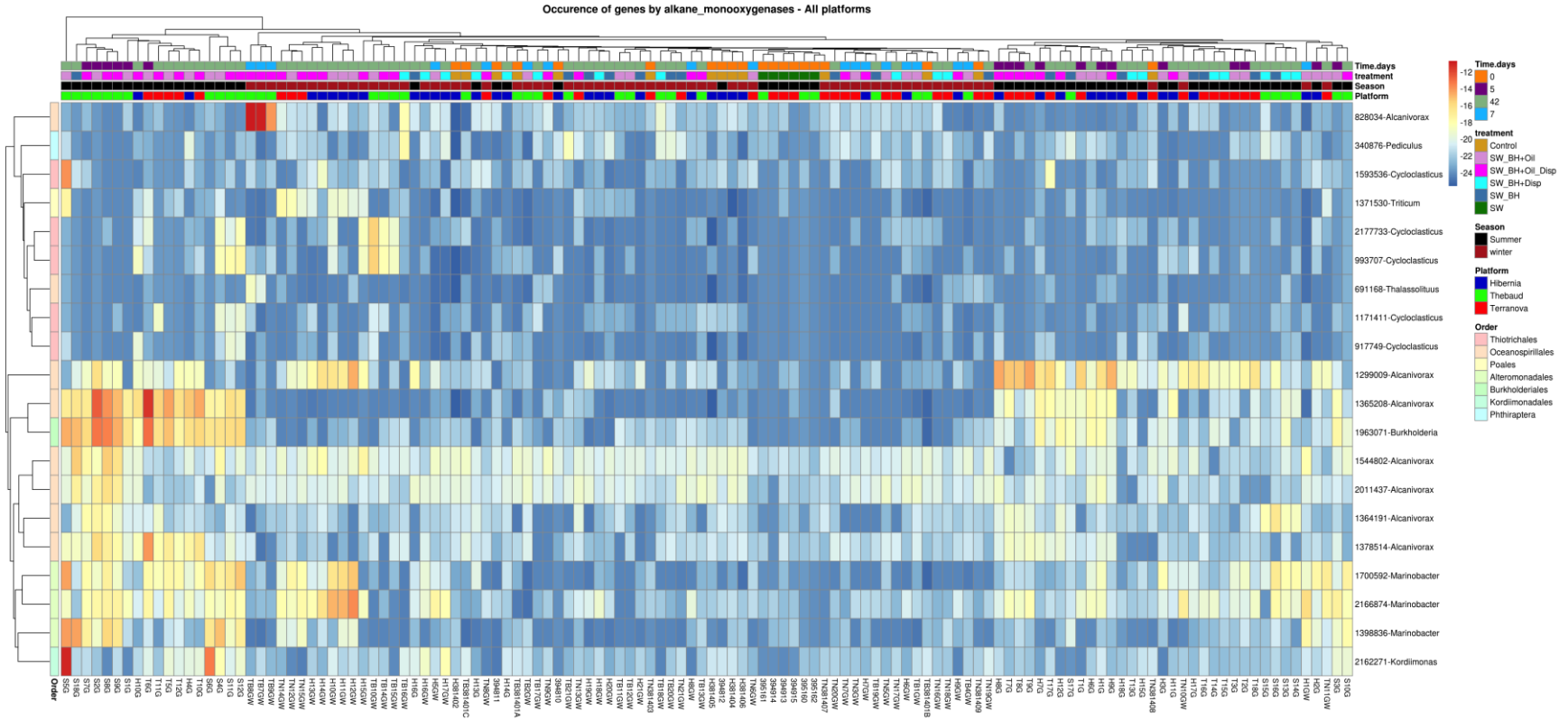

Figure 21: Metatranscriptomic analysis of all three sites (Hibernia, Thebaud (Sable), Terra Nova) showing up-regulation of alkane 1-monooxygenases, a key gene in alkane degradation. The colored horizontal bars along the top of the heatmap provide a color-key for the three sites (lowest bar), followed by sampling season, then microcosm treatment and finally time of microcosm sacrificing (days), as presented on the right side of the heatmap. The identities/producers of the individual alkane 1-monoxygenases is shown on the right y-axis, while sample identities are shown on the x-axis. Results have been trimmed to show only the most up-regulated pathways (log fold-change ≥ 3). Cell color intensity represents log_2 transformed gene expression values to enhance visual contrast.

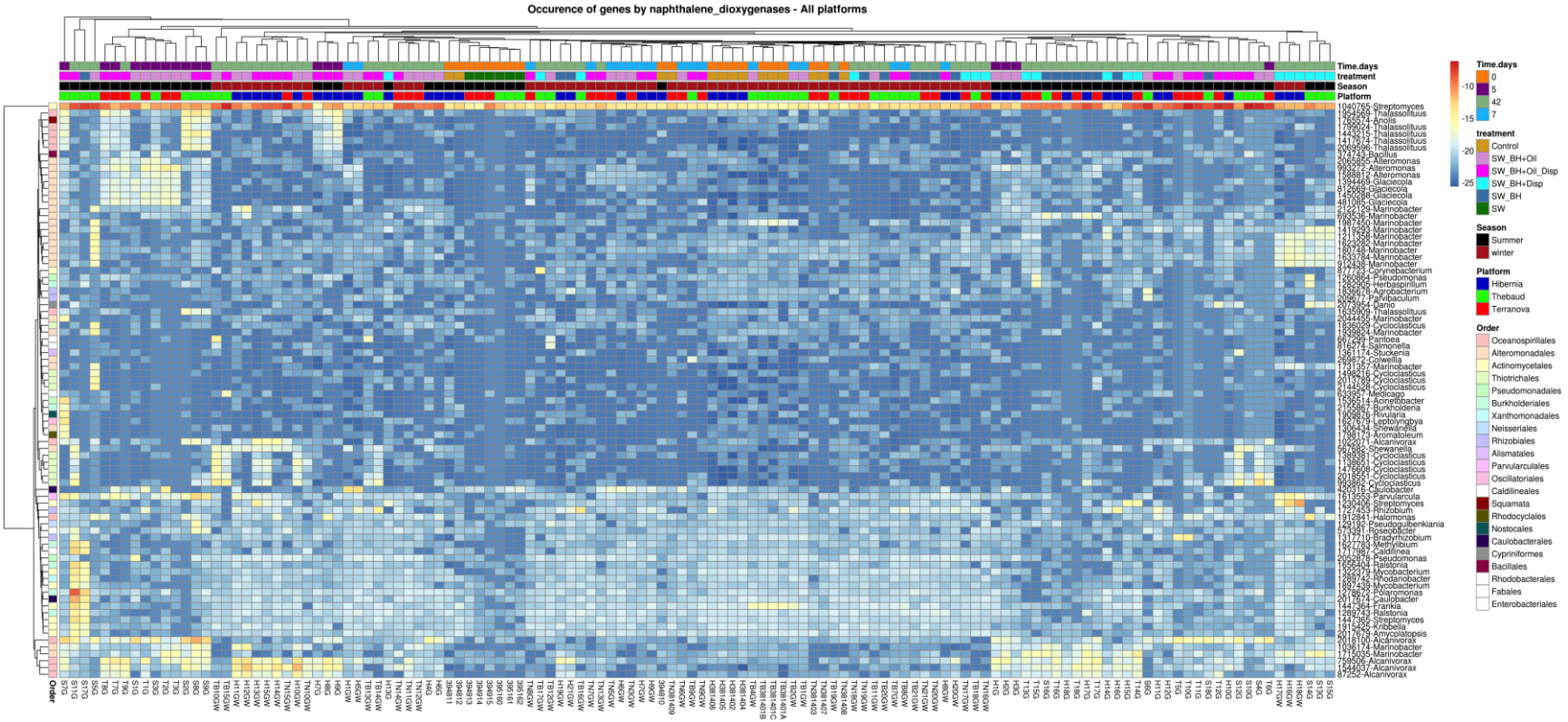

Figure 22: Metatranscriptomic analysis of all three sites (Hibernia, Thebaud (Sable), Terra Nova) showing up-regulation of naphthalene dioxygenases, a key gene in low molecular weight PAH degradation. The colored horizontal bars along the top of the heatmap provide a color-key for the three sites (lowest bar), followed by sampling season, then microcosm treatment and finally time of microcosm sacrificing (days), as presented on the right side of the heatmap. The identities/producers of the individual naphthalene dixygenases is shown on the right y-axis, while sample identities are shown on the x-axis. Results have been trimmed to show only the most up-regulated pathways (log fold-change ≥ 4). Cell color intensity represents log_2 transformed gene expression values to enhance visual contrast.

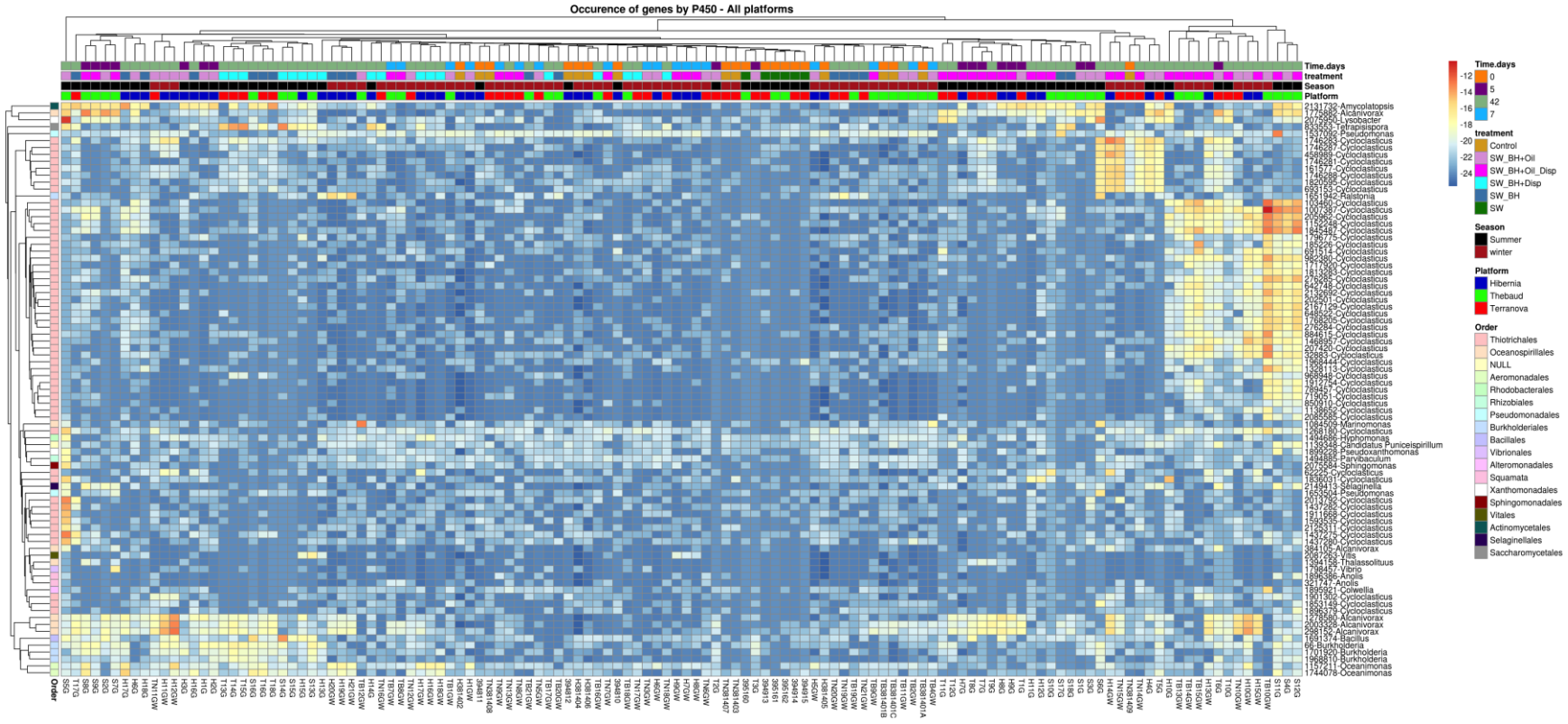

Figure 23: Metatranscriptomic analysis of all three sites (Hibernia, Thebaud (Sable), Terra Nova) showing up-regulation of P450 monooxygenases, a key gene involved in hydrocarbon degradation. The colored horizontal bars along the top of the heatmap provide a color-key for the three sites (lowest bar), followed by sampling season, then microcosm treatment and finally time of microcosm sacrificing (days), as presented on the right side of the heatmap. The identities/producers of the individual P450 genes is shown on the right y-axis, while sample identities are shown on the x-axis. Results have been trimmed to show only the most up-regulated pathways (log fold-change ≥ 3). Cell color intensity represents log_2 transformed gene expression values to enhance visual contrast.

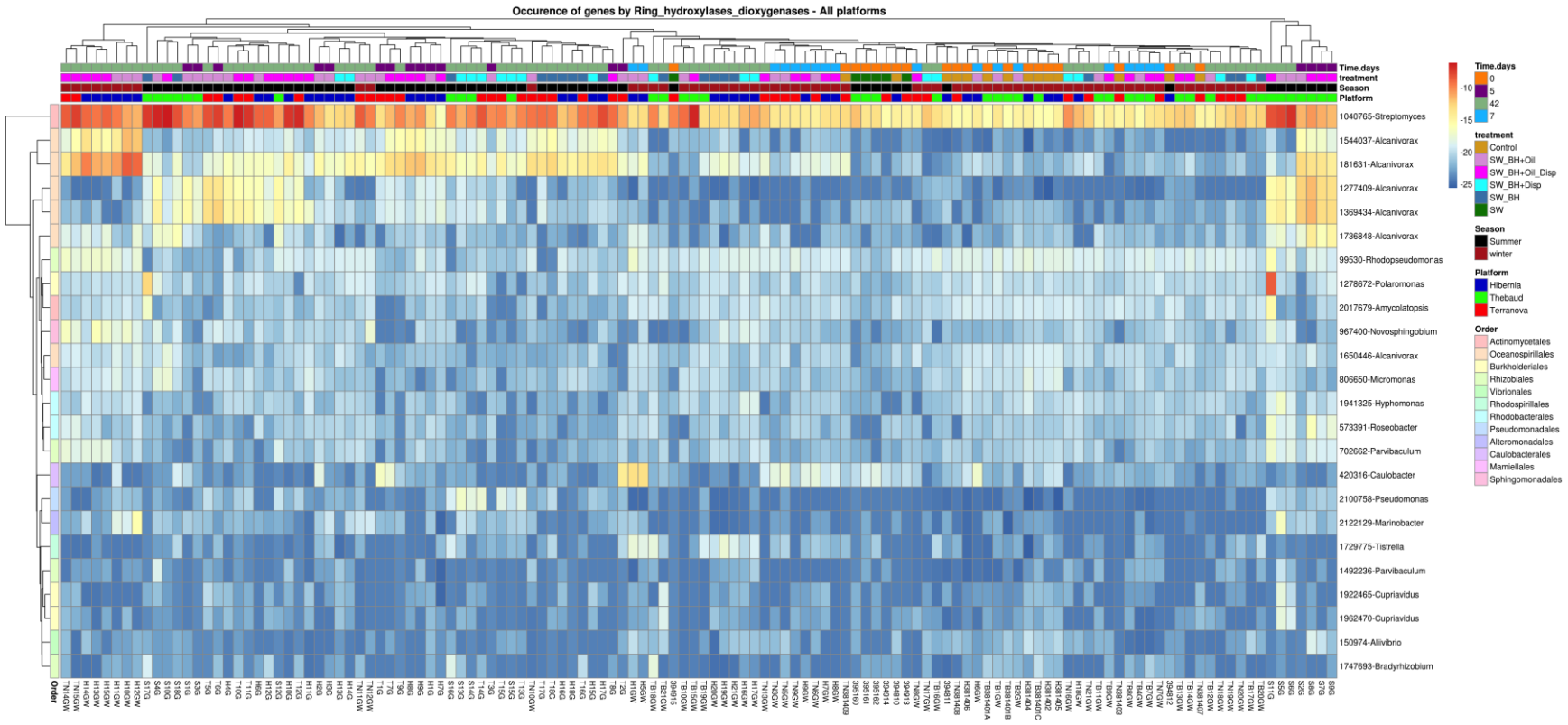

Figure 24: Metatranscriptomic analysis of all three sites (Hibernia, Thebaud (Sable), Terra Nova) showing up-regulation of ring hydroxylases/dioxygenases, key genes involved in aromatic hydrocarbon degradation. The colored horizontal bars along the top of the heatmap provide a color-key for the three sites (lowest bar), followed by sampling season, then microcosm treatment and finally time of microcosm sacrificing (days), as presented on the right side of the heatmap. The identities/producers of the individual ring hydroxylase/dioxygenase are shown on the right y-axis, while sample identities are shown on the x-axis. Results have been trimmed to show only the most up-regulated pathways (log fold-change ≥ 3). Cell color intensity represents log_2 transformed gene expression values to enhance visual contrast.

Figure 25: Metatranscriptomic analysis of all three sites (Hibernia, Thebaud (Sable), Terra Nova) showing up-regulation of nitrogen cycle genes. The colored horizontal bars along the top of the heatmap provide a color-key for the three sites (lowest bar), followed by sampling season (summer, winter), then microcosm treatment and finally time of microcosm sacrificing (days), as presented on the right side of the heatmap. The first vertical bar on the heatmap at the left side identifies which Order is the origin of the nitrogen metabolizing gene identified on the right side of the heatmap. The identities/producers of the individual nitrogen metabolizing genes are shown on the right y-axis, sample identities are shown on the left y-axis and the x-axis has the sample identities. Results have been trimmed to show only the most up-regulated pathways (log fold-change ≥ 3). Cell color intensity represents log_2 transformed gene expression values to enhance visual contrast.

7.0 Conclusions

The present study evaluated the natural attenuation ability of indigenous microbial communities adjacent of offshore eastern Canada oil and gas installations (Hibernia, Terra Nova and Thebaud) to biodegrade oil in the absence and presence of dispersant at two different times (summer and winter). A combination of several techniques was used to evaluate microbial presence and activity, including respirometry and microcosms incubated under ambient conditions at the time of seawater sampling, in addition to chemical and genomic analyses.

Seawater from the Hibernia and Terra Nova sites were effective at degrading crude oil hydrocarbons in the summer (13 °C) as well as the winter (6-7 °C) and degradation kinetics were similar for these two sites. Degradation rates were up to seven times faster for alkanes in the summer, at both sites, than they were in the winter. The positive effects of dispersant on crude oil biodegradation were most apparent in the winter: although slight rate increases were observed for alkane degradation in the summer, at both sites, the biodegradation rate for the alkane fraction was almost 3 times higher in the winter in comparison to without dispersant. The biodegradation of PAHs and Alkylated PAHs was typically two to three times faster in the summer in comparison to the winter and dispersant appeared to have only a slight effect on the biodegradation rates under the same seasonal conditions. Although the data were quite variable, the degradation rate for PAHs and Alkylated PAHs may have decreased somewhat in the presence of dispersant in both the summer and winter, especially at the Hibernia site.

Biodegradation of the alkane fraction in gas condensate, using seawater from the Thebaud site, was extremely fast in the summer, but more than 4 times slower in the winter. It appears that dispersant had a negative impact on the biodegradation of the chemical fractions (alkanes, PAHs and Alkylated PAHs) associated with gas condensate in the winter, but in general, degradation rates were so fast in the summer that differences between with and without dispersant were not evident. There was no clear effect of dispersant on degradation of any of the fractions in the winter for most of the incubation period, although the last sampling point suggested that dispersant might have a slight negative impact.

Dispersant (Corexit 9500) had the most obvious positive impact on alkane degradation in the crude oil, especially in the winter when conditions were possibly less conducive for biodegradation. It is possible that factors, other than temperature and dispersant, such as seasonal variations (e.g. oceanographic conditions related to ocean productivity, availability of nutrients, etc.) are clearly contributing to the observed biodegradation rates. It is also clear that the use of dispersants to address oil spills on a large scale remains quite controversial (Prince, 2015) and a recent study has suggested that dispersant may actually be suppressing hydrocarbon degradation (Kleindienst et al. 2015).

The microbial community structures (metagenomic profile) from the three sites were examined prior to and following incubation with oil alone or with dispersant. The presence of the oil alone caused considerable shifts in the microbial community structure, with known hydrocarbon degrading genera (many from the *Gammaproteobacteria*), becoming predominant after only a few days and persisting for the entire incubation period (42 days), although there were differences in the population members between the short and longer incubation times. The inclusion of dispersant with the oil resulted in

similar but distinctive shifts in the microbial community structure. With the dispersant other *Gammaproteobacteria* became dominant, especially during the early stages of the incubation period, and again later in the incubation other hydrocarbon degrading bacterial genera became dominant. There was clearly a succession of bacterial taxa over time during the incubation, something that would likely be occurring in situ, and was observed previously during the monitoring of the Deepwater Horizon blowout (Dubinsky et al. 2013; Gutierrez et al. 2013; Hazen et al. 2010; Mason et al. 2012; Redmond and Valentine, 2012; Yang et al. 2014). Of interest were differences between the three sites with respect to the succession of bacterial taxa: different genera with different hydrocarbon degradation potentials being predominant in either the early stages or the late stages of microcosm incubation.

The activity of the microbial population (metagenomics profile) was evaluated by looking at the frequencies of genes in the overall metabolism (combined metabolic pathways) and by targeting specific key genes (metatranscriptomics) involved in hydrocarbon degradation (alkane monooxygenases, naphthalene dioxygenases, cytochrome P450 oxygenases, ring hydroxylases/dioxygenases) or other cellular processes (nitrogen metabolism). There was a substantial increase in metabolic gene frequencies with several key orders of bacteria, notably the *Alteromonadales, Oceanospirillales, Rhodobacterales,* and *Pseudomonadales*, all of which are rich in hydrocarbon degrading bacteria, in the presence of oil/gas condensate with dispersant, indicating that these bacteria had responded positively to the presence of the oil/gas condensate and dispersant. The targeted key hydrocarbon degradation genes were up-regulated (metatranscriptomics) under these conditions, especially in genera such as *Marinobacter (Alteromonadales)* and *Alcanivorax (Oceanospirillales),* which were producing numerous variants of each of these target enzymes. The increased expression was observed at all the sites when the microbial population was exposed to oil/gas condensate alone or with dispersant, in both the summer and the winter, although up-regulation was considerably less in the winter. In addition to the increased expression of hydrocarbon degradation genes and increases in overall metabolic gene frequencies in these key orders of bacteria, it was also noted that nitrogen metabolism was increased. This is expected for these organisms, because in order to incorporate carbon from the hydrocarbons into their cellular macromolecules, nitrogen would also be required. This confirms that the actively metabolizing bacteria were degrading the hydrocarbons.

Overall the results demonstrate that the indigenous microbial populations in the marine environment in the areas of the Hibernia, Terra Nova and Thebaud (Sable) facilities possess hydrocarbon-degrading bacteria that respond positively to exposure to oil under ambient temperature conditions in the summer (13 °C) and winter (6-7 °C). Their population densities are typically quite low to non-detectable prior to oil exposure, but they did become dominant components of the total population when oil/gas condensate was present. This is possibly not entirely surprising, since some members of these bacterial groups are known obligate hydrocarbon degraders, meaning that the only substrates they can use are hydrocarbons. Under conditions where the substrates are not present these bacteria undergo modifications to conserve energy, such as dormancy. Under appropriate conditions when substrate is present and other conditions are favourable, they respond rapidly. The exposure to oil/gas condensate resulted in increased numbers and activity of known degrader genera of bacteria in addition to the increased expression of their hydrocarbon degradation genes.

Crude oil and gas condensate were rapidly degraded under summer conditions, but more slowly under winter conditions, with the alkane fraction being the most rapidly degraded. The presence of dispersant had a positive impact on the degradation kinetics, especially for the alkane fraction, and in the winter. The effect of dispersant on the degradation of PAHs and Alkylated PAHs was not as clear with slight enhancements in some cases and potential detrimental effects in other instances, but statistically significant results were less clear with these latter two substrates. Other oceanographic factors that will impact hydrocarbon degradation rates in situ will be nutrient availability (notably nitrogen and phosphorus), competition for nutrients, predation, temperature, etc. What has been demonstrated in this study is that natural populations of hydrocarbon degrading bacteria are present, in the offshore eastern Canada environment, and are responsive to inputs of oil or gas condensate. The evidence shows that natural attenuation and more specifically enhanced natural attenuation (e.g. nutrient and possibly dispersant application) is a potential oil spill strategy to increase the rate of natural biodegradation, especially alkanes under winter conditions, and possibly prevent the dispersion of oil to more vulnerable habitats.

Acknowledgements

The NRC and COOGER would like to thank Drs. Kenneth Lee (Commonwealth Science Industrial Research Organization (CSIRO) Australia; scientific advice), Simon Courtenay (DFO; project management), William Li (DFO; bacteria enumeration), Youyu Lu (DFO; project management), Haibo Niu (Dalhousie University; modelling work), and Yongsheng Wu (DFO; modelling work), Ms. Carol Anstey (DFO; nutrients), and Mr. Rod Doane (DFO; administrative support and editing) for their contributions to this study. We would also like to acknowledge Robert Dunphy (Hibernia Management Corporation), Trudy Wells (Suncor), Megan Tuttle (ExxonMobil) for the representative samples of crude oil and condensate and the Captain and Crew (Canadian Coast Guard Ship, Hudson) for their dedicated at sea support for both summer and winter cruises.

8.0 References

American Academy of Microbiology (2011) Microbes and Oil Spills.

Armstrong, F.A.J., Sterns, C.R., and Strickland, J.D.H.. (1967). The Measurement of Upwelling and Subsequent Biological Processes by Means of the Technicon Autoanalyzer and Associated Equipment. *Deep-Sea Res.*, *14,* 381-389.

Ausubel, F.M., Brent, R., Kingston, R.E., Moore, D.D., Seidman, J.G., Smith, J.A., and Struhl, K. **(**2002). *Short protocols in molecular biology: a compendium of methods, from 'Current protocols in molecular biology'* (5th ed). Wiley, New York.

Brakstad, O.G., Throne-Holst, M., Netzer, R., Stoeckel, D.M., and Atlas, R.M. (2015). Microbial communities related to biodegradation of dispersed Macondo oil at low seawater temperature with Norwegian coastal seawater. *Microbial. Biotechnol.* DOI: 10.1111/1751-7915.12303.

Cappello S., Caneso, G., Zampino, D., Monticelli, L., Maimone, G., Dnearo, R., Tripod, B., Troussellier, M., Yakimov, N., and Giuliano, L. (2007). Microbial community dynamics during assays of harbour oil spill bioremediation: a microscale simulation study. *J. Appl. Microbiol*., *102,* 184–194.

Cole, M., King, T., and Lee, K. (2007). Analytical technique for extracting hydrocarbons from water using sample container as extraction vessel in combination with a roller apparatus. *Canadian Technical Report of Fisheries and Aquatic Sciences, 2733,* 1-40.

Crompton, T.R. (ed). (2006). *Analysis of seawater: a guide for the analytical and environmental chemist*. Springer, New York.

Dubinsky, E. A., Conrad, M.E., Chakraborty, R., Bill, M., Borglin, S.E., Hollibaugh, J.T., Mason, O.A., Piceno, Y.M., Reid, F.C., and Stringfellow, W.T. (2013). Succession of hydrocarbon degrading bacteria in the aftermath of the Deepwater Horizon oil spill in the Gulf of Mexico. *Environ. Sci. Technol., 47,* 10860-10867.

Grasshoff, K., 1969. Technicon International Congress, June Technicon Industrial Systems, Tarrytown, New York, NY.

Gutierrez, T., Singleton, D.R., Berry, D., Yang, T., Aitken, M.D., and Teske, A. (2013). Hydrocarbon-degrading bacteria enriched by the Deepwater Horizon oil spill identified by cultivation and DNA-SIP. *ISME J., 7,* 2091-2104.

Hazen, T.C., Dubinsky, E.A., DeSantis, T.Z., Andersen, G.L., Piceno, Y.M., Singh, N., Jansson, J.K., Probst, A., Borglin, S.E., Fortney, J.L., Stringfellow, W.T., Bill, M., Conrad, M.E., Tom, L.M., Chavarria, K.L., Alusi, T.R., Lamendella, R., Joyner, D.C., Spier, C., Baelum, J., Auer, M., Zemla, M.L., Chakraborty, R., Sonnenthal, E.L., D'Haeseleer, P., Holman, H.Y.N., Osman, S., Lu, Z.M., Van Nostrand, J.D., Deng, Y., Zhou, J.Z., and Mason, O.U. (2010). Deep-Sea Oil Plume Enriches Indigenous Oil-Degrading Bacteria. *Science, 330,* 204-208.

Holm-Hansen, O., Lorenzen, C.J., Holmes, R.W., and Strickland, J.D.H. (1965). Fluorometric determination of chlorophyll. *J. Cons. Cons. Int. Expl. Mer., 30*, 3-15.

Kasai, Y., Kishira, H., and Harayama, S. (2002). Bacteria Belonging to the Genus *Cycloclasticus* Play a Primary Role in the Degradation of Aromatic Hydrocarbons Released in a Marine Environment. *Appl. Environ. Microbiol., 68*, 5623-5633.

Kerouel, R. and Aminot, A. (1997). Fluorometric determination of ammonia in sea and estuarine waters by direct segmented flow analysis. *Marine Chemistry, 57*, 265-275.

King, T., Robinson, B., McIntyre, C., Toole, P., Ryan, S., Saleh, F., Boufadel, M., and Lee, K. (2015). Fate of surface spills Cold Lake Blend diluted bitumen treated dispersant and mineral fines in a wave tank. *Environmental Engineering Science, 32(3),* 250-261.

Kleindienst, S., Seidel, M., Ziervogel, K., Grim, S., Loftis, K., Harrison, S., Malkin, S.Y., Perkins, M.J., Field, J., Sogin, M.L., Dittmar, T., Passow, U., Medeiros, P.M., and Joye, S.B. (2015). Chemical dispersants can suppress the activity of natural oil-degrading microorganisms. *Proc. Natl. Acad. Sci. USA* Doi/10.1073/pnas.1507380112.

Lee, K., Nedwed, T., and Prince, R.C. (2011). Biodegradation of Dispersed Oil in Marine Environments is Substantial and Rapid, and Not Significantly Limited by Either Oxygen, Nutrients or Temperature. *In Proceedings of the International Oil Spill Conference*, Paper # 245.

Li, W.K.W. and Dickie, P.M. (2001). Monitoring phytoplankton, bacterioplankton, and virioplankton in a coastal inlet (Bedford Basin) by flow cytometry. *Cytometry, 44,* 236-246.

Li, W.K.W. (2014). The state of phytoplankton and bacterioplankton on the Scotian Shelfand Slope: Atlantic Zone Monitoring Program 1997-2013. *Can. Tech. Rep. Hydrogr. Ocean. Sci., 303,* xx + 140 p

Li, W.K.W. and Harrison, W.G. (2014). The state of phytoplankton and bacterioplankton in the Labrador Sea: Atlantic Zone Off-Shelf Monitoring Program 1994-2013. *Can. Tech. Rep. Hydrogr. Ocean. Sci., 302,* xviii + 181 p.

Mason, O. U., Hazen, T.C., Borglin, S., Chain,P.S.G., Dubinsky, E.D., Fortney, J.L., Han, J., Holman, H.Y.N., Hultman, J., Lamendella, R., Mackelprang, R., Malfatti, S., Tom, L.M., Tringe, S.G., Woyke, T., Zhou, J., Rubin, E.B., and Jansson, J.K. (2012). Metagenome, metatranscriptome and single-cell sequencing reveal microbial response to Deepwater Horizon oil spill. *ISME J., 6,* 1715-1727.

Mellor, G.L. and Kantha, L. (1989). An ice-ocean coupled model. *Journal of Geophysical Research, 94,* 10937-10954.

Mitchell, M.R., Harrison, G., Pauley, K., Gagné, A., Maillet, G., and Strain, P. (200). Atlantic Zonal Monitoring Program Sampling Protocol. *Can. Tech. Rep. Hydrogr. Ocean Sci., 223,* iv + 23 pp.

Murphy, J. and Riley, J.P. (1962). A Modified Single Solution Method for the Determination of Phosphate in Natural Waters. *Anal. Chim. Acta, 27,* p.30.

Prince, R. C. (2010). Eukaryotic Hydrocarbon Degraders. *In* K.M. Timmis (ed.), *Handbook of Hydrocarbon and Lipid Microbiology (*pp. 2065-2078). Springer, Germany.

Prince, R. C., A. Gramain and T. J. McGenity. 2010. Prokaryotic Hydrocarbon Degraders. *In* K.M. Timmis (ed.), *Handbook of Hydrocarbon and Lipid Microbiology.* pp. 1669-1692.

Prince, R.C. 2015. Oil Spill dispersants: Boon or Bane. *Environ. Sci. Technol.* 49: 6376-6384. DOI: 10.1021/acs.est.5b00961.

Prince, R.C., Elmendorf, D.L., Lute, L.J., Hsu, C.S., Haith, C.E., Senius, J.D., Dechert, G.J., Douglas, G.S., and Butler, E.L. (1994). 17α(H),21β(H)-Hopane as a conserved internal marker for estimating the biodegradation of crude oil. *Environ. Sci. Technol., 28,* 142-145.

Redmond, M.C. and Valentine, D.L. (2012). Natural gas and temperature structured a microbial community response to the Deepwater Horizon oil spill. *P. Natl. Acad. Sci. USA, 109,* 20292-20297.

SL Ross, 2015. http://www.etc-cte.ec.gc.ca/databases/Oilproperties/pdf/WEB_Sable_Island_Condensate.pdf

Strickland, J.D.H. and Parsons, T.R. 1972. A Practical Handbook of Seawater Analysis. Fisheries Research Board of Canada, Ottawa, Bulletin 167 (2nd ed), 310 p.

US Department of the Interior (1969) FWPCA methods for chemical analysis of water and wastes November, 1969. Federal Water Pollution Control Administration, Cincinnati, 280 p.

Venosa, A.D., Suidan, M.T., King, D. and B.A. Wrenn, 1997. Use of hopane as a conservative biomarker for monitoring the bioremediation effectiveness of crude oil contaminating a sandy beach. J. Ind. Microbiol. Biotechnol. 18 (2-3):131-139.

Yang, T., Nigro, L.M., Gutierrez, T., D'Ambrosio, L., Joye, S.B., Highsmith, R., and Teske, A. (2014). Pulsed blooms and persistent oil-degrading bacterial populations in the water column during and after the Deepwater Horizon blowout. *Deep Sea Res., Part II In press*: DOI:10.1016/j.dsr2.2014.01.014.

Zhai, L., Platt, T., Tang, C., Sathyendranath, S., and Hernandez Walls, R. (2011). Phytoplankton phenology on the Scotian Shelf. *ICES Journal of Marine Science, 68*(4)*,* 781-791.

APPENDICES

Appendix 1: Field Data

The station locations the Grand Banks and Sable regions, in summer and winter, are found in Tables 1-1 to 1-2. Data collected, from the Seabird SBE9, is presented in Tables 1-3 to 1-5. Figure 1-1 is collage of photos showing the setup of microcosm in the refrigerated reefer on board the CCGS *Hudson*.

Table 1-1: Station locations names, direction and distance, and latitude and longitude at all three sites for summer sampling.

SUMMER

Region	Station Name Name	Direction/Distance from platform	Latitude	Longitude
Grand Banks Hibernia	R50	West 50km (reference)	46.696	-49.427
	HS5k	South 5 km	46.707	-48.785
	HNW2k	North-west 2km	46.764	-48.803
	HW5k	West 5km	46.751	-48.847
	HN5k	North 5 km	46.795	-48.782
	HE5k	East 5 km	46.752	-48.716
Grand Banks Terra Nova	TNS5k	South 5 km	46.431	-48.480
	TNW2k	West 2 km	46.488	-48.498
	TNN5k	North 5 km	46.520	-48.480
	TNE5k	East 5 km	46.477	-48.412
	TNSE5k	South-east 5 km	46.443	-48.435
	TNNW20k	North-west 20 km	46.602	-48.666
	TNNW10k	North-west 10 km	46.538	-48.576
	TNSE10k	South-east 10 km	46.411	-48.390
	TNSE20k	South-east 20 km	46.348	-48.296
	TNSE50k	South-east 50 km (reference)	46.156	-48.020
Scotian Shelf Sable Thebaud	TSE5k	South-east 5 km	43.859	-60.157
	TSE2k	South-east 2 km	43.878	-60.182
	TS5k	South 5 km	43.847	-60.201
	TW5k	West 5 km	43.891	-60.261
	TNW5k	North-west 5 km	43.923	-60.243
	TSE10k	South-east 10 km	43.826	-60.115
	TSE20k	South-east 20 km	43.761	-60.030
	TNW10k	North-west 10 km	43.957	-60.283
	TNW20_Ref	North-west 20 km (reference)	44.023	-60.366

Table 1-2: Station locations names, direction and distance, and latitude and longitude at all three sites for winter sampling.

WINTER

Region	Station Name	Direction/Distance from platform	Latitude	Longitude
Grand Banks Hibernia	Hibernia-Winter	North 36 km	47.000	-48.4711
Grand Banks Terra Nova	Terra Nova-Winter	North 60 km	47.000	-48.2884
Scotian Shelf	Sable-Winter	South-east 5 km	43.859	-60.157

Table 1-3: Nutrient and salinity data from Hibernia sampling stations (microcosm station in Grey).

HIBERNIA							
Station	Depth (m)	NITRATE µM	NITRITE µM	PHOSPHATE µM	SILICATE µM	AMMONIA µM	Salinity PSU
R50	69.4	2.36	0.13	0.75	6.24	2.40	32.964
R50	50.2	2.67	0.13	0.75	6.28	2.41	32.963
R50	25.2	0.45	0.05	0.20	0.40	0.52	32.793
R50	10.4	0.77	0.05	0.22	0.30	0.53	32.781
R50	3.4	0.94	0.05	0.20	0.26	0.60	32.774
HS5k	73.9	4.21	0.11	0.93	4.73	4.15	32.884
HS5k	49.7	2.18	0.08	0.67	2.23	1.48	32.858
HS5k	25.3	0.20	0.05	0.27	0.36	0.61	32.758
HS5k	10.0	0.18	DL	0.24	0.23	1.27	32.710
HS5k	2.2	0.11	DL	0.26	0.40	0.63	32.713
HNW2k	77.2	2.94	0.08	0.89	3.88	3.84	32.877
HNW2k	50.7	2.09	0.07	0.78	2.59	2.69	32.871
HNW2k	24.2	0.09	DL	0.28	0.25	0.61	32.651
HNW2k	9.9	0.16	DL	0.27	0.27	0.62	32.642
HNW2k	3.0	0.17	0.05	0.28	0.33	0.57	32.653
HW5k	73.3	2.73	0.09	0.84	3.92	3.48	32.871
HW5k	50.4	2.50	0.10	0.83	4.11	3.27	32.868
HW5k	25.6	0.25	0.05	0.29	0.50	0.56	-
HW5k	9.8	0.25	DL	0.24	0.18	0.49	32.692
HW5k	3.1	0.18	0.04	0.25	0.20	0.49	32.684
HN5k	75.3	2.86	0.10	0.88	3.63	3.93	32.878
HN5k	50.4	2.95	0.12	0.92	3.95	3.84	32.873
HN5k	25.2	0.22	0.05	0.30	0.30	0.77	32.626
HN5k	10.2	0.22	0.04	0.28	0.32	0.51	32.631
HN5k	3.0	0.22	0.05	0.26	0.26	0.52	32.622
HE5k	78.4	3.53	0.11	0.96	4.17	4.26	32.884
HE5k	50.3	2.61	0.10	0.85	3.02	3.49	32.879
HE5k	25.1	0.27	0.05	0.26	0.21	0.57	32.728
HE5k	10.4	0.30	0.04	0.24	0.17	0.50	32.656
HE5k	3.0	0.27	0.04	0.24	0.16	0.50	32.681
Hib-Winter	5.4	0.64	0.05	0.36	1.38	0.59	

Table 1-4: Nutrient and salinity data for Terra Nova sampling stations (microcosm station in Grey).

TERRA NOVA							
Station	Depth (m)	NITRATE µM	NITRITE µM	PHOSPHATE µM	SILICATE µM	AMMONIA µM	Salinity PSU
TNS5k	88.9	5.38	0.12	1.17	5.27	5.03	32.946
TNS5k	50.4	0.33	0.04	0.43	0.46	0.56	32.037
TNS5k	25.0	0.21	0.05	0.27	0.18	0.51	32.703
TNS5k	10.1	0.25	0.06	0.23	0.18	0.51	32.654
TNS5k	3.1	0.19	0.06	0.24	0.21	0.82	32.657
TNS5k	3.1	0.28	0.04	0.27	0.18	0.56	-
TNW2k	89.2	5.95	0.11	1.20	5.09	5.63	32.960
TNW2k	50.4	1.00	0.06	0.56	0.51	1.27	32.845
TNW2k	25.0	0.27	0.05	0.31	0.28	0.58	32.715
TNW2k	10.2	0.28	0.05	0.27	0.22	0.50	32.677
TNW2k	3.1	0.20	0.05	0.23	0.19	0.52	-
TNN5k	89.7	6.44	0.11	1.28	5.28	5.73	32.974
TNN5k	50.5	0.22	0.06	0.42	0.11	0.62	32.811
TNN5k	25.5	0.23	0.04	0.29	0.14	0.43	32.745
TNN5k	9.8	0.30	0.05	0.28	0.12	0.38	32.593
TNN5k	3.3	0.33	0.04	0.23	0.10	0.47	32.641
TNE5km	93.0	5.81	0.10	1.21	4.80	5.14	32.973
TNE5km	50.4	0.34	0.04	0.41	0.12	0.46	32.799
TNE5km	25.2	0.32	0.04	0.29	0.17	0.54	32.696
TNE5km	10.5	0.28	0.07	0.27	0.21	0.48	32.611
TNE5km	3.4	0.16	0.05	0.25	0.30	0.53	32.671
TNSE5k	91.0	5.35	0.11	1.04	3.87	4.43	32.967
TNSE5k	49.9	0.23	0.04	0.37	0.12	0.48	32.775
TNSE5k	25.3	0.22	0.04	0.28	0.17	0.60	32.687
TNSE5k	10.3	0.18	DL	0.28	0.44	0.46	32.647
TNSE5k	3.2	0.22	0.04	0.24	0.26	0.42	32.658
TNNW20k	79.8	5.67	0.13	1.07	5.20	4.84	32.914
TNNW20k	50.7	0.93	0.07	0.38	0.45	0.77	32.823
TNNW20k	25.3	0.64	0.04	0.23	0.23	0.49	32.725
TNNW20k	9.8	0.44	0.05	0.21	0.18	0.54	32.696
TNNW20k	2.7	DL	0.05	0.20	0.36	0.57	32.690
TNNW10k	88.9	5.54	0.12	1.18	4.97	5.41	32.955
TNNW10k	50.3	DL	0.05	0.35	0.13	0.49	32.817
TNNW10k	24.9	DL	0.07	0.24	0.12	0.61	32.740

TNNW10k	9.7	DL	0.05	0.22	0.14	0.52	-
TNNW10k	3.1	DL	0.06	0.21	0.17	0.52	-
TNSE10k	93.9	5.23	0.11	1.11	4.70	4.80	32.970
TNSE10k	50.3	DL	0.06	0.36	0.15	0.68	32.816
TNSE10k	25.2	DL	0.05	0.25	0.09	0.51	32.591
TNSE10k	9.5	DL	0.05	0.23	0.10	0.47	-
TNSE10k	3.2	DL	0.05	0.21	0.24	0.52	-
TNSE20k	95.9	5.96	0.11	1.18	5.27	5.05	33.012
TNSE20k	50.7	1.14	0.07	0.48	0.16	1.14	32.806
TNSE20k	24.7	DL	0.04	0.20	0.12	0.44	32.662
TNSE20k	9.8	DL	0.04	0.19	0.10	0.48	32.576
TNSE20k	3.2	DL	0.05	0.15	0.18	0.46	32.605
TNSE50k	113.9	7.15	0.12	0.84	5.78	1.98	33.099
TNSE50k	50.0	5.69	0.12	0.78	1.92	1.46	32.847
TNSE50k	25.0	DL	DL	0.35	0.24	0.50	32.521
TNSE50k	9.8	DL	0.05	0.33	0.16	0.46	32.314
TNSE50k	3.2	DL	DL	0.31	0.09	0.43	32.314
TN-Winter	6.0	1.17	0.07	0.44	2.15	0.60	

Table 1-5: Nutrient and salinity data for Sable sampling stations (microcosm station in Grey).

SABLE (THEBAUD)							
Station	Depth (m)	NITRATE µM	NITRITE µM	PHOSPHATE µM	SILICATE µM	AMMONIA µM	Salinity PSU
TSE5k	33.0	DL	0.08	0.43	1.01	0.68	31.759
TSE5k	9.4	DL	0.07	0.32	0.22	0.58	31.493
TSE5k	4.3	DL	0.05	0.29	0.13	0.46	31.378
TSE2k	30.4	DL	0.05	0.40	0.68	0.68	31.673
TSE2k	11.0	DL	0.04	0.29	0.18	0.48	31.478
TSE2k	4.6	DL	0.04	0.28	0.15	0.50	-
TS5k	40.6	0.44	0.07	0.51	1.62	1.00	31.857
TS5k	10.5	DL	0.05	0.30	0.14	0.57	31.338
TS5k	4.7	DL	0.05	0.29	0.13	0.44	-
TW5k	30.3	DL	0.05	0.38	0.58	0.49	-
TW5k	9.9	DL	0.05	0.28	0.12	0.47	31.360
TW5k	4.5	DL	0.05	0.23	0.02	0.45	31.267
TNW5k	16.8	DL	0.06	0.34	0.20	0.52	31.483
TNW5k	9.7	DL	0.06	0.32	0.17	0.44	31.743
TNW5k	4.2	DL	0.07	0.35	0.29	0.54	31.473
TSE10k	42.7	0.69	0.13	0.58	2.40	1.36	31.956
TSE10k	10.1	DL	0.08	0.31	0.18	0.60	31.378
TSE10k	4.0	DL	0.06	0.29	0.10	0.47	31.357
Tse20k	52.5	3.66	0.26	0.78	5.92	2.20	32.536
Tse20k	10.6	DL	0.06	0.28	0.23	0.58	31.377
Tse20k	4.4	DL	0.04	0.29	0.16	0.45	31.375
TNW10k	14.1	DL	0.05	0.34	0.31	0.47	31.529
TNW10k	9.3	DL	0.05	0.36	0.40	0.48	31.492
TNW10k	4.0	DL	0.05	0.32	0.35	0.51	31.460
TNW20	11.4	DL	0.05	0.35	0.36	0.42	31.537
TNW20	9.3	DL	0.06	0.35	0.40	0.53	31.537
TNW20	4.1	DL	0.05	0.35	0.34	0.49	31.538
T-winter	2.5	0.70	0.11	0.38	1.77	0.83	

Table 1-6: Data from Seabird SBE9 collected at Hibernia (microcosm station in Grey).

Hibernia							
Station	**Decimal Latitude**	**Decimal Longitude**	**Oxygen mL/L**	**Salinity PSU**	**Temperature °C**	**Pressure db**	**Fluorescence µg/L**
R50	46.696	-49.427	8.0690	32.9608	1.814	69.44	0.22
	46.696	-49.427	8.0710	32.9594	1.808	50.20	0.23
	46.696	-49.427	7.7699	32.7762	9.068	25.21	0.16
	46.696	-49.427	7.4115	32.7445	11.188	10.39	0.10
	46.696	-49.427	7.2842	32.7697	11.582	3.39	0.09
HS5k	46.707	-48.785	8.1762	32.8821	0.053	73.85	0.07
	46.707	-48.785	8.9289	32.8534	0.388	49.73	1.55
	46.707	-48.785	8.0149	32.7829	7.709	25.30	0.19
	46.707	-48.785	7.4817	32.7018	10.141	10.01	0.08
	46.707	-48.785	7.1897	32.7102	11.907	2.17	0.07
	46.707	-48.785	7.1988	32.7101	11.866	2.67	0.06
HNW2k	46.764	-48.803	8.3428	32.8755	0.045	77.15	0.09
	46.764	-48.803	8.4823	32.8712	0.210	50.66	0.79
	46.764	-48.803	7.7691	32.6476	8.634	24.21	0.07
	46.764	-48.803	7.4243	32.6350	10.506	9.87	0.05
	46.764	-48.803	7.1891	32.6485	11.856	3.05	0.04
HW5k	46.751	-48.847	8.4442	32.8695	0.160	73.30	0.15
	46.751	-48.847	8.4287	32.8663	0.473	50.40	0.42
	46.751	-48.847	8.1265	32.7640	7.033	25.58	0.11
	46.751	-48.847	7.4732	32.6876	10.171	9.82	0.04
	46.751	-48.847	7.1707	32.6885	12.524	3.10	0.03
HN5k	46.795	-48.782	8.2119	32.8778	0.092	75.30	0.07
	46.795	-48.782	8.2460	32.8752	0.266	50.44	0.72
	46.795	-48.782	8.1283	32.6324	6.917	25.19	0.09
	46.795	-48.782	7.5693	32.6277	9.999	10.20	0.05
	46.795	-48.782	7.3417	32.6187	11.261	3.02	0.04
HE5k	46.752	-48.716	8.1125	32.8838	-0.031	78.42	0.05
	46.752	-48.716	8.2397	32.8756	0.253	50.26	1.08
	46.752	-48.716	7.6721	32.7216	9.285	25.07	0.10
	46.752	-48.716	7.3914	32.6606	11.020	10.40	0.05
	46.752	-48.716	7.1547	32.6775	12.578	3.00	0.05

Table 1-7: Data from Seabird SBE9 collected at Terra Nova (microcosm station in Grey).

TERRA NOVA							
Station	**Decimal Latitude**	**Decimal Longitude**	**Oxygen mL/L**	**Salinity PSU**	**Temperature °C**	**Pressure db**	**Fluorescence µg/L**
TNS5k	46.431	-48.480	7.667	32.9463	-0.178	88.94	0.05
	46.431	-48.480	9.672	32.8338	0.325	50.37	0.29
	46.431	-48.480	7.927	32.7079	7.955	25.05	0.11
	46.431	-48.480	7.103	32.6523	12.452	10.07	0.07
TNS5k	46.431	-48.480	7.075	32.6538	12.820	3.09	0.07
TNW2k	46.488	-48.498	7.587	32.9614	-0.296	89.18	0.07
	46.488	-48.498	9.471	32.8420	-0.029	50.42	0.55
	46.488	-48.498	7.869	32.7107	8.457	25.02	0.11
	46.488	-48.498	7.420	32.6730	10.892	10.21	0.06
	46.488	-48.498	7.043	32.6677	13.022	3.09	0.05
TNN5k	46.520	-48.480	7.415	32.9735	-0.301	89.71	0.05
	46.520	-48.480	10.009	32.8106	0.263	50.53	0.19
	46.520	-48.480	8.483	32.7489	5.958	25.47	0.09
	46.520	-48.480	7.537	32.5742	10.174	9.76	0.05
	46.520	-48.480	7.151	32.6354	12.351	3.30	0.07
TNE5k	46.477	-48.412	7.559	32.9716	-0.297	92.98	0.05
	46.477	-48.412	10.118	32.7955	0.470	50.37	0.13
	46.477	-48.412	8.053	32.6918	7.658	25.17	0.10
	46.477	-48.412	7.563	32.6051	10.141	10.50	0.07
	46.477	-48.412	7.220	32.6360	12.276	3.36	0.09
TNSE5k	46.443	-48.435	7.889	32.9647	-0.315	91.01	0.05
	46.443	-48.435	9.782	32.7714	1.834	49.86	0.14
	46.443	-48.435	7.953	32.6760	8.248	25.26	0.09
	46.443	-48.435	7.256	32.6402	12.003	10.27	0.07
	46.443	-48.435	7.058	32.6554	13.078	3.22	0.09
TNNW20k	46.602	-48.666	7.757	32.9122	-0.170	79.82	0.05
	46.602	-48.666	9.959	32.8161	0.166	50.71	0.11
	46.602	-48.666	7.779	32.7238	8.700	25.27	0.14
	46.602	-48.666	7.455	32.6931	10.573	9.80	0.08
	46.602	-48.666	7.347	32.6911	11.289	2.69	0.06
TNNW10k	46.538	-48.576	7.498	32.9542	-0.273	88.88	0.05

Table 1-8: Data from Seabird SBE9 collected at Sable (microcosm stations in Grey).

SABLE (THEBAUD)							
Station	**Decimal Latitude**	**Decimal Longitude**	**Oxygen mL/L**	**Salinity PSU**	**Temperature °C**	**Pressure db**	**Fluorescence µg/L**
TSE5k	43.859	-60.157	7.490	31.7695	9.540	32.99	0.26
	43.859	-60.157	7.555	31.5436	12.403	9.45	0.12
	43.859	-60.157	7.151	31.3670	14.830	4.32	0.07
TSE5k	43.859	-60.157	7.027	31.3448	15.330	4.25	0.06
	43.859	-60.157	7.012	31.3532	15.123	4.35	0.05
	43.859	-60.157	7.069	31.3555	15.173	4.28	0.05
TSE2k	43.878	-60.182	7.597	31.6934	10.193	30.37	0.29
	43.878	-60.182	7.610	31.5353	12.368	10.98	0.16
	43.878	-60.182	7.270	31.4001	14.287	4.57	0.10
TS5k	43.847	-60.201	7.453	31.8782	8.624	40.62	0.21
	43.847	-60.201	6.942	31.3535	15.502	10.55	0.09
	43.847	-60.201	6.948	31.3538	15.382	4.70	0.09
TW5k	43.891	-60.261	7.437	31.6768	10.594	30.35	0.28
	43.891	-60.261	7.090	31.3610	15.015	9.87	0.10
	43.891	-60.261	6.836	31.2882	15.949	4.54	0.09
TNW5k	43.923	-60.243	7.197	31.5002	13.501	16.77	0.19
	43.923	-60.243	7.177	31.4924	13.674	9.71	0.19
	43.923	-60.243	7.184	31.4922	13.696	4.15	0.19
TSE10k	43.826	-60.115	7.323	32.0111	7.738	42.72	0.15
	43.826	-60.115	7.017	31.5278	14.716	10.06	0.11
	43.826	-60.115	6.993	31.3779	15.096	3.99	0.09
TSE20k	43.761	-60.030	7.241	32.5523	4.709	52.53	0.07
	43.761	-60.030	7.040	31.3994	14.946	10.56	0.14
	43.761	-60.030	7.016	31.3959	15.053	4.43	0.11
TNW10k	43.957	-60.283	7.433	31.5531	12.068	14.07	0.26
	43.957	-60.283	7.345	31.5037	12.738	9.31	0.17
	43.957	-60.283	7.331	31.4892	12.983	3.99	0.18
TNW20_Ref	44.023	-60.366	7.329	31.5559	12.839	11.44	0.22
	44.023	-60.366	7.324	31.5569	12.820	9.33	0.23
	44.023	-60.366	7.322	31.5562	12.829	4.05	0.20

Figure 1-1: Photos showing the setup of microcosms in the refrigerated reefer. The copper colored disk next to label 370 (right side photo) is the oxygen sensor.

Appendix 1-a: Inorganics (Nutrients) and Salinity

Water column nutrient samples were collected from all stations and depths as part of the baseline oceanographic survey of the Grand Banks and Sable regions. Nutrient samples were collected using clean silicone tubing attached to the spigot of the Niskin bottle. Wearing gloves to avoid contamination, 60 mL acid rinsed (10 % HCl) plastic bottles were rinsed three times with sample water before filling the bottle to ¾ full. Duplicate samples were taken and all immediately frozen upright in a rack at -20°C until analysis at BIO.

Ammonia, silicate, nitrite, nitrate and phosphate were analysed by segmented flow analysis (Technicon II) at BIO. The determination of soluble silicates (Technicon Industrial Method No. 186-72W released March 1973, adapted from Strickland and Parsons 1972) in seawater was based on the reduction of a silicomolybdate in acidic acid solution to ''molybdenum blue' by ascorbic acid, which was read colorimetrically at 660nm. Oxalic acid was introduced to the sample stream, before the addition of ascorbic acid, to eliminate interference from phosphate.

The determination of nitrate/nitrite followed Technicon Industrial Method No. 158-71W released December 1972 (adapted from Armstrong et al. 1967; Grasshoff 1969; U.S. Department of the Interior 1969). The method was based on the principle of nitrate reduction to nitrite by a copper-cadmium redactor column. The nitrite ion then reacts with sulphanilamide under acidic conditions to form a diazo compound. This compound then couples with N-1-naphlylethylenediamine dihydrochloride to form a reddish-purple azo dye, which is read colorimetrically at 550 nm. Nitrite is determined with identical chemistry but omitting the copper-cadmium column from the sample stream.

The method for ammonia (Kerouel and Aminot, 1997) was based on the reaction of ammonia with ortho-phthalaldehyde (OPA) and sulfite to form an intense fluorescent product. Determination is done fluorometrically with excitation at 370 nm and emission at 418-700 nm.

The determination of ortho phosphate (followed Technicon Industrial Method 155-71W released January 1973 adapted from Murphy and Riley, 1972) was based on the formation of a phosphomolybdenum blue complex, read colorimetrically at 880 nm, produced by the reaction of phosphate with an acidic ammonium molybdate solution containing a small amount of antimony and ascorbic acid. The original method called for combining ammonium molybdate, antimony potassium tartrate and ascorbic acid into one working reagent. In house, the ascorbic acid is introduced into the sample stream separately. Nutrient data, for all three sites, are found in Tables 1-6 to 1-8.

Salinity samples were collected, from all stations and depths, directly from a clean silicone tube attached to the spigot of the Niskin bottle. Sampling procedure involved rinsing a glass Kimax 200 mL bottle (2 x) with sample prior to collection, subsequently capping and stored at room temperature until analysis using a Guildline Autosal laboratory salinometer and data reported as Practical Salinity Units (psu) (Tables 1-6 to 1-8).

Appendix 1-b: Organics (PAHs, Aliphatics and BTEX)

Water samples were collected directly from the Niskin bottle into 2.3 L amber glass bottles (solvent rinsed, but not rinsed with sample) filled with 2 L of seawater and then acidified with 2 mL of 6 N HCl. Sample bottle caps were wrapped with Teflon tape and samples were stored in the refrigerated container while at sea, subsequently transferred to a 4 °C cold room at Bedford Institute of Oceanography (BIO) prior to analysis. Background levels of alkanes, PAHs and alkylated PAHs were measured from selected water samples collected at various depths in the study area.

Samples were analysed using a modified version of EPA method 8270. The 2 L water sample was spiked with a surrogate standard containing a series of deuterated aliphatic and aromatic hydrocarbons, and extracted with 3 x 50 mL of DCM in a separatory funnel. The solvent was concentrated on a TurboVap and the extract purified on a silica gel column. The purified extract was exchanged into isooctance and spiked with internal standards. Samples were analysed using an Agilent 6890 Gas Chromatograph (GC) coupled to a 5975 Mass Spectrometer (MS). The column was a Supelco MDN-5s of 30 m length x 250µm internal diameter x 0.25µm film thickness, with a 1 m retention gap of deactivated fused silica. A 1µL aliquot was injected using the oven track mode. Helium was the carrier gas with a flow rate of one mL/min. The oven temperature program was set to hold at 85° C for 2 min, followed by a ramp to 280° C at 4 °C/min held for 20 min. Total run time was 70.75 min. The MS was operated in the selected ion monitoring (SIM) mode. Samples were calibrated against a seven-point curve containing a mixture of aliphatic hydrocarbons as well as parent and alkyl PAH. For some of the alkyl PAH where standards were not available, the response of the parent PAH was used for quantification.

Briefly, according to EPA method 8240, water samples for BTEX (benzene, toluene, ethylbenzene and xylene) analysis were collected in 40 mL purge and trap vials. The vials were spiked with 40 µL of 6N HCl to serve as a preservative, so that they can be stored at 4°C for up to 14 days. The purge and trap system was a Teledyne Tekmar velocity XPT purge and trap concentrator equipped with a Tenax/silica gel/charcoal trap. The auto-sampler was a Teledyne Tekmar Aquatek 70-vial unit, which transferred a 5 mL aliquot of sample into the purge and trap chamber, where it was purged with helium for 11 minutes. During this process, the volatiles were trapped on the Tenax trap and then desorbed at 225°C for 2 min., where they enter a heated transfer line connected to the Agilent 6890 GC injector and subsequently proceed to the GC column (Supelco SLB-5ms 30 m × 250 µm × 0.25 µm length × i.d. × film thickness with a 1 m retention gap of fused silica). The GC oven was programmed at an initial oven temperature of 50ºC, held for 8 min, followed by an increase to 280ºC at 40ºC/min, and held at 280ºC for 2 min, for a total run time of 18 min. The gases exiting the GC column were detected by an Agilent 5973 mass selective detector (MS) used in selective ion mode (SIM) monitoring for six ions: 77, 78, 91, 92, 105 and 106 amu. BTEX standards were prepared in 40 mL purge and trap vials and analyzed using this method, along with sample blanks, samples, and duplicates. All background water samples (e.g. BTEX, saturates, PAHs, and Alk-PAHs) analysed had negligible values.

Appendix 2: Water Sample Analyses (Microbiology)

Appendix 2-a: Chlorophyll-a and Phaeopigments by Fluorometric Analysis

Chlorophyll-a is a universal pigment found in all taxa. Phaeopigments are commonly produced by a wide variety of zooplankton, including copepods, euphausids, salps, and phagotrophic flagellates. Chlorophyll-a and phaeopigment samples were collected from all stations at various depths directly from the niskin bottle using clean silicone tubing attached to the spigot. Sample bottles (1 L Nalgene) were rinsed 2x with sample and filled to approximately 500 mL.

Chlorophyll-a and phaeopigment measurements have historically provided a useful estimate of algal biomass, and their spatial and temporal variability. The fluorometric method (Holm-Hansen et al. 1965) is extensively used for the quantitative analysis of chlorophyll-a and phaeopigments. Methods used are described in Mitchell et al. 2002. Duplicate 100 mL samples from each depth were decanted into a graduated cylinder and filtered through Whatman 25 mm GF/F filters at < 10 psi. Each filter was placed in a 20 mL glass scintillation vial (with a polycone lid) that contained 10 mL of 90% acetone and subsequently were capped and stored in the dark at -20 °C for a minimum of 24 hours.

The vials were removed from the freezer and covered to keep in the dark for approximately two hours prior to fluorescence readings. A Turner Designs Trilogy® Laboratory fluorometer fitted with a red sensitive photomultiplier, a blue lamp, 5-60 blue filter and 2-64 red filter was used to measure fluorescence.

Vials were gently mixed and the acetone overlaying the filter was added to a cuvette that was placed into the fluorometer cell and reading, range and sensitivity were recorded. The sample was then acidified with two drops of 10% HCl and measurements repeated. Algal pigments, particularly chlorophyll-a, fluoresce in the red wavelengths after extraction in acetone when they are excited by blue wavelengths of light. The fluorometer excites the extracted sample with a broadband blue light and the resulting fluorescence in the red is detected by a photomultiplier. The significant fluorescence by phaeopigments is corrected for by acidifying the sample which converts all of the chlorophyll-a to phaeopigments. By applying a measured conversion for the relative strength of chlorophyll and phaeopigment fluorescence, the two values can be used to calculate both the chlorophyll-a and phaeopigment concentrations. Chlorophyll (Mean C) and phaeopigments (Mean P) data for all three sites are found in Tables 2-1 to 2-3.

Table 2-1: Chlorophyll concentrations in samples collected at various depths near Hibernia (microcosm station in Grey).

HIBERNIA					
Station	Sampling Depth (m)	Chlorophyll			
		MEAN C $mg \cdot m^3$	MEAN P $mg \cdot m^3$	Average of all depths (Mean C) $mg \cdot m^3$	Average of all depths (Mean P) $mg \cdot m^3$
R50	69.4	0.982	0.380	0.711	0.262
	50.2	0.982	0.380		
	25.2	0.706	0.350		
	10.4	0.457	0.123		
	3.4	0.429	0.078		
HS5km	73.9	0.177	0.268	0.857	0.310
	49.7				
	25.3	0.828	0.261		
	10.0	1.319	0.452		
	2.2	1.105	0.258		
HNW2k	77.2	0.364	0.258	1.268	0.232
	50.7	5.061	0.665		
	24.2	0.289	0.094		
	9.9	0.308	0.086		
	3.0	0.317	0.056		
HW5k	73.3	0.798	0.292	0.979	0.254
	50.4	2.725	0.732		
	25.6	0.653	0.144		
	9.8	0.373	0.072		
	3.1	0.345	0.028		
HN5k	75.3	0.205	0.219	0.797	0.254
	50.4	2.725	0.732		
	25.2	0.439	0.090		
	10.2	0.317	0.087		
	3.1	0.299	0.054		
HE5k	78.4	0.118	0.250	1.320	0.259
	50.3	5.547	0.826		
	25.1	0.345	0.100		
	10.4	0.289	0.063		
	3.0	0.299	0.054		

Table 2-2: Chlorophyll (Mean C) and phaeopigments (Mean P) concentrations in samples collected at various depths near Terra Nova (microcosm station in Grey).

TERRA NOVA					
Station	Sampling Depth (m)	Chlorophyll			
		MEAN C $mg \cdot m^3$	MEAN P $mg \cdot m^3$	Average of all depths (MEAN C) $mg \cdot m^3$	Average of all depths (MEAN P) $mg \cdot m^3$
TNS5k	88.9	0.063	0.269	0.554	0.199
	50.4	1.749	0.431		
	25.0	0.383	0.135		
	10.1	0.271	0.092		
	3.1	0.303	0.070		
TNW2k	89.2	0.081	0.255	0.840	0.218
	50.4	3.017	0.548		
	25.0	0.429	0.161		
	10.2	0.345	0.069		
	3.1	0.327	0.057		
TNN5k	89.2	0.093	0.311	0.414	0.189
	50.4	0.951	0.343		
	25.0	0.336	0.141		
	10.2	0.345	0.079		
	3.1	0.345	0.069		
TNE5km	93.0	0.072	0.286	0.377	0.151
	50.4	0.588	0.168		
	25.2	0.411	0.118		
	10.5	0.401	0.096		
	3.4	0.411	0.087		
TNSE5k	91.0	0.098	0.254	0.358	0.134
	49.9	0.607	0.233		
	25.3	0.345	0.090		
	10.3	0.364	0.050		
	3.2	0.373	0.041		
TNNW20k	79.8	0.058	0.211	0.385	0.150
	50.7	0.672	0.209		
	25.3	0.597	0.159		
	9.8	0.299	0.095		
	2.7	0.299	0.074		
TNNW10k	88.9	0.089	0.259	0.356	0.145
	50.3	0.635	0.153		
	24.9	0.411	0.138		

	9.7	0.336	0.089		
	3.1	0.308	0.086		
TNSE10k	93.9	0.081	0.271	0.524	0.213
	50.3	1.473	0.503		
	25.2	0.317	0.107		
	9.5	0.373	0.103		
	3.2	0.373	0.083		
TNSE20k	95.9	0.072	0.293	0.502	0.203
	50.7	1.381	0.390		
	24.7	0.364	0.123		
	9.8	0.336	0.120		
	3.2	0.355	0.091		
TNSE50k	113.9	0.150	0.128	0.592	0.165
	50.0	2.119	0.517		
	25.0	0.224	0.076		
	9.8	0.207	0.045		
	3.2	0.261	0.060		

Table 2-3: Chlorophyll (Mean C) and phaeopigments (Mean P) concentrations in samples collected at various depths near Sable (microcosm station in Grey).

SABLE (THEBAUD)					
Station	Sampling Depth (m)	Chlorophyll			
		MEAN C $mg \cdot m^3$	MEAN P $mg \cdot m^3$	Average of all depths (MEAN C) $mg \cdot m^3$	Average of all depths (MEAN P) $mg \cdot m^3$
TSE5k	33.0	1.289	0.550	0.793	0.276
	9.4	0.614	0.204		
	4.3	0.476	0.073		
TSE2k	30.4	1.258	0.547	0.803	0.287
	11.0	0.675	0.210		
	4.6	0.476	0.104		
TS5k	40.6	1.289	0.550	0.675	0.235
	10.5	0.392	0.074		
	4.7	0.345	0.079		
TW5k	30.3	1.350	0.523	0.718	0.235
	9.9	0.457	0.112		
	4.5	0.345	0.069		
TNW5k	16.8	0.828	0.295	0.767	0.289
	9.7	0.736	0.251		
	4.2	0.736	0.319		
TSE10k	42.7	0.859	0.571	0.588	0.262
	10.1	0.476	0.115		
	4.0	0.429	0.099		
TSE20k	52.5	0.308	0.324	0.553	0.203
	10.6	0.644	0.139		
	4.4	0.706	0.146		
TNW10k	14.1	1.013	0.418	0.931	0.341
	9.3	0.890	0.336		
	4.0	0.890	0.268		
TNW20_Ref	11.4	0.951	0.411	0.921	0.408
	9.3	0.890	0.404		
	4.1	0.921	0.408		

Appendix 2-b: Bacterial Enumeration by Flow Cytometry

At all stations and depth, samples for enumeration of bacteria were collected directly from a clean silicone tube attached to the spigot of the Niskin bottle. Sample bottles (1 L Nalgene) were rinsed twice with sample and filled to approximately 500 mL. As soon as possible after collection, duplicate aliquots of 1.8 mL were removed using an Eppendorf pipette and dispensed into a 2 mL capacity cryogenic vials, then fixed with 10% paraformaldehyde (e.g. by adding 200 µL to the sample and vortex mixing) and maintained at room temperature for 15 minutes, subsequently frozen in liquid nitrogen, and stored at -80 °C until analyses as outlined in Li and Dickie, 2001. The results for the bacterial enumeration for all three sites are shown in Figure 2-1.

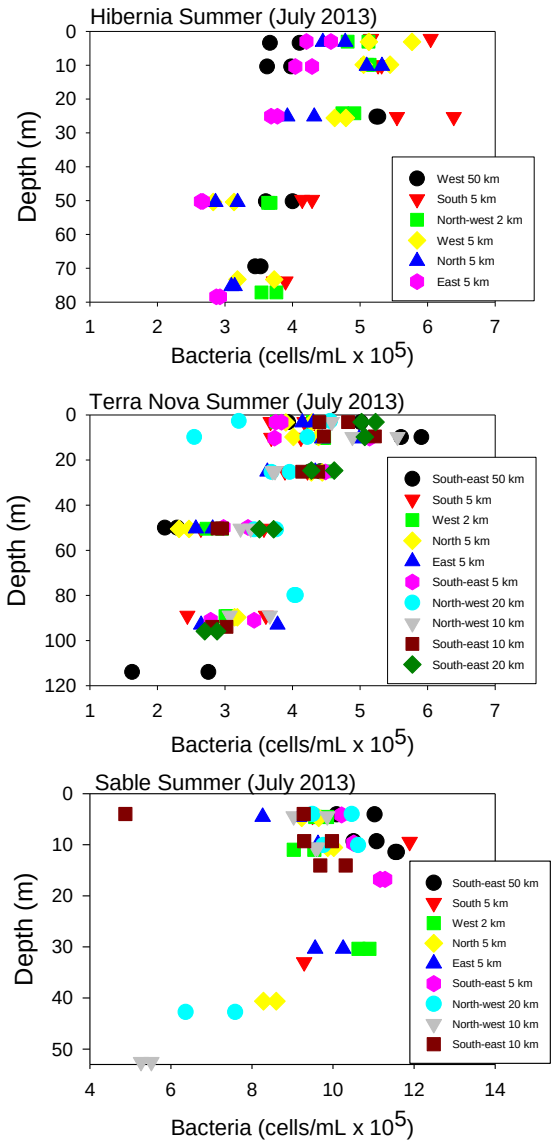

Figure 2-1: Bacterial Enumeration results for Hibernia (top), Terra Nova (middle) and Sable (bottom).

Appendix 3: Hydrocarbon products' composition data

Table 3-1: Chemical composition of oils and condensate used in the study.

Compound	WEATHERED		
	Thebaud Scotian Shelf Condensate weathered 45.2% $ng \cdot g^{-1}$	Hibernia Crude Oil weathered 10.0% $ng \cdot g^{-1}$	Terra Nova Crude Oil weathered 8.9% $ng \cdot g^{-1}$
n-decane	4,049,788	3,679,542	3,348,315
undecane	3,815,488	3,982,687	3,745,693
dodecane	3,038,297	4,004,330	3,987,100
tridecane	2,315,197	3,794,737	3,963,321
tetradecane	1,826,573	4,138,230	4,239,957
pentadecane	1,285,994	4,291,837	4,453,525
hexadecane	1,346,632	3,941,152	4,364,836
heptadecane	889,105	3,846,024	4,207,432
2,6,10,14-TMPdecane (pristane)	319,219	2,313,937	3,234,666
octadecane	693,376	3,273,549	3,820,834
2,6,10,14-TMHdecane (phytane)	114,211	2,572,047	3,247,208
nonadecane	443,252	3,236,239	3,511,359
eicosane	195,372	2,376,444	2,227,299
heneicosane	130,818	2,338,684	2,200,777
docosane	76,345	2,186,175	1,991,737
tricosane	46,370	2,109,719	1,876,687
tetracosane	29,462	2,056,231	1,795,393
pentacosane	21,691	2,158,452	1,864,926
hexacosane	16,309	2,111,117	1,927,680
heptacosane	12,477	1,976,254	1,824,365
octacosane	10,029	1,890,989	1,754,437
tricontane	9,298	979,896	924,791
n-heneicontane	8,836	989,588	953,059
dotriacontane	8,577	830,397	813,016
tritriacontane	4,189	1,134,282	1,146,114
tetratriacontane	3,510	873,442	909,015
n-pentatriacontane		649,373	668,934
17β(H), 21α (H)-hopane		19,392	15,284
naphthalene	1,881,022	743,303	641,015
1-methylnaphthalene	1,555,112	1,217,478	1,223,933
methylnaphthalene	2,715,742	1,616,292	1,489,315
2,6-dimethlynaphthalen	1,184,612	689,795	558,899
dimethylnaphthalene	2,297,340	1,991,764	1,886,680
2,3,5-trimethylnaphthalene	284,408	443,788	441,203

trimethylnaphthalene	1,023,677	1,462,325	1,467,062
tetramethylnaphthalene	320,999	694,390	763,357
acenaphthene	19,186	19,866	15,248
acenaphthylene			
fluorene	838	1,083	854
methylfluorene	78,034	221,521	199,133
dimethylfluorene	49,080	273,899	270,430
trimethylfluorene	20,784	205,626	215,321
dibenzothiophene	4,003	74,955	88,356
methyldibenzothiophene	5,833	146,033	182,863
dimethyldibenzothiophene	3,935	215,165	270,201
trimethyldibenzothiophene		142,661	182,146
tetramethyldibenzothiophene		77,259	99,829
phenanthrene	39,895	228,366	173,314
anthracene			
methylphenanthrene	46,354	472,841	444,024
2-methylphenanthrene	19,777	135,696	104,743
dimethylphenanthrene	27,079	446,463	435,423
3,6-dimethylphenanthrene	4,371	29,791	27,433
trimethylphenanthrene	13,488	293,278	304,678
tetramethylphenanthrene	5,227	150,959	163,013
fluoranthene		4,949	3,963
pyrene		8,516	6,623
methylpyrene	5,107	67,470	56,842
dimethylpyrene	4,384	93,118	87,146
trimethylpyrene	3,148	95,751	92,666
tetramethylpyrene		100,454	115,576
naphthobenzothiophene		18,514	20,747
methylnaphthobenzothiophene		75,313	87,235
dimethylNBenzothiophene		188,760	198,939
trimethylNbenzothiophene		67,352	79,534
tetramethylNbenzothiophene		34,274	41,629
benz[*a*]anthracene		6,401	3,858
chrysene		40,157	30,638
methylchrysene		78,118	54,752
dimethylchrysene		88,247	82,726
trimethylchrysene		59,838	57,962
tetramethylchrysene		52,767	55,193
benzo[*b*]fluoranthene		65	54
benzo[*k*]fluoranthene			
benzo[*e*]pyrene		9,642	8,635
benzo[*a*]pyrene		2,852	2,819
perylene		3,931	3,713

indeno[1,2,3-*cd*]pyrene			
dibenz[*a*,*h*]anthracene		3,117	3,124
benzo[*ghi*]perylene		3,521	4,230
ΣAlkanes ($ng \cdot g^{-1}$)	20,710,417	67,754,746	69,017,760
ΣAlkylated PAHs ($ng \cdot g^{-1}$)	4,607,279	7,863,962	7,938,198
ΣPAHs ($ng \cdot g^{-1}$)	1,944,944	1,169,238	1,007,191

Appendix 4: Respirometric data

Table 4-1: Hibernia summer % oxygen saturation in the headspace of the microcosm flasks.

Day	% Oxygen Saturation								
	Oil Avg	StDev	Oil+Dispersant		Dispersant		Seawater		Sterile Control
			Avg	StDev	Avg	StDev	Avg	StDev	
0	21.70	0.40	21.06	0.32	21.02	0.28	21.07	0.05	20.54
1	20.50	0.09	20.78	0.10	21.69	0.22	21.50	0.14	20.51
2	20.19	0.33	20.25	0.07	21.23	0.28	21.49	0.01	20.06
3	18.81	0.74	18.14	0.14	19.34	0.08	19.50	0.13	17.93
4	18.64	0.19	17.81	0.20	19.48	0.05	19.72	0.04	18.32
5	20.13	0.06	19.32	0.22	21.45	0.41	21.52	0.16	19.72
6	20.41	0.13	18.99	0.04	21.48	0.10	21.75	0.10	20.09
7	20.49	0.06	19.80	0.22	21.89	0.03	22.34	0.12	20.09
10	20.69	1.17	19.12	0.45	21.84	0.15	22.17	0.42	19.57
14	19.31	0.50	17.97	0.14	21.03	0.08	21.39	0.22	18.89
18	18.59	0.24	17.58	0.29	21.28	0.14	21.61	0.10	19.16
21	18.14	0.11	17.49	0.28	21.26	0.06	21.76	0.17	19.10
26	18.23	0.12	17.36	0.22	20.76	0.11	21.02	0.21	19.54
33	17.41	0.05	17.09	0.30	21.08	0.08	21.65	0.17	19.07
41	16.85	0.04	16.52	0.23	20.57	0.12	21.05	0.16	18.55

Table 4-2: Hibernia winter % oxygen saturation in the headspace of the microcosm flasks.

		% Oxygen Saturation								
Day	Oil Avg	StDev	Oil+Dispersant		Dispersant		Seawater		Sterile Control	
			Avg	StDev	Avg	StDev	Avg	StDev	Avg	Stdev
0	21.38	0.07	21.64	0.17	21.38	0.08	21.74	0.19	21.29	0.29
1	19.93	0.29	19.50	0.11	20.53	0.35	20.57	0.18	19.36	0.56
2	20.27	0.22	19.67	0.05	21.47	0.34	21.37	0.18	19.68	0.57
3	20.06	0.21	19.61	0.03	21.88	0.26	21.81	0.36	19.31	0.47
4	18.47	0.13	18.01	0.11	20.42	0.18	20.48	0.25	18.06	0.55
5	18.23	0.20	17.82	0.14	20.50	0.40	20.46	0.20	17.80	0.46
6	18.91	0.29	18.42	0.19	21.57	0.39	21.56	0.46	18.59	0.57
7	19.08	0.26	18.52	0.26	21.83	0.32	21.87	0.19	18.78	0.59
8	19.07	0.13	18.74	0.27	22.09	0.33	22.18	0.28	18.73	0.49
10	18.54	0.35	18.04	0.51	21.39	0.19	21.53	0.17	17.97	0.43
11	18.54	0.44	17.74	0.26	21.56	0.27	21.64	0.19	17.94	0.39
12	18.98	0.52	17.93	0.25	22.09	0.14	22.18	0.18	18.40	0.45
14	18.36	0.53	17.13	0.26	21.51	0.27	21.60	0.17	17.73	0.40
17	18.62	0.66	17.17	0.28	21.83	0.20	22.02	0.22	17.62	0.39
22	16.81	0.69	15.48	0.23	20.33	0.20	20.50	0.24	16.36	0.34
25	17.81	1.07	16.42	0.16	21.61	0.29	21.44	0.19	17.36	0.92
28	17.22	0.65	15.87	0.55	20.76	0.27	20.88	0.20	16.30	0.38
32	17.10	0.80	15.87	0.26	21.40	0.26	21.52	0.22	16.83	0.52
35	17.32	0.52	15.86	0.19	21.51	0.37	21.57	0.21	16.60	0.26
38	16.63	0.73	15.50	0.18	21.02	0.20	21.22	0.40	15.83	0.33
43	17.40	0.68	16.26	0.19	22.00	0.23	22.26	0.21	16.76	0.35

Table 4-3: Terra Nova summer % oxygen saturation in the headspace of the microcosm flasks.

Day	% Oxygen Saturation								
	Oil		Oil+Dispersant		Dispersant		Seawater		Sterile Control
	Avg	StDev	Avg	StDev	Avg	StDev	Avg	StDev	
0	21.51	0.18	21.56	0.17	22.21	0.26	21.72	0.36	21.84
1	20.12	0.11	19.96	0.12	21.00	0.08	20.87	0.29	20.04
2	18.31	0.19	18.18	0.16	19.10	0.21	19.21	0.30	18.21
3	18.13	0.07	18.03	0.19	19.10	0.12	19.27	0.25	18.12
4	20.28	0.05	19.96	0.24	21.37	0.09	21.49	0.20	20.21
5	20.04	0.16	19.29	0.28	21.09	0.08	21.31	0.15	20.13
6	20.56	0.28	19.41	0.38	21.72	0.03	21.85	0.12	20.42
9	20.08	0.39	18.81	0.38	21.33	0.28	21.55	0.28	19.98
13	19.01	0.11	17.87	0.63	20.67	0.06	20.77	0.15	19.51
17	18.92	0.16	17.73	0.16	21.09	0.15	21.29	0.13	19.73
20	18.61	0.14	17.71	0.14	21.07	0.18	21.32	0.15	19.64
25	18.23	0.12	17.36	0.22	20.76	0.11	21.02	0.21	19.54
32	18.20	0.21	17.52	0.18	21.10	0.16	21.35	0.16	19.55
40	17.62	0.07	16.92	0.18	20.52	0.11	20.74	0.19	19.09
42	17.59	0.04	17.07	0.08	20.70	0.11	20.82	0.21	19.06

Table 4-4: Terra Nova winter % oxygen saturation in the headspace of the microcosm flasks.

Day	% Oxygen Saturation									
	Oil		Oil+Dispersant		Dispersant		Seawater		Sterile Control	
	Avg	StDev	Avg	StDev	Avg	StDev	Avg	StDev	Avg	StDev
0	20.54	0.25	20.62	0.14	20.67	0.22	20.93	0.15	20.90	0.09
1	19.96	0.57	20.30	0.18	20.66	0.80	20.41	0.24	20.03	0.44
2	20.28	0.54	20.39	0.08	21.49	0.59	21.21	0.39	20.32	0.41
3	20.10	0.57	20.30	0.15	21.67	0.48	21.50	0.45	20.14	0.31
4	18.71	0.42	18.68	0.04	20.30	0.33	20.33	0.50	18.69	0.22
5	18.62	0.46	18.43	0.05	20.20	0.38	20.09	0.52	18.46	0.15
6	19.48	0.51	19.17	0.05	21.27	0.38	21.16	0.54	19.24	0.18
7	19.62	0.51	19.23	0.10	21.64	0.44	21.46	0.64	19.44	0.19
8	19.59	0.44	19.21	0.08	21.76	0.12	21.87	0.63	19.47	0.18
10	18.79	0.77	18.34	0.12	21.13	0.21	21.03	0.48	18.80	0.19
11	18.69	0.74	18.20	0.15	21.13	0.15	21.12	0.49	18.56	0.05
12	19.13	0.73	18.43	0.17	21.61	0.08	21.61	0.53	19.07	0.07
14	18.58	0.97	17.81	0.30	21.39	0.17	21.17	0.51	18.43	0.05
17	18.69	1.01	17.90	0.32	21.70	0.17	21.62	0.47	18.38	0.10
22	17.43	1.14	16.66	0.41	20.60	0.17	20.42	0.40	17.38	0.10
25	17.96	1.26	17.64	1.35	21.41	0.17	21.34	0.48	17.86	0.17
28	17.27	1.33	16.37	0.48	20.63	0.20	20.80	0.61	17.20	0.09
32	17.91	1.46	16.73	0.52	21.57	0.31	21.37	0.43	17.69	0.08
35	17.86	1.22	16.33	0.43	20.83	0.18	21.12	0.45	17.48	0.15
38	17.59	1.76	16.81	0.58	21.20	0.26	21.27	0.89	16.81	0.11
43	18.06	1.57	16.82	0.26	21.70	0.21	21.93	0.49	17.68	0.12

Table 4-5: Sable summer % oxygen saturation in the headspace of the microcosm flasks.

	% Oxygen Saturation							
	Condensate		Cond+ Disp*	Dispersant		Seawater		Sterile Control
	Avg	StDev		Avg	StDev	Avg	StDev	
0	20.46	0.18	21.25	21.30	0.25	21.69	0.44	20.87
1	17.40	0.44	17.75	20.92	0.49	21.15	0.23	18.74
2	17.24	0.51	17.19	21.25	0.41	21.66	0.17	18.53
5	15.99	0.51	15.45	20.73	0.37	21.33	0.17	17.66
9	14.77	0.27	12.88	20.29	0.39	20.77	0.34	16.93
13	14.81	0.25	12.14	20.80	0.46	21.30	0.27	17.33
16	14.66	0.28	12.31	20.79	0.32	21.26	0.24	17.33
21	14.29	0.22	12.22	20.42	0.45	21.20	0.42	16.90
28	14.09	0.19	12.56	20.74	0.48	21.37	0.12	17.10
36	13.47	0.26	12.40	20.29	0.40	20.85	0.30	16.69
42	13.45	0.22	12.43	21.02	0.63	21.15	0.09	16.79

*2 replicates dropped due to loose caps

Table 4-6: Sable winter % oxygen saturation in the headspace of the microcosm flasks.

	% Oxygen Saturation									
Day	Condensate		Condensate +Dispersant		Dispersant		Seawater		Sterile Control	
	Avg	StDev	Avg	StDev	Avg	StDev	Avg	StDev	Avg	StDev
0	18.59	0.57	18.53	0.13	21.78	0.33	21.54	0.27	18.37	0.07
1	16.24	0.09	16.33	0.07	21.11	0.33	21.06	0.14	16.21	0.03
2	15.52	0.81	15.36	0.46	20.78	0.69	20.52	0.34	14.90	0.05
3	15.29	0.11	15.54	0.30	21.59	0.39	21.64	0.42	15.27	0.05
4	15.08	0.15	15.26	0.11	22.16	0.52	22.61	1.51	15.31	0.35
5	14.41	0.11	14.47	0.05	21.16	0.05	21.20	0.15	14.29	0.03
6	13.66	0.12	13.71	0.09	20.33	0.12	20.46	0.19	13.42	0.04
7	12.79	0.11	12.77	0.05	19.44	0.07	19.61	0.13	12.89	0.03
8	14.16	0.12	14.19	0.08	22.00	0.00	22.26	0.11	14.30	0.00
9	13.63	0.11	13.66	0.05	21.13	0.05	21.32	0.19	13.70	0.00
10	13.46	0.12	13.47	0.05	21.27	0.18	21.34	0.15	13.40	0.00
11	12.37	0.14	12.27	0.05	20.66	0.49	20.23	0.35	12.26	0.09
13	12.72	0.15	12.63	0.10	20.97	0.48	20.81	0.25	12.60	0.00
14	12.71	0.23	12.59	0.08	21.06	0.51	20.90	0.17	13.08	0.77
15	11.88	0.21	11.71	0.08	19.82	0.39	19.74	0.23	11.77	0.05
16	11.80	0.44	11.60	0.09	19.64	0.42	19.54	0.15	11.57	0.05
17	12.27	0.35	12.02	0.07	20.60	0.58	20.42	0.16	12.07	0.05
18	12.47	0.39	12.29	0.20	20.93	0.58	20.77	0.18	12.17	0.05
19	12.56	0.35	12.42	0.19	21.02	0.29	21.11	0.25	12.27	0.05
21	12.18	0.36	12.12	0.21	20.66	0.51	20.50	0.17	11.78	0.30
22	12.22	0.37	12.11	0.53	20.61	0.32	20.59	0.15	11.90	0.09
23	12.52	0.40	12.52	0.26	21.11	0.25	21.20	0.21	12.17	0.05
24	12.24	0.39	12.37	0.26	20.87	0.48	20.79	0.16	11.83	0.07
27	12.16	0.32	12.31	0.25	20.79	0.39	20.73	0.13	11.76	0.05
32	11.77	0.23	11.89	0.25	20.06	0.39	19.96	0.22	11.14	0.07
35	12.47	0.64	12.31	0.28	20.78	0.25	20.81	0.16	11.46	0.12
35	13.48	1.05	14.47	0.18	21.38	0.10	21.61	0.22	12.08	0.07
38	13.33	0.79	14.38	0.26	20.91	0.16	21.00	0.09	12.44	0.11
42	13.90	0.86	14.97	0.30	21.46	0.15	21.62	0.11	13.03	0.11

Appendix 5: Hydrocarbon Fraction degradation kinetics (%biodegradation) for Hibernia, Terra Nova and Thebaud.

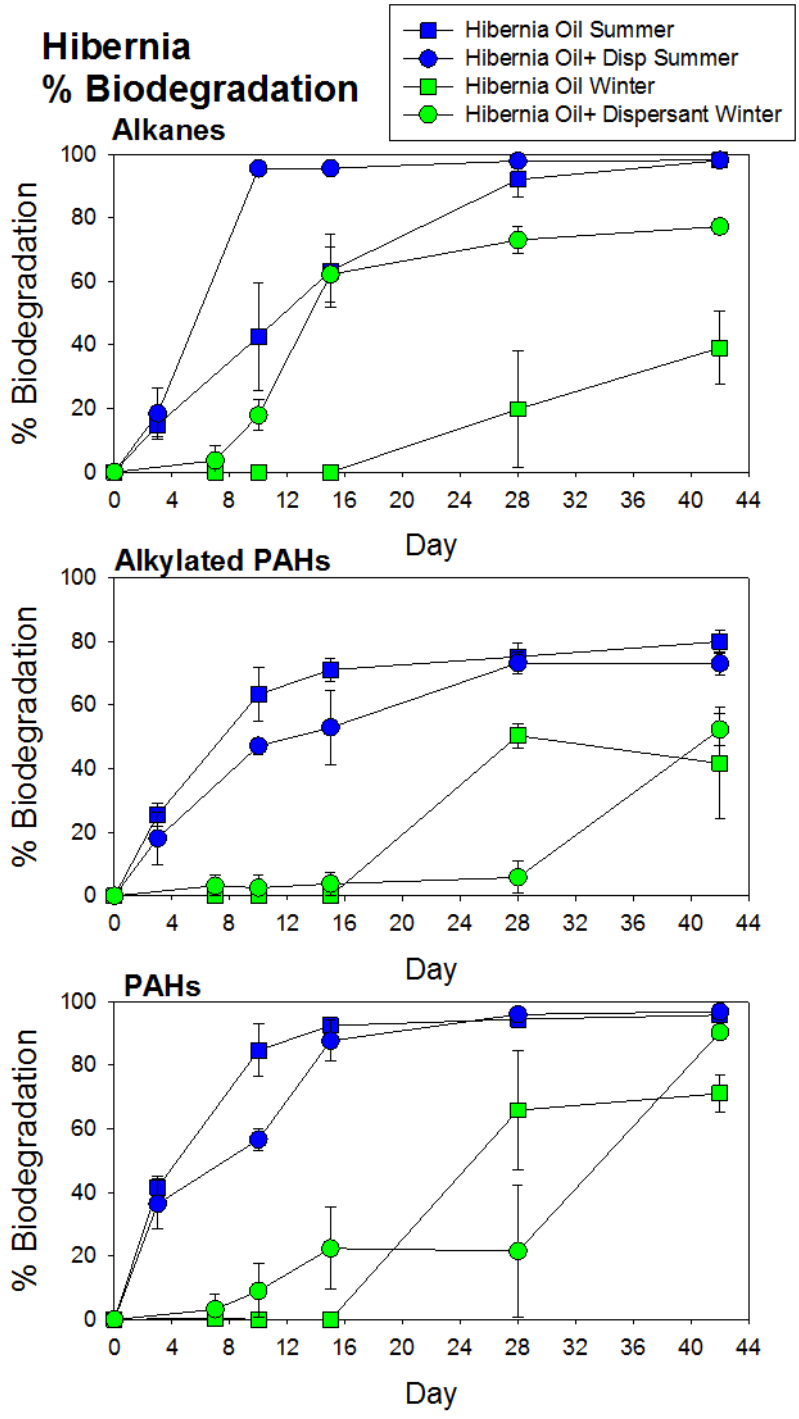

Figure 5-1: Hydrocarbon degradation rates for Hibernia in summer and winter for alkanes, Alkylated PAHs and PAHs.

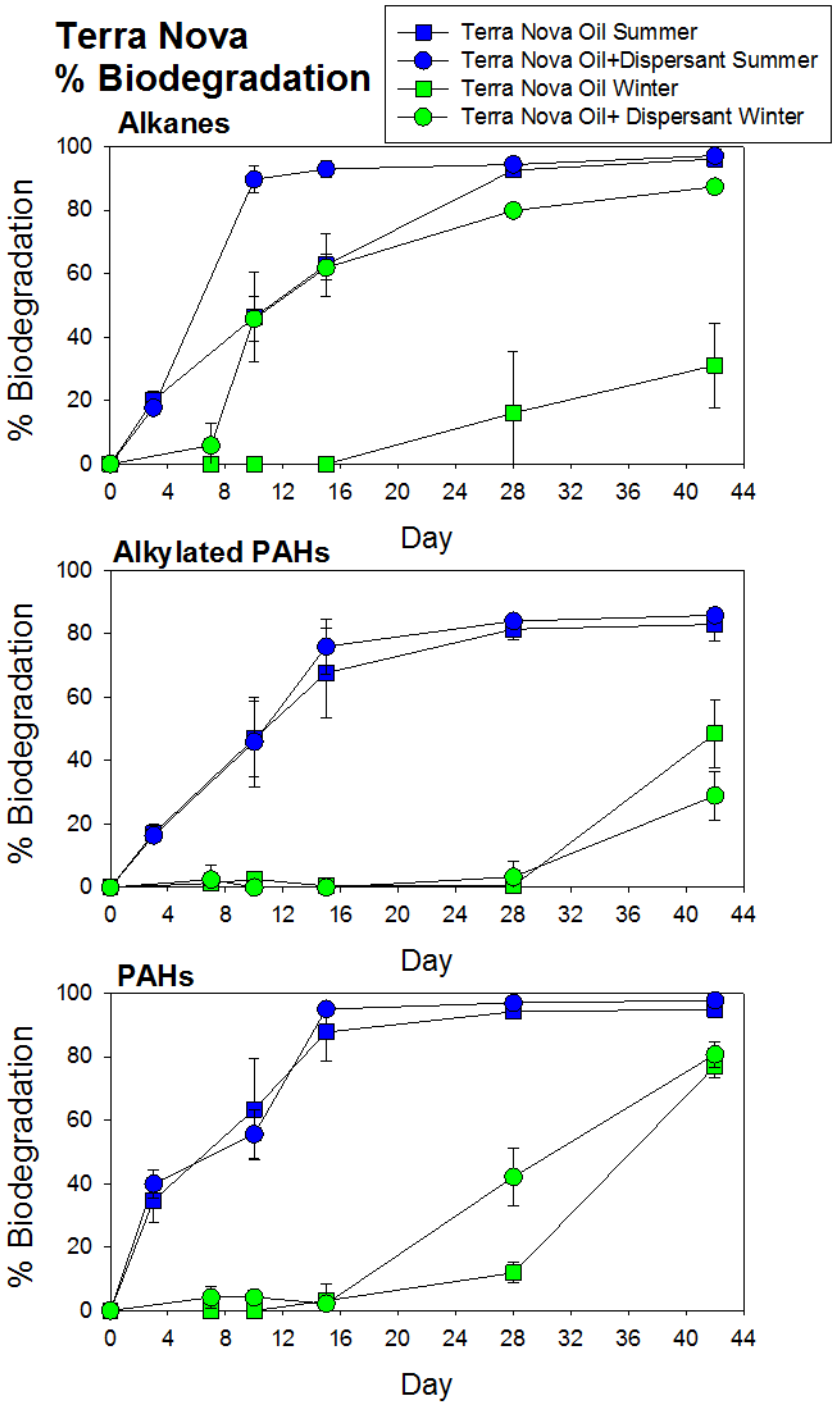

Figure 5-2: Hydrocarbon degradation rates for Terra Nova in summer and winter for alkanes, Alkylated PAHs and PAHs.

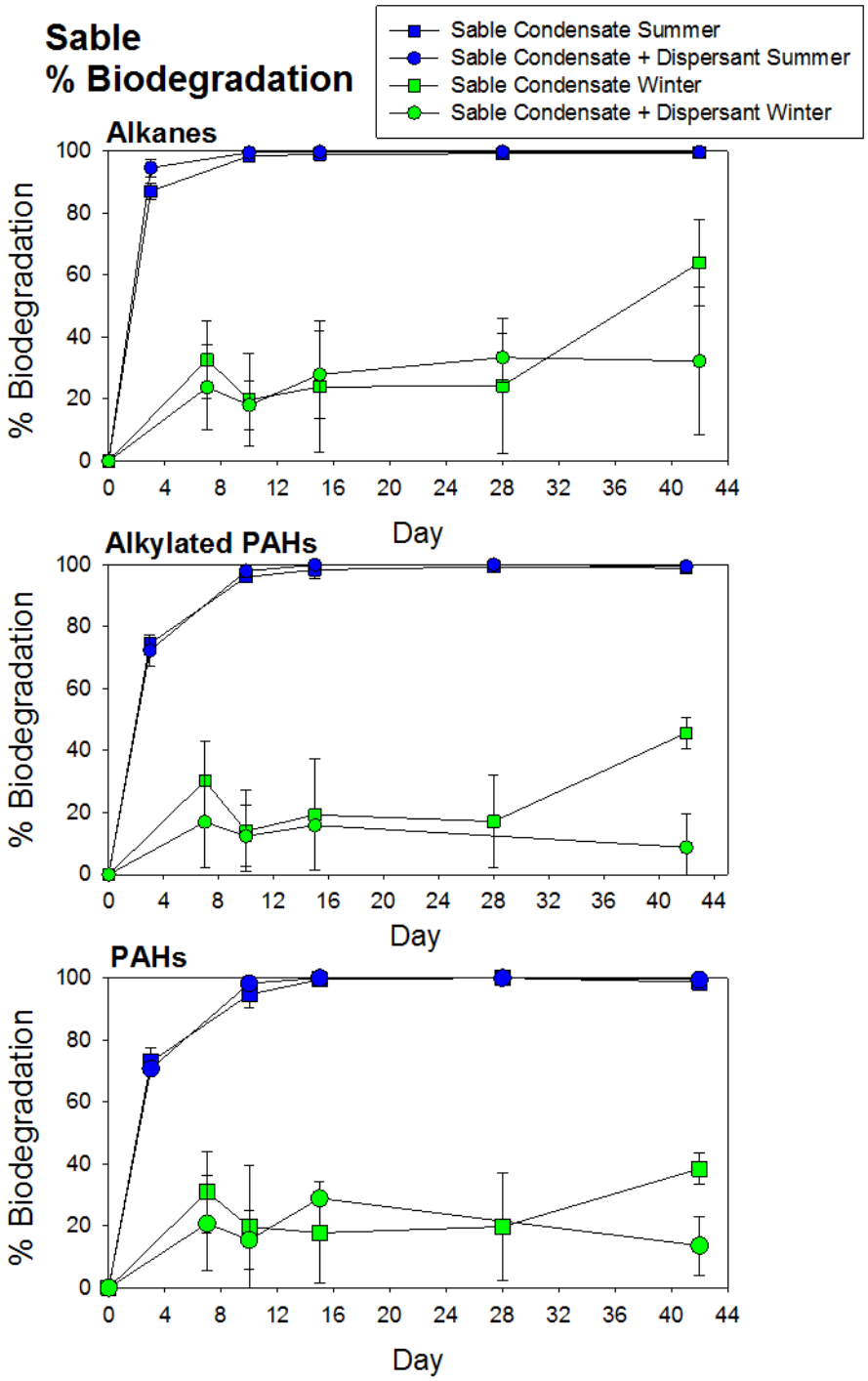

Figure 5-3: Hydrocarbon degradation rates for Thebaud (Sable) in summer and winter for alkanes, Alkylated PAHs and PAHs.

Appendix 6: Sample ID key table

Table 6-1: Sample ID key table

Sample ID	Platform	Season	Treatment	Time point (days)
394810	Hibernia	Summer	Control	0
394811	Hibernia	Summer	Control	0
394812	Hibernia	Summer	Control	0
H1G	Hibernia	Summer	SW/BH + Oil	5
H2G	Hibernia	Summer	SW/BH + Oil	5
H3G	Hibernia	Summer	SW/BH + Oil	5
H4G	Hibernia	Summer	SW/BH + Oil	42
H6G	Hibernia	Summer	SW/BH + Oil	42
H7G	Hibernia	Summer	SW/BH + Oil/Disp	5
H8G	Hibernia	Summer	SW/BH + Oil/Disp	5
H9G	Hibernia	Summer	SW/BH + Oil/Disp	5
H10G	Hibernia	Summer	SW/BH + Oil/Disp	42
H11G	Hibernia	Summer	SW/BH + Oil/Disp	42
H12G	Hibernia	Summer	SW/BH + Oil/Disp	42
H13G	Hibernia	Summer	SW/BH + Disp	42
H14G	Hibernia	Summer	SW/BH + Disp	42
H15G	Hibernia	Summer	SW/BH + Disp	42
H16G	Hibernia	Summer	SW/BH	42
H17G	Hibernia	Summer	SW/BH	42
H18G	Hibernia	Summer	SW/BH	42
H381402	Hibernia	winter	Control	0
H381404	Hibernia	winter	Control	0
H381405	Hibernia	winter	Control	0
H381406	Hibernia	winter	Control	0
H1GW	Hibernia	winter	SW/BH + Oil	7
H5GW	Hibernia	winter	SW/BH + Oil	7
H6GW	Hibernia	winter	SW/BH + Oil	7
H7GW	Hibernia	winter	SW/BH + Oil/Disp	7
H8GW	Hibernia	winter	SW/BH + Oil/Disp	7
H9GW	Hibernia	winter	SW/BH + Oil/Disp	7
H10GW	Hibernia	winter	SW/BH + Oil	42
H11GW	Hibernia	winter	SW/BH + Oil	42
H12GW	Hibernia	winter	SW/BH + Oil	42
H13GW	Hibernia	winter	SW/BH + Oil/Disp	42
H14GW	Hibernia	winter	SW/BH + Oil/Disp	42
H15GW	Hibernia	winter	SW/BH + Oil/Disp	42
H16GW	Hibernia	winter	SW/BH + Disp	42
H17GW	Hibernia	winter	SW/BH + Disp	42
H18GW	Hibernia	winter	SW/BH + Disp	42
H19GW	Hibernia	winter	SW/BH	42
H20GW	Hibernia	winter	SW/BH	42
H21GW	Hibernia	winter	SW/BH	42

395160	Thebaud	Summer	Control	0
395161	Thebaud	Summer	Control	0
395162	Thebaud	Summer	Control	0
S1G	Thebaud	Summer	SW/BH + Oil	5
S2G	Thebaud	Summer	SW/BH + Oil	5
S3G	Thebaud	Summer	SW/BH + Oil	5
S4G	Thebaud	Summer	SW/BH + Oil	42
S5G	Thebaud	Summer	SW/BH + Oil	42
S6G	Thebaud	Summer	SW/BH + Oil	42
S7G	Thebaud	Summer	SW/BH + Oil/Disp	5
S8G	Thebaud	Summer	SW/BH + Oil/Disp	5
S9G	Thebaud	Summer	SW/BH + Oil/Disp	5
S10G	Thebaud	Summer	SW/BH + Oil/Disp	42
S11G	Thebaud	Summer	SW/BH + Oil/Disp	42
S12G	Thebaud	Summer	SW/BH + Oil/Disp	42
S13G	Thebaud	Summer	SW/BH + Disp	42
S14G	Thebaud	Summer	SW/BH + Disp	42
S15G	Thebaud	Summer	SW/BH + Disp	42
S16G	Thebaud	Summer	SW/BH	42
S17G	Thebaud	Summer	SW/BH	42
S18G	Thebaud	Summer	SW/BH	42
TB381401A	Thebaud	winter	Control	0
TB381401B	Thebaud	winter	Control	0
TB381401C	Thebaud	winter	Control	0
TB1GW	Thebaud	winter	SW/BH + Oil	7
TB2GW	Thebaud	winter	SW/BH + Oil	7
TB4GW	Thebaud	winter	SW/BH + Oil	7
TB7GW	Thebaud	winter	SW/BH + Oil/Disp	7
TB8GW	Thebaud	winter	SW/BH + Oil/Disp	7
TB9GW	Thebaud	winter	SW/BH + Oil/Disp	7
TB10GW	Thebaud	winter	SW/BH + Oil	42
TB11GW	Thebaud	winter	SW/BH + Oil	42
TB12GW	Thebaud	winter	SW/BH + Oil	42
TB13GW	Thebaud	winter	SW/BH + Oil/Disp	42
TB14GW	Thebaud	winter	SW/BH + Oil/Disp	42
TB15GW	Thebaud	winter	SW/BH + Oil/Disp	42
TB16GW	Thebaud	winter	SW/BH + Disp	42
TB17GW	Thebaud	winter	SW/BH + Disp	42
TB18GW	Thebaud	winter	SW/BH + Disp	42
TB19GW	Thebaud	winter	SW/BH	42
TB20GW	Thebaud	winter	SW/BH	42
TB21GW	Thebaud	winter	SW/BH	42
394913	Terranova	Summer	Control	0
394914	Terranova	Summer	Control	0
394915	Terranova	Summer	Control	0

T1G	Terranova	Summer	SW/BH + Oil	5
T2G	Terranova	Summer	SW/BH + Oil	5
T3G	Terranova	Summer	SW/BH + Oil	5
T5G	Terranova	Summer	SW/BH + Oil	42
T6G	Terranova	Summer	SW/BH + Oil	42
T7G	Terranova	Summer	SW/BH + Oil/Disp	5
T8G	Terranova	Summer	SW/BH + Oil/Disp	5
T9G	Terranova	Summer	SW/BH + Oil/Disp	5
T10G	Terranova	Summer	SW/BH + Oil/Disp	42
T11G	Terranova	Summer	SW/BH + Oil/Disp	42
T12G	Terranova	Summer	SW/BH + Oil/Disp	42
T13G	Terranova	Summer	SW/BH + Disp	42
T14G	Terranova	Summer	SW/BH + Disp	42
T15G	Terranova	Summer	SW/BH + Disp	42
T16G	Terranova	Summer	SW/BH	42
T17G	Terranova	Summer	SW/BH	42
T18G	Terranova	Summer	SW/BH	42
TN381403	Terranova	winter	Control	0
TN381407	Terranova	winter	Control	0
TN381408	Terranova	winter	Control	0
TN381409	Terranova	winter	Control	0
TN3GW	Terranova	winter	SW/BH + Oil	7
TN5GW	Terranova	winter	SW/BH + Oil	7
TN6GW	Terranova	winter	SW/BH + Oil	7
TN7GW	Terranova	winter	SW/BH + Oil/Disp	7
TN8GW	Terranova	winter	SW/BH + Oil/Disp	7
TN9GW	Terranova	winter	SW/BH + Oil/Disp	7
TN10GW	Terranova	winter	SW/BH + Oil	42
TN11GW	Terranova	winter	SW/BH + Oil	42
TN12GW	Terranova	winter	SW/BH + Oil	42
TN13GW	Terranova	winter	SW/BH + Oil/Disp	42
TN14GW	Terranova	winter	SW/BH + Oil/Disp	42
TN15GW	Terranova	winter	SW/BH + Oil/Disp	42
TN16GW	Terranova	winter	SW/BH + Disp	42
TN17GW	Terranova	winter	SW/BH + Disp	42
TN18GW	Terranova	winter	SW/BH + Disp	42
TN19GW	Terranova	winter	SW/BH	42
TN20GW	Terranova	winter	SW/BH	42
TN21GW	Terranova	winter	SW/BH	42

Appendix 7: Metagenomics sequencing reads: processing statistics.

Table 7-1: Metagenomics sequencing reads

Sample name	Raw fragments	Surviving fragments	Surviving fragments %	Total reads QCed	Mapped Reads	Mapped reads %
394773	4,325,569	4,296,096	99%	8,336,230	5,815,395	69%
394774	7,093,402	7,009,808	98%	13,474,750	9,716,244	72%
394775	12,035,062	11,903,647	98%	22,418,232	16,389,241	73%
394777	3,152,021	3,122,450	99%	6,041,014	4,009,234	66%
394778	4,072,546	3,987,815	97%	7,563,880	5,042,355	66%
394779	9,958,763	9,887,337	99%	19,090,252	13,983,000	73%
394781	6,279,343	6,172,318	98%	11,916,892	8,291,844	69%
394782	11,959,336	11,845,812	99%	22,920,448	16,786,348	73%
394783	11,880,339	11,803,968	99%	22,361,960	17,502,917	78%
394785	9,266,380	9,076,313	97%	17,598,326	11,985,900	68%
394786	10,968,178	10,855,821	98%	20,928,084	15,189,989	72%
394787	8,286,087	8,204,499	99%	15,744,284	11,266,413	71%
394789	9,421,979	9,317,750	98%	18,103,800	12,910,803	71%
394790	15,296,366	15,069,319	98%	28,673,744	22,119,371	77%
394791	12,245,546	12,125,631	99%	23,417,154	16,259,685	69%
394794	12,210,634	12,114,816	99%	23,362,918	18,184,048	77%
394795	7,064,579	6,922,230	97%	13,260,100	10,499,811	79%
394796	6,658,429	6,583,560	98%	12,819,770	9,155,731	71%
394798	4,025,842	3,976,287	98%	7,786,098	5,115,554	65%
394799	4,735,137	4,666,043	98%	9,004,432	6,009,081	66%
394800	1,154,944	1,127,264	97%	2,105,640	1,679,141	79%
394802	12,121,215	12,007,312	99%	22,902,268	17,171,674	74%
394803	4,220,959	4,173,155	98%	8,122,610	5,748,678	70%
394804	4,088,628	3,972,477	97%	7,281,724	5,727,374	78%
394806	9,237,245	9,153,384	99%	17,854,694	12,792,536	71%
394807	1,861,070	1,839,120	98%	3,570,018	2,545,937	71%
394808	8,689,011	8,595,956	98%	16,707,106	11,344,764	67%
394897	5,815,771	5,775,525	99%	11,161,712	8,639,537	77%
394898	14,629,948	14,513,026	99%	27,809,272	23,093,172	83%
394899	1,297,852	1,229,853	94%	2,160,178	1,966,257	91%
394901	2,337,124	2,257,671	96%	4,262,408	3,449,585	80%
394902	7,591,195	7,502,903	98%	14,312,548	10,744,808	75%
394903	3,010,856	2,938,590	97%	5,571,476	4,290,549	77%
394905	4,186,407	4,063,437	97%	7,825,102	5,639,727	72%
394906	3,815,382	3,732,139	97%	7,067,192	5,457,606	77%
394907	8,631,208	8,558,023	99%	16,258,518	12,545,076	77%
394909	4,502,380	4,431,461	98%	8,214,122	7,302,562	88%
394910	5,996,326	5,877,104	98%	11,101,632	8,267,601	74%

394911	8,041,631	7,945,327	98%	15,388,856	10,925,522	70%
394940	15,247,292	15,016,297	98%	28,558,202	23,727,663	83%
394941	10,258,517	10,152,846	98%	19,457,906	15,177,426	78%
394942	7,135,379	7,068,223	99%	13,619,156	10,125,414	74%
394944	9,856,469	9,745,512	98%	18,675,288	13,374,707	71%
394945	14,574,767	14,231,420	97%	26,868,480	19,310,324	71%
394946	10,851,042	10,762,228	99%	20,731,192	14,128,155	68%
394948	657,055	637,848	97%	1,185,056	809,162	68%
394949	7,821,958	7,745,773	99%	14,764,218	10,521,714	71%
394950	8,714,272	8,569,687	98%	16,599,646	10,225,250	61%
394952	3,762,625	3,711,604	98%	7,254,810	5,048,912	69%
394953	4,324,181	4,241,156	98%	8,221,826	5,730,426	69%
394954	3,426,798	3,368,943	98%	6,472,354	4,668,809	72%
394956	4,865,715	4,811,841	98%	9,302,810	6,656,375	71%
394957	4,817,607	4,628,317	96%	8,691,368	6,740,721	77%
394958	7,233,403	7,062,911	97%	13,610,896	9,672,722	71%
395154	3,740,364	3,669,423	98%	7,103,370	4,630,245	65%
395158	3,787,140	3,694,987	97%	7,001,904	4,976,492	71%
395257	989,890	965,640	97%	1,893,852	1,287,488	67%
395258	1,582,794	1,547,545	97%	3,004,686	1,979,966	65%
395260	1,422,039	1,385,336	97%	2,673,388	1,670,246	62%
395261	3,574,912	3,542,092	99%	6,856,738	4,790,715	69%
395262	3,244,028	3,197,561	98%	6,109,358	4,125,415	67%
H10G	6,793,707	6,682,348	98%	12,565,992	12,246,266	97%
H10GW	6,105,117	6,032,288	98%	11,875,260	11,239,632	94%
H11G	10,948,887	10,776,134	98%	20,732,184	20,339,399	98%
H11GW	3,561,190	3,508,857	98%	6,968,796	6,757,145	96%
H12G	25,565,798	25,207,348	98%	48,808,578	47,995,098	98%
H12GW	11,601,894	11,359,688	97%	22,136,780	21,638,552	97%
H13G	22,732,872	22,411,389	98%	43,707,024	42,183,579	96%
H13GW	12,424,527	12,216,062	98%	23,686,292	23,259,808	98%
H14G	25,610,187	25,184,367	98%	48,966,634	47,388,749	96%
H14GW	11,019,606	10,817,136	98%	21,195,070	20,768,783	97%
H15G	23,897,142	23,572,077	98%	45,673,668	44,238,548	96%
H15GW	10,813,322	10,634,701	98%	20,682,298	20,345,310	98%
H16G	22,593,976	22,330,135	98%	42,991,446	40,644,484	94%
H16GW	10,295,076	10,161,792	98%	19,802,564	18,618,128	94%
H17G	6,102,475	6,025,031	98%	11,864,894	11,306,033	95%
H17GW	7,025,629	6,901,338	98%	13,475,520	12,663,134	93%
H18G	20,924,054	20,639,705	98%	40,117,066	38,523,654	96%
H18GW	11,880,238	11,654,232	98%	22,352,776	20,865,639	93%
H19GW	7,446,726	7,397,167	99%	14,534,896	12,962,232	89%
H1G	23,830,361	23,549,653	98%	45,358,608	44,804,052	98%

H20GW	12,925,302	12,823,126	99%	24,957,164	22,860,729	91%
H21GW	8,147,637	8,064,525	98%	15,704,688	14,546,535	92%
H2G	26,099,575	25,828,607	98%	49,577,542	47,670,532	96%
H2GW	8,348,416	8,291,818	99%	16,245,480	13,097,502	80%
H381402	11,035,710	10,868,616	98%	20,910,978	13,770,850	65%
H381404	9,547,549	9,424,711	98%	18,124,294	11,571,800	63%
H381405	12,839,165	12,703,128	98%	24,539,244	17,049,709	69%
H381406	2,191,892	2,156,555	98%	4,264,444	2,576,580	60%
H3G	30,303,076	30,061,804	99%	57,596,462	57,103,402	99%
H3GW	4,766,656	4,737,356	99%	9,287,508	7,726,304	83%
H4G	10,654,706	10,537,611	98%	20,025,130	19,535,748	97%
H4GW	7,326,342	7,267,435	99%	14,181,870	12,100,806	85%
H6G	21,243,898	20,955,942	98%	40,239,016	39,741,302	98%
H7G	20,476,983	20,210,170	98%	38,865,382	37,989,749	97%
H7GW	11,161,318	11,092,263	99%	21,611,030	20,832,736	96%
H8G	21,387,775	21,051,017	98%	40,497,404	39,790,501	98%
H8GW	7,669,907	7,604,361	99%	14,936,036	14,363,298	96%
H9G	16,737,153	16,498,042	98%	31,770,606	30,841,283	97%
H9GW	8,780,854	8,738,521	99%	17,008,290	16,547,794	97%
S10G	14,404,271	14,215,276	98%	27,791,242	26,920,957	96%
S11G	9,572,095	9,448,646	98%	16,752,634	16,465,704	98%
S12G	8,685,401	8,544,573	98%	15,915,744	15,498,028	97%
S13G	20,817,800	20,593,016	98%	39,411,238	37,053,778	94%
S14G	22,089,989	21,835,951	98%	41,729,654	38,791,895	92%
S15G	22,707,679	22,336,057	98%	42,103,978	39,835,263	94%
S16G	24,405,536	24,162,832	99%	46,022,882	43,752,630	95%
S17G	14,564,298	14,385,668	98%	27,692,886	25,586,026	92%
S18G	18,109,243	17,989,246	99%	33,853,986	31,752,110	93%
S1G	16,881,835	16,725,084	99%	32,739,260	27,788,367	84%
S2G	17,760,409	17,503,598	98%	34,222,484	32,637,306	95%
S394918A	2,688,956	2,626,432	97%	5,164,098	1,793,719	34%
S394918B	3,964,185	3,837,845	96%	7,496,194	2,835,784	37%
S394918C	7,825,009	7,642,918	97%	14,812,752	6,655,087	44%
S395099A	5,218,363	5,101,157	97%	9,842,356	4,207,142	42%
S395099B	7,640,721	7,477,866	97%	14,134,074	6,819,371	48%
S395099C	4,855,468	4,753,807	97%	9,314,412	3,772,179	40%
S395263A	555,547	535,929	96%	1,043,056	453,210	43%
S395263B	298,980	293,166	98%	569,472	249,619	43%
S395263C	887,346	855,354	96%	1,659,550	659,200	39%
S3G	22,626,807	22,347,913	98%	43,518,720	41,153,184	94%
S4G	23,538,209	23,218,446	98%	45,325,292	43,765,692	96%
S5G	15,519,235	15,256,264	98%	29,892,162	28,990,628	96%
S6G	17,447,386	17,195,768	98%	33,410,474	32,369,547	96%

S7G	23,572,448	23,307,421	98%	45,235,690	44,337,700	98%
S8G	19,133,419	18,922,952	98%	36,994,106	35,153,690	95%
S9G	26,097,961	25,822,093	98%	49,209,242	47,272,518	96%
T10G	18,432,090	18,104,530	98%	35,250,118	34,120,053	96%
T11G	18,068,820	17,769,472	98%	34,569,106	33,317,987	96%
T12G	3,235,820	3,147,505	97%	6,030,758	5,851,916	97%
T13G	21,220,643	20,954,493	98%	40,603,346	38,317,547	94%
T14G	22,287,906	22,004,152	98%	42,631,706	39,584,205	92%
T15G	11,772,348	11,629,736	98%	22,728,814	20,901,004	91%
T16G	20,956,556	20,689,240	98%	39,660,392	37,880,796	95%
T17G	22,390,850	22,132,228	98%	42,362,224	40,880,129	96%
T18G	22,281,265	22,011,116	98%	41,889,136	40,688,178	97%
T1G	20,473,490	20,242,246	98%	39,246,254	35,644,172	90%
T2G	22,172,048	21,998,701	99%	43,034,494	39,551,332	91%
T3G	26,477,961	26,200,363	98%	51,096,726	46,251,201	90%
T5G	17,103,040	16,868,006	98%	33,079,484	32,345,716	97%
T6G	18,069,101	17,728,357	98%	34,597,490	33,146,918	95%
T7G	22,480,782	22,232,779	98%	43,384,858	41,458,979	95%
T8G	26,799,528	26,520,979	98%	51,572,974	50,110,257	97%
T9G	17,857,966	17,719,918	99%	34,475,216	33,479,727	97%
TB10GW	12,523,976	12,428,721	99%	24,245,250	23,577,239	97%
TB11GW	2,523,477	2,486,128	98%	4,865,970	3,152,546	64%
TB12GW	10,633,019	10,539,121	99%	20,386,102	20,098,597	98%
TB13GW	13,774,070	13,632,094	98%	26,462,708	25,712,169	97%
TB14GW	14,126,648	14,019,582	99%	27,307,444	26,563,686	97%
TB15GW	10,584,167	10,420,696	98%	20,341,680	19,487,873	95%
TB16GW	13,397,780	13,229,887	98%	25,627,014	21,348,874	83%
TB17GW	15,692,761	15,452,464	98%	30,030,986	25,384,056	84%
TB18GW	10,218,207	10,062,312	98%	19,532,520	15,377,695	78%
TB19GW	7,637,285	7,507,752	98%	14,748,366	11,172,835	75%
TB20GW	6,983,874	6,871,241	98%	13,392,878	10,039,308	74%
TB21GW	11,259,280	11,103,342	98%	21,427,408	15,571,448	72%
TB381401A	12,448,605	12,292,975	98%	23,254,254	16,278,460	70%
TB381401B	14,518,476	14,294,244	98%	27,333,454	18,163,763	66%
TB381401C	69,338	62,111	89%	116,408	73,753	63%
TB3GW	13,472,218	13,299,808	98%	25,397,222	16,612,780	65%
TB4GW	6,567,105	6,466,132	98%	12,651,160	9,242,817	73%
TB5GW	10,889,663	10,761,437	98%	20,669,030	15,676,298	75%
TB7GW	11,453,135	11,348,911	99%	21,957,624	19,893,337	90%
TB8GW	10,574,797	10,458,591	98%	20,361,590	17,872,589	87%
TB9GW	13,504,661	13,379,033	99%	25,423,608	23,270,321	91%
TN10GW	8,192,545	8,033,329	98%	15,768,278	15,445,044	97%
TN11GW	10,952,642	10,781,775	98%	20,865,320	20,400,555	97%

TN12GW	11,889,763	11,715,373	98%	22,480,000	18,903,633	84%
TN14GW	10,169,482	10,010,417	98%	19,516,102	19,272,356	98%
TN15GW	14,078,619	13,844,316	98%	26,738,692	26,444,039	98%
TN16GW	9,406,391	9,275,294	98%	18,029,300	16,662,800	92%
TN17GW	12,793,102	12,629,078	98%	24,555,674	23,432,493	95%
TN18GW	10,809	5,344	49%	4,708	3,818	81%
TN19GW	12,533,668	12,407,091	98%	23,998,154	21,832,793	90%
TN1GW	10,931,870	10,738,516	98%	20,710,854	17,050,738	82%
TN20GW	10,708,860	10,580,045	98%	20,467,006	18,804,531	91%
TN21GW	12,745,252	12,589,052	98%	24,564,532	21,779,148	88%
TN381403	13,463,964	13,238,535	98%	25,522,860	16,728,635	65%
TN381407	11,237,961	11,066,803	98%	21,138,186	14,722,005	69%
TN381408	10,834,795	10,609,253	97%	20,114,334	13,666,630	67%
TN381409	14,394,206	14,091,784	97%	26,559,838	18,991,030	71%
TN3GW	12,009,639	11,890,072	99%	22,928,998	19,841,115	86%
TN7GW	15,492,902	15,336,958	98%	29,777,100	28,369,026	95%
TN8GW	9,913,001	9,846,896	99%	19,145,136	18,206,349	95%
TN9GW	11,128,122	11,024,678	99%	21,478,534	20,715,335	96%
_394810	10,912,556	10,766,413	98%	20,911,010	14,863,352	71%
_394811	19,393,831	19,188,203	98%	36,568,874	28,826,065	78%
_394812	22,933,680	22,676,738	98%	42,584,322	30,487,233	71%
_394913	11,492,396	11,266,516	98%	21,779,092	14,918,753	68%
_394914	8,502,599	8,292,406	97%	15,938,902	10,612,545	66%
_394915	16,480,963	16,331,149	99%	31,675,960	23,420,487	73%
_395152	8,247,797	8,113,691	98%	14,791,976	10,953,087	74%
_395153	3,602,833	3,536,004	98%	6,495,690	4,679,393	72%
_395156	4,690,942	4,591,301	97%	8,344,720	6,165,165	73%
_395157	1,138,100	1,104,021	97%	2,124,644	1,386,700	65%
_395160	18,743,363	18,551,545	98%	34,881,078	26,917,297	77%
_395161	18,472,545	18,245,441	98%	34,569,346	25,587,834	74%
_395162	16,478,490	16,263,093	98%	31,585,180	23,514,367	74%
_395252	418,050	398,324	95%	746,360	514,110	68%
_395253	3,154,455	3,105,127	98%	6,076,106	3,929,691	64%
_395256	3,652,681	3,574,112	97%	6,824,882	4,377,349	64%

Appendix 8: Expression Heatmaps of Target Genes by Location

8-1: Hibernia - Alkane-1-monooxygenase

8-2: Terra Nova - Alkane-1-monooxygenase

8-3: Thebaud - Alkane-1-monooxygenase

8-4: Hibernia - Naphthalene dioxygenase

8-5: Terra Nova - Naphthalene dioxygenase

8-6: Thebaud - Naphthalene dioxygenase

8-7: Hibernia - Cytochrome P450

8-8: Terra Nova - Cytochrome P450

8-9: Thebaud - Cytochrome P450

8-10: Hibernia – Ring Hydroxylases/dioxygenases

8-11: Terra Nova – Ring Hydroxylases/dioxygenases

8-12: Thebaud – Ring Hydroxylases/dioxygenases

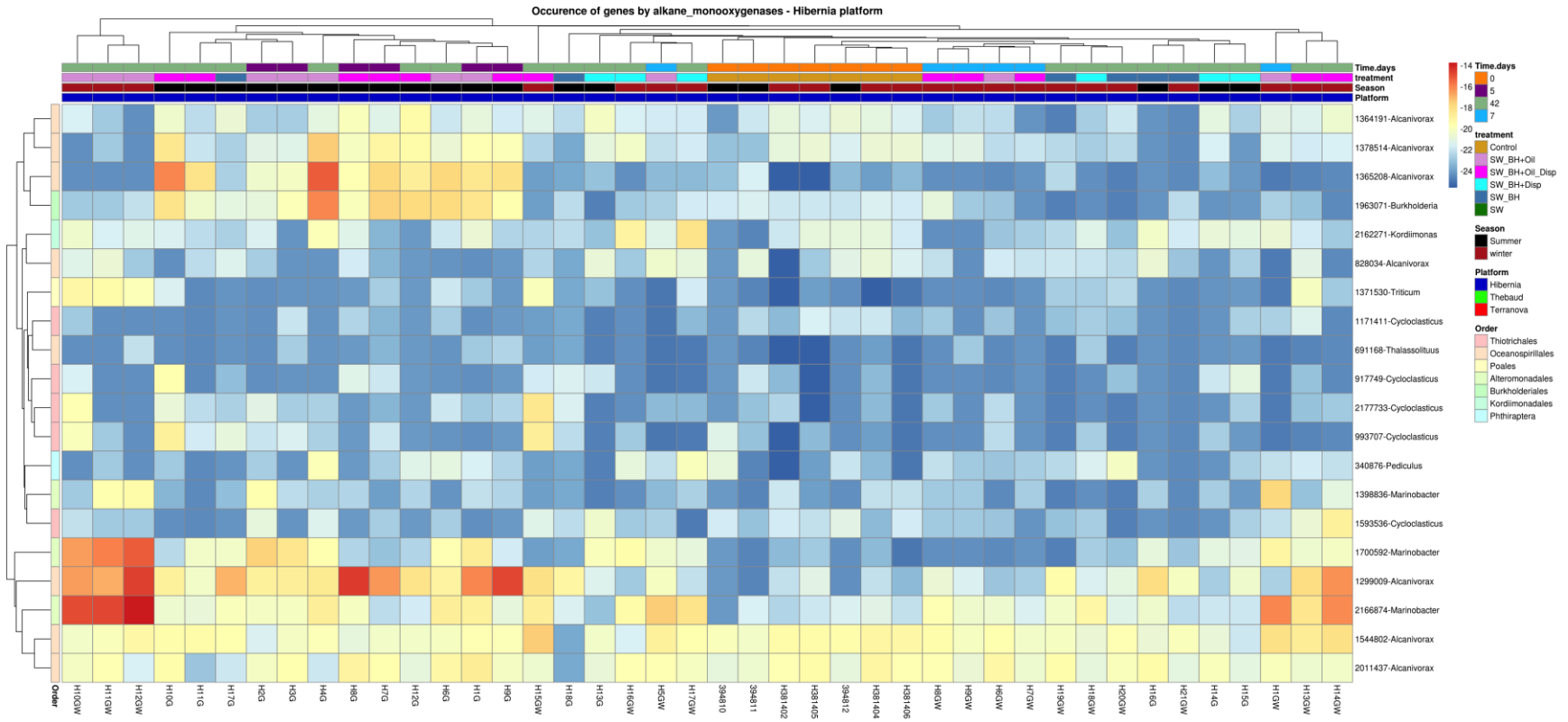

Figure 8-1: Metatranscriptomic analysis of the Hibernia site showing up-regulation of alkane 1-monooxygenases in comparison to time zero. The colored horizontal bars along the top of the heatmap provide a color-key for the site (lowest bar), followed by sampling season, then microcosm treatment and finally time of microcosm sacrificing (days), as presented on the right side of the heatmap. The identities/producers of the individual alkane 1-monoxygenases are shown on the right y-axis, while sample identities are shown on the x-axis. Results have been trimmed to show only the most up-regulated pathways (log fold-change ≥ 3). Cell color intensity represents $\log_2$ transformed gene expression values to enhance visual contrast.

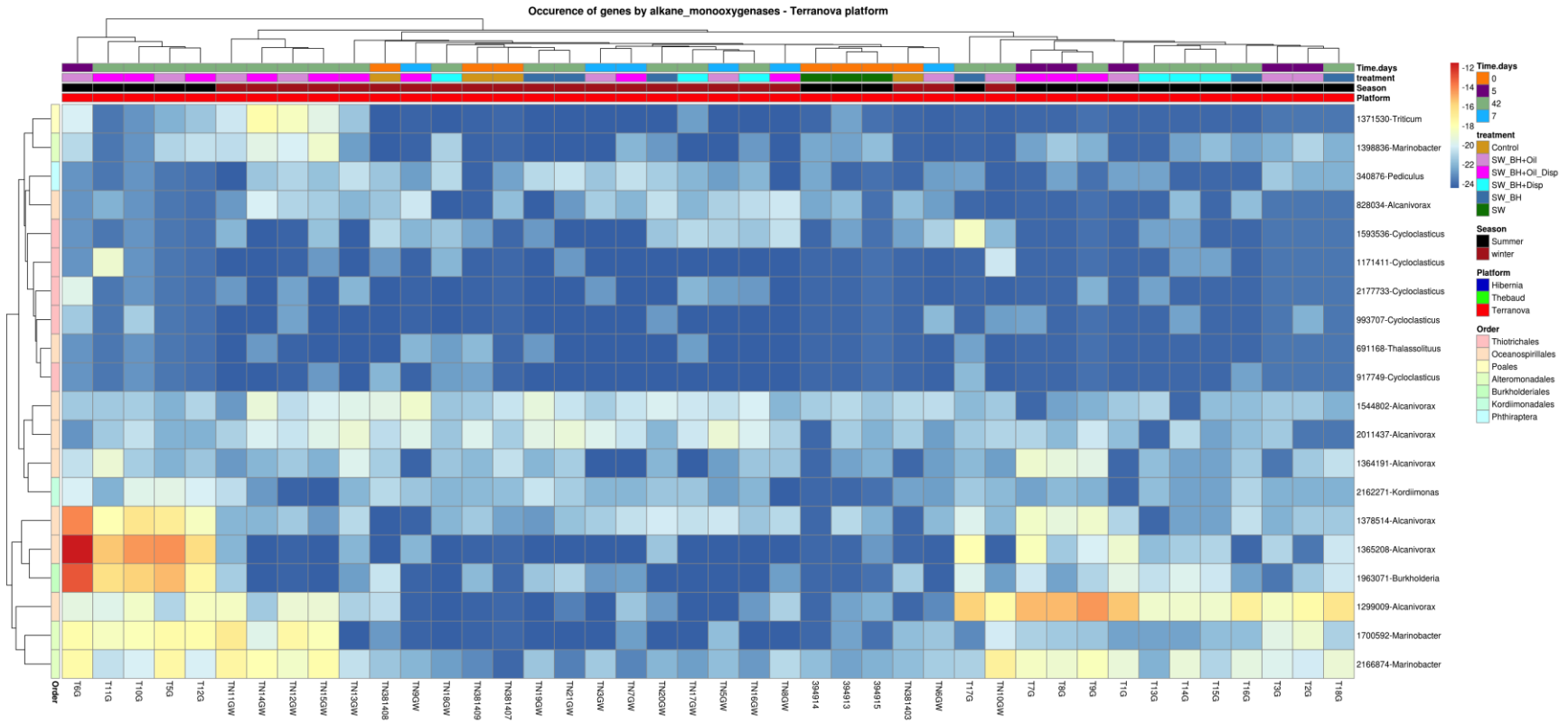

Figure 8-2: Metatranscriptomic analysis of the Terra Nova site showing up-regulation of alkane 1-monooxygenases in comparison to time zero. The colored horizontal bars along the top of the heatmap provide a color-key for the site (lowest bar), followed by sampling season, then microcosm treatment and finally time of microcosm sacrificing (days), as presented on the right side of the heatmap. The identities/producers of the individual alkane 1-monoxygenases are shown on the right y-axis, while sample identities are shown on the x-axis. Results have been trimmed to show only the most up-regulated pathways (log fold-change ≥ 3). Cell color intensity represents log_2 transformed gene expression values to enhance visual contrast.

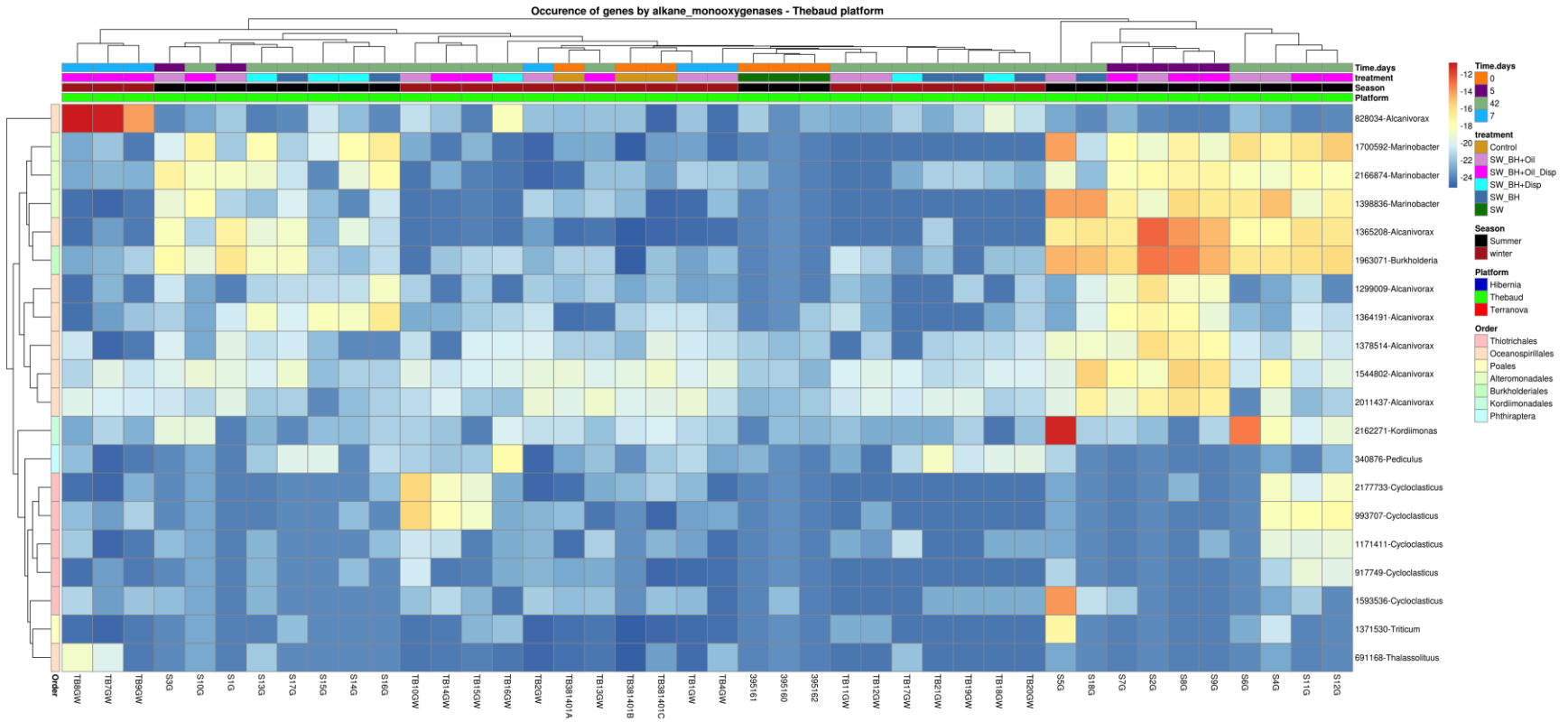

Figure 8-3: Metatranscriptomic analysis of the Thebaud (Sable) site showing up-regulation of alkane 1-monooxygenases in comparison to time zero. The colored horizontal bars along the top of the heatmap provide a color-key for the site (lowest bar), followed by sampling season, then microcosm treatment and finally time of microcosm sacrificing (days), as presented on the right side of the heatmap. The identities/producers of the individual alkane 1-monoxygenases are shown on the right y-axis, while sample identities are shown on the x-axis. Results have been trimmed to show only the most up-regulated pathways (log fold-change ≥ 3). Cell color intensity represents $\log_2$ transformed gene expression values to enhance visual contrast.

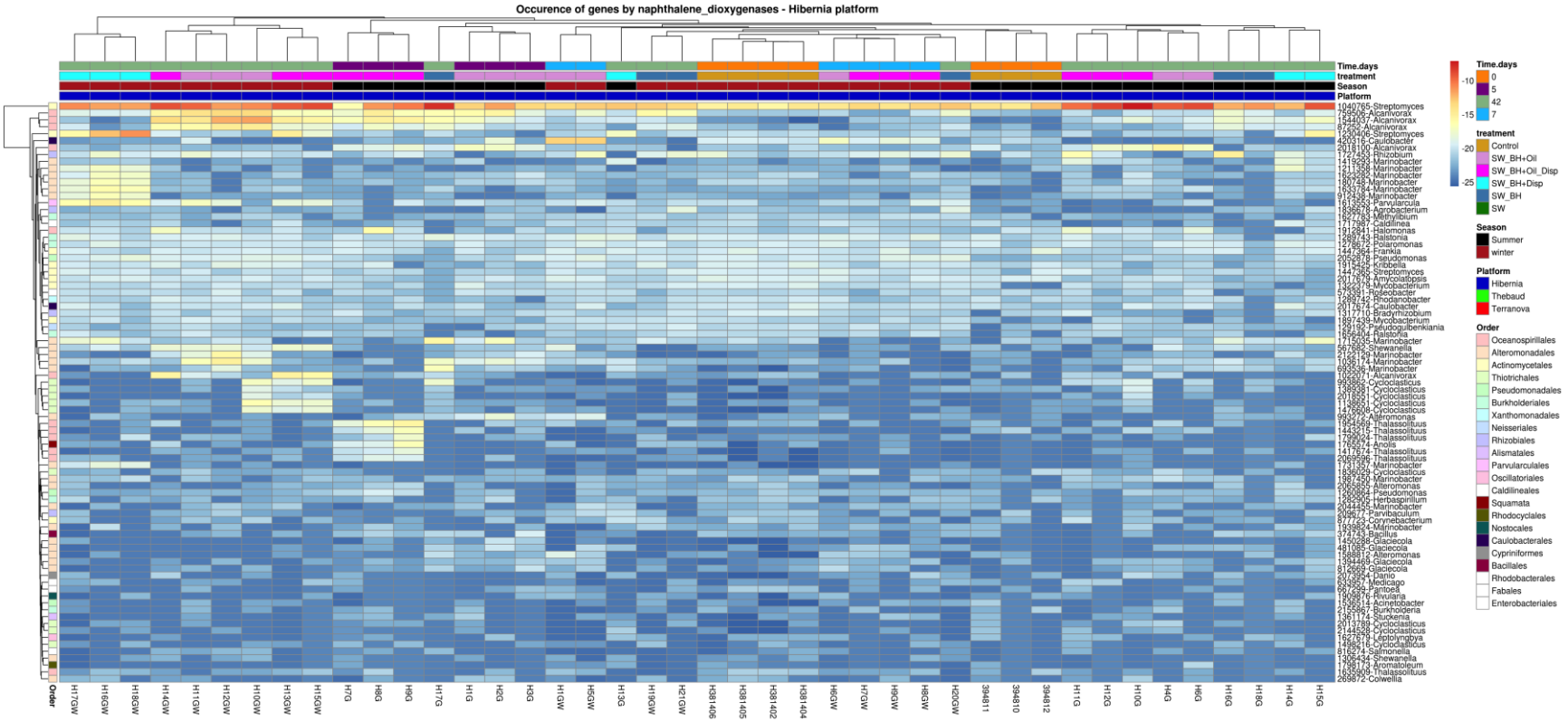

Figure 8-4: Metatranscriptomic analysis of the Hibernia site showing up-regulation of naphthalene dioxygenases in comparison to time zero. The colored horizontal bars along the top of the heatmap provide a color-key for the site (lowest bar), followed by sampling season, then microcosm treatment and finally time of microcosm sacrificing (days), as presented on the right side of the heatmap. The identities/producers of the individual naphthalene dioxygenases are shown on the right y-axis, while sample identities are shown on the x-axis. Results have been trimmed to show only the most up-regulated pathways (log fold-change ≥ 4). Cell color intensity represents log_2 transformed gene expression values to enhance visual contrast.

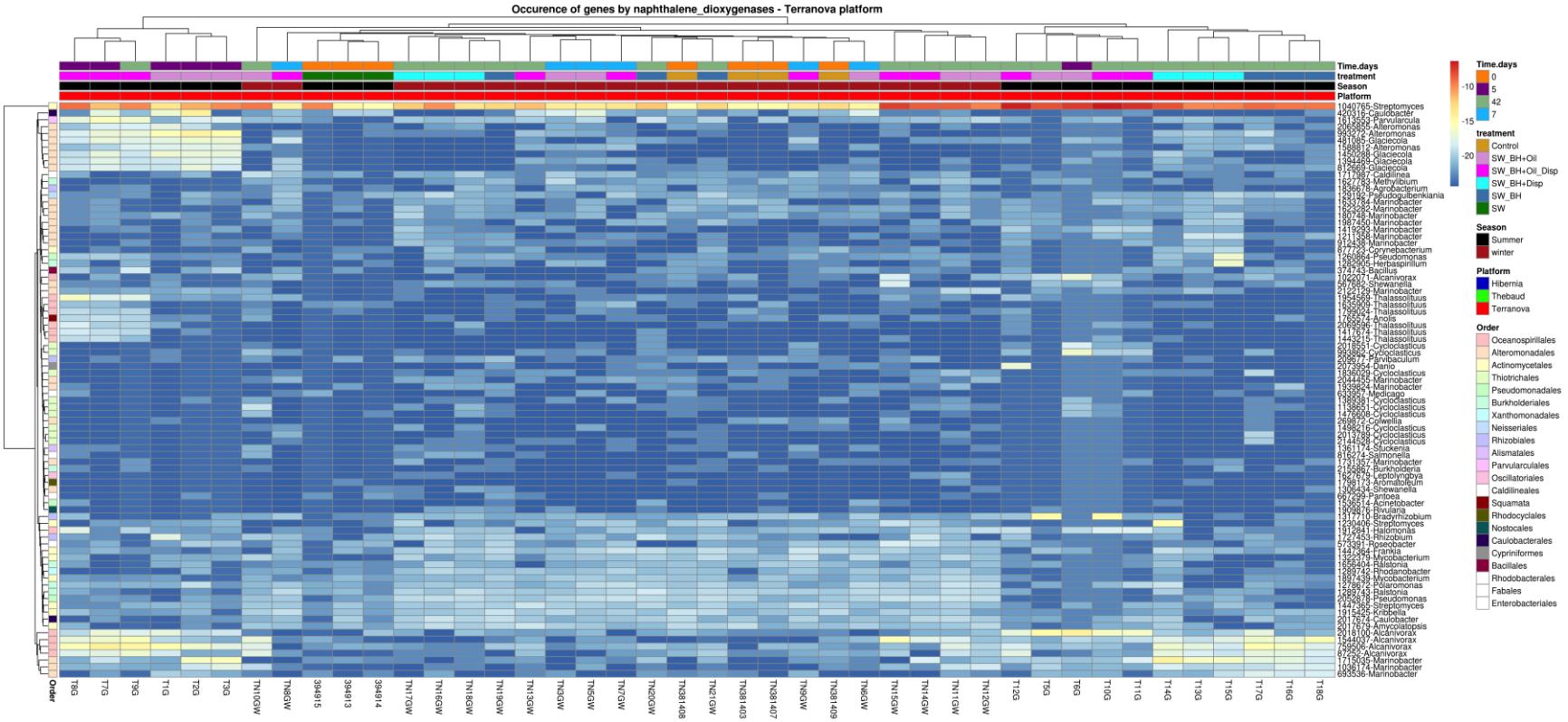

Figure 8-5: Metatranscriptomic analysis of the Terra Nova site showing up-regulation of naphthalene dioxygenases in comparison to time zero. The colored horizontal bars along the top of the heatmap provide a color-key for the site (lowest bar), followed by sampling season, then microcosm treatment and finally time of microcosm sacrificing (days), as presented on the right side of the heatmap. The identities/producers of the individual naphthalene dioxygenases are shown on the right y-axis, while sample identities are shown on the x-axis. Results have been trimmed to show only the most up-regulated pathways (log fold-change ≥ 4). Cell color intensity represents log_2 transformed gene expression values to enhance visual contrast.

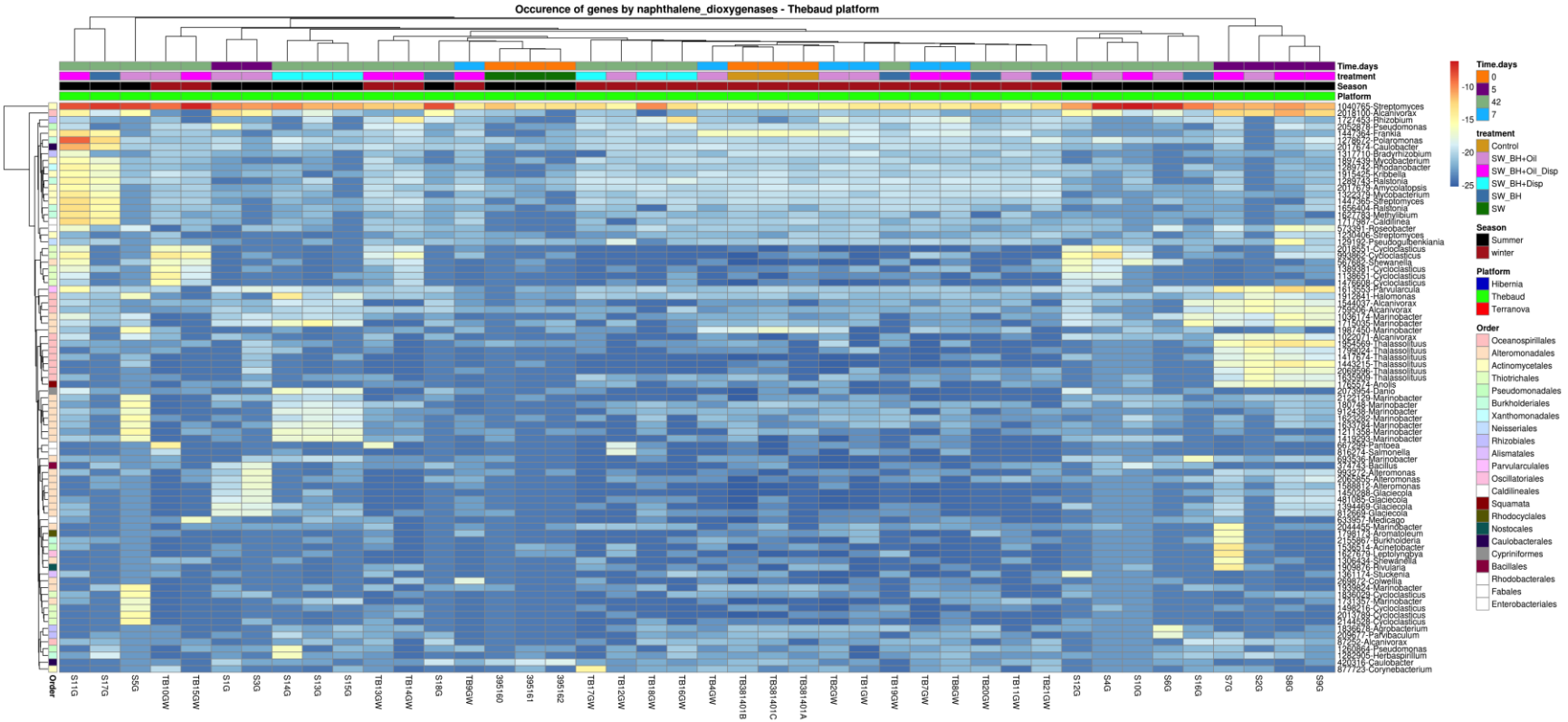

Figure 8-6: Metatranscriptomic analysis of the Thebaud (Sable) site showing up-regulation of naphthalene dioxygenases in comparison to time zero. The colored horizontal bars along the top of the heatmap provide a color-key for the site (lowest bar), followed by sampling season, then microcosm treatment and finally time of microcosm sacrificing (days), as presented on the right side of the heatmap. The identities/producers of the individual naphthalene dioxygenases are shown on the right y-axis, while sample identities are shown on the x-axis. Results have been trimmed to show only the most up-regulated pathways (log fold-change ≥ 4). Cell color intensity represents log_2 transformed gene expression values to enhance visual contrast.

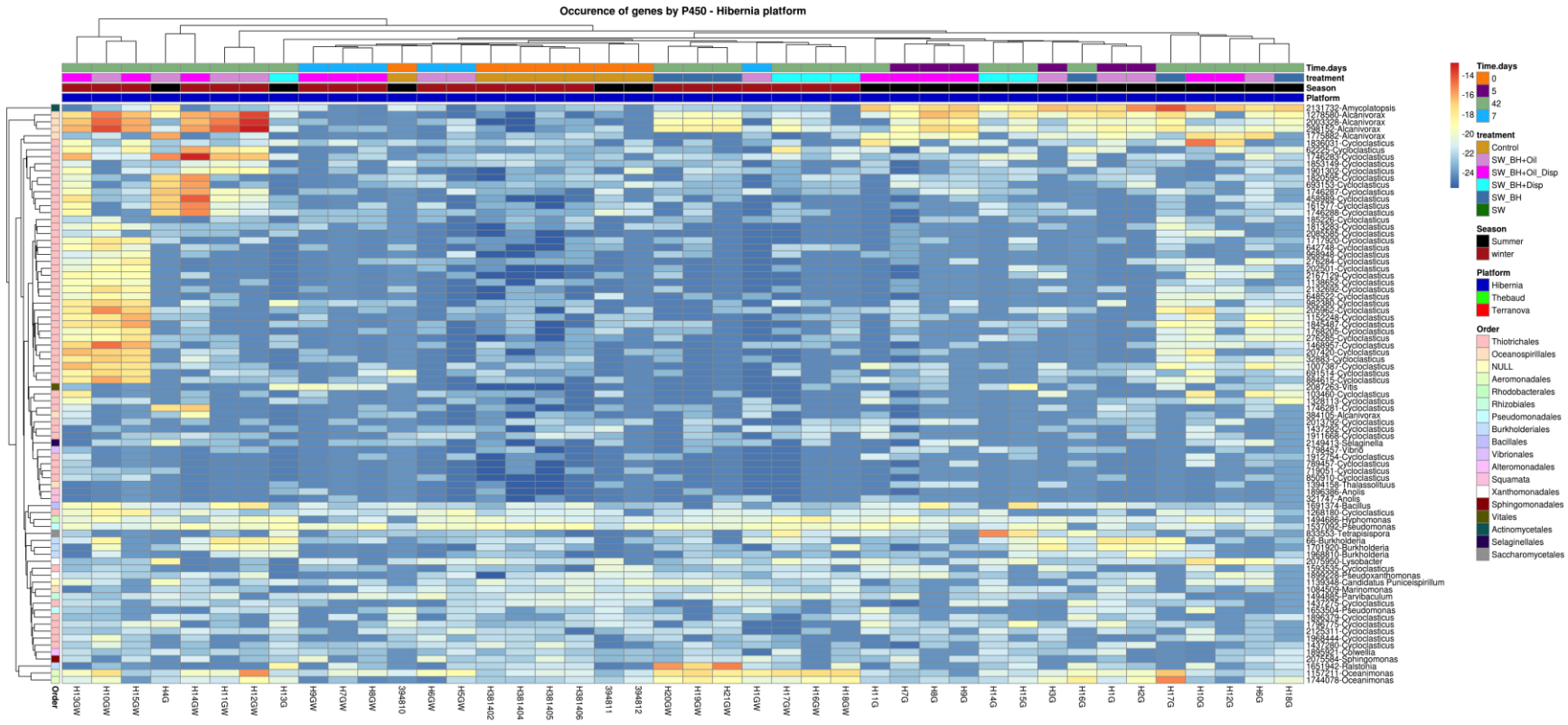

Figure 8-7: Metatranscriptomic analysis of the Hibernia site showing up-regulation of P450 dioxygenases in comparison to time zero. The colored horizontal bars along the top of the heatmap provide a color-key for the site (lowest bar), followed by sampling season, then microcosm treatment and finally time of microcosm sacrificing (days), as presented on the right side of the heatmap. The identities/producers of the individual P450 dioxygenases are shown on the right y-axis, while sample identities are shown on the x-axis. Results have been trimmed to show only the most up-regulated pathways (log fold-change ≥ 3). Cell color intensity represents log_2 transformed gene expression values to enhance visual contrast.

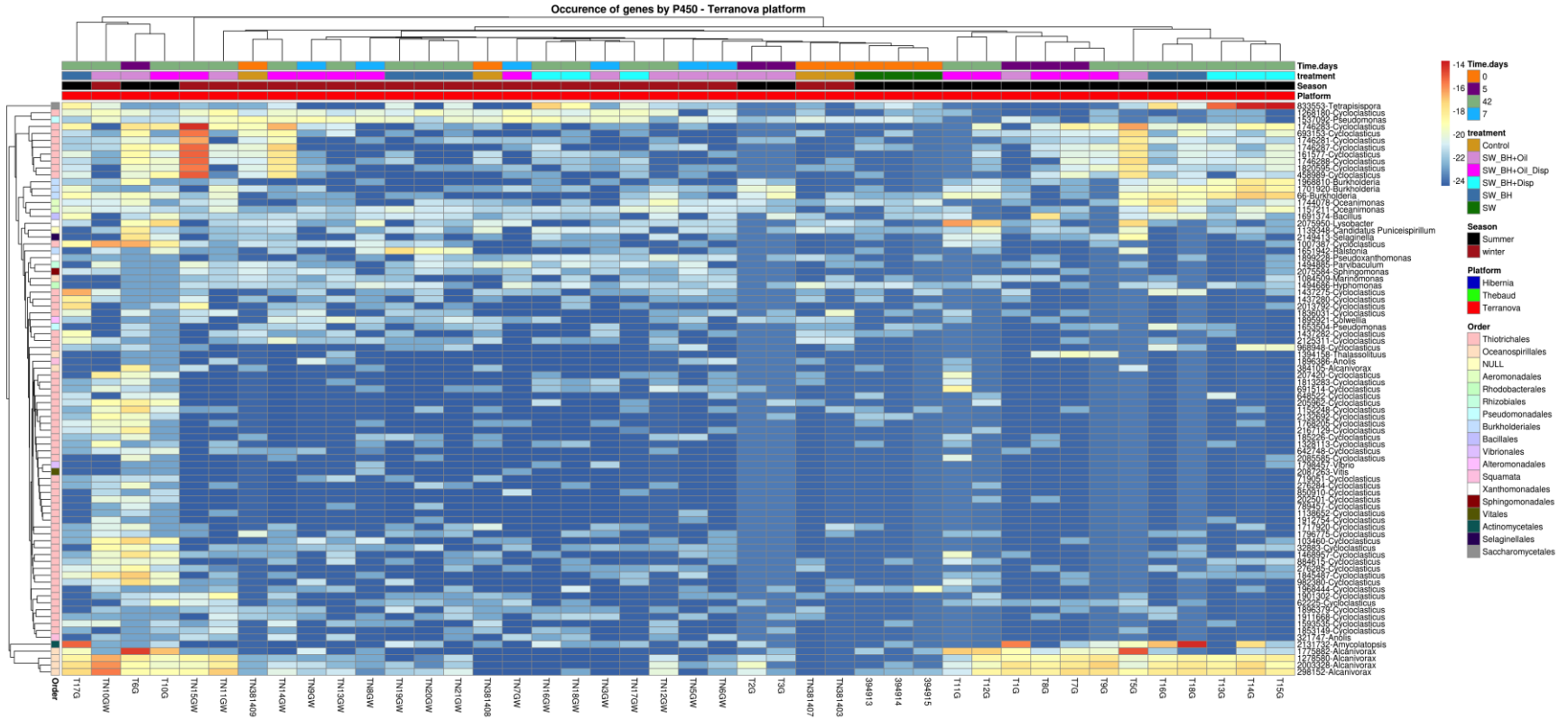

Figure 8-8: Metatranscriptomic analysis of the Terra Nova site showing up-regulation of P450 dioxygenases in comparison to time zero. The colored horizontal bars along the top of the heatmap provide a color-key for the site (lowest bar), followed by sampling season, then microcosm treatment and finally time of microcosm sacrificing (days), as presented on the right side of the heatmap. The identities/producers of the individual P450 dioxygenases are shown on the right y-axis, while sample identities are shown on the x-axis. Results have been trimmed to show only the most up-regulated pathways (log fold-change ≥ 3). Cell color intensity represents log_2 transformed gene expression values to enhance visual contrast.

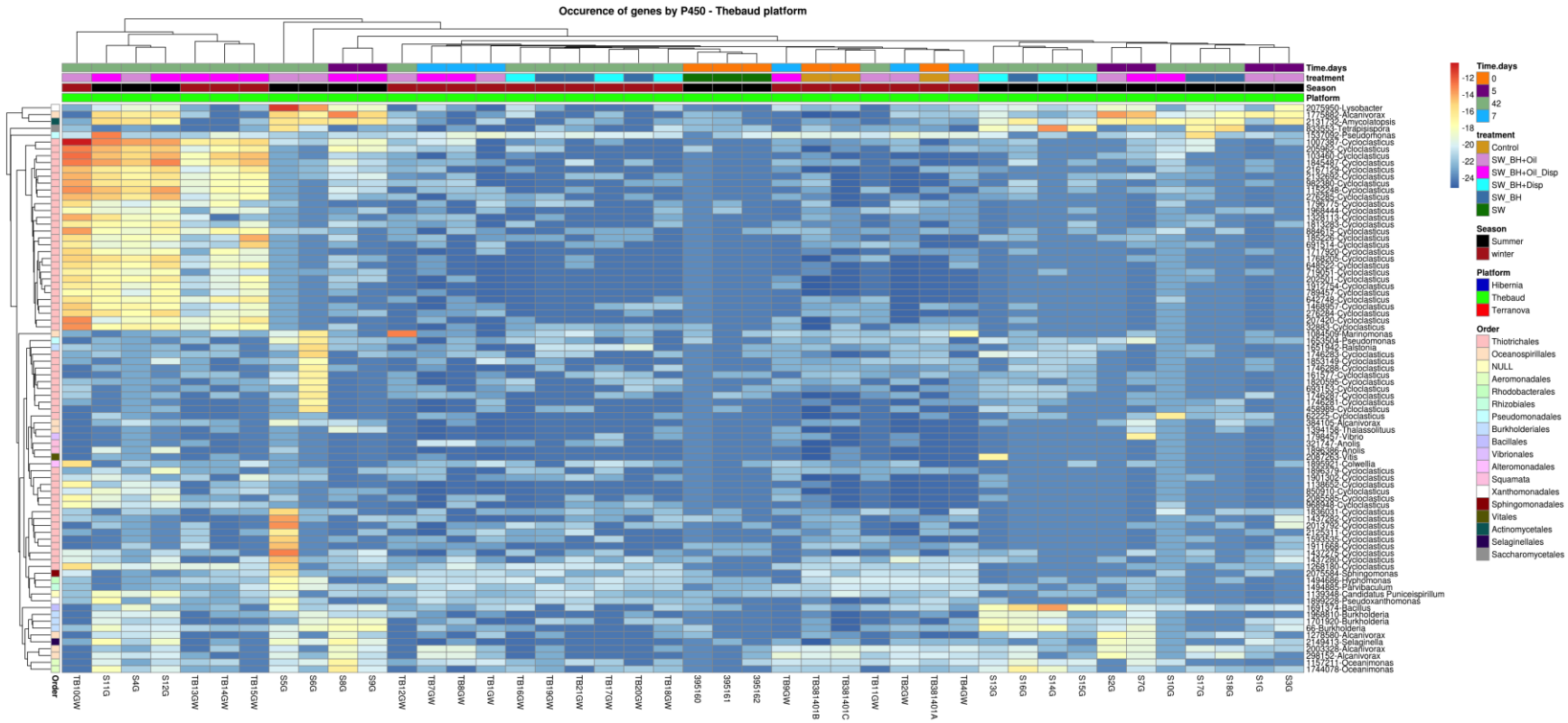

Figure 8-9: Metatranscriptomic analysis of the Thebaud (Sable) site showing up-regulation of P450 dioxygenases in comparison to time zero. The colored horizontal bars along the top of the heatmap provide a color-key for the site (lowest bar), followed by sampling season, then microcosm treatment and finally time of microcosm sacrificing (days), as presented on the right side of the heatmap. The identities/producers of the individual P450 dioxygenases is shown on the right y-axis, while sample identities are shown on the x-axis. Results have been trimmed to show only the most up-regulated pathways (log fold-change ≥ 3). Cell color intensity represents log_2 transformed gene expression values to enhance visual contrast.

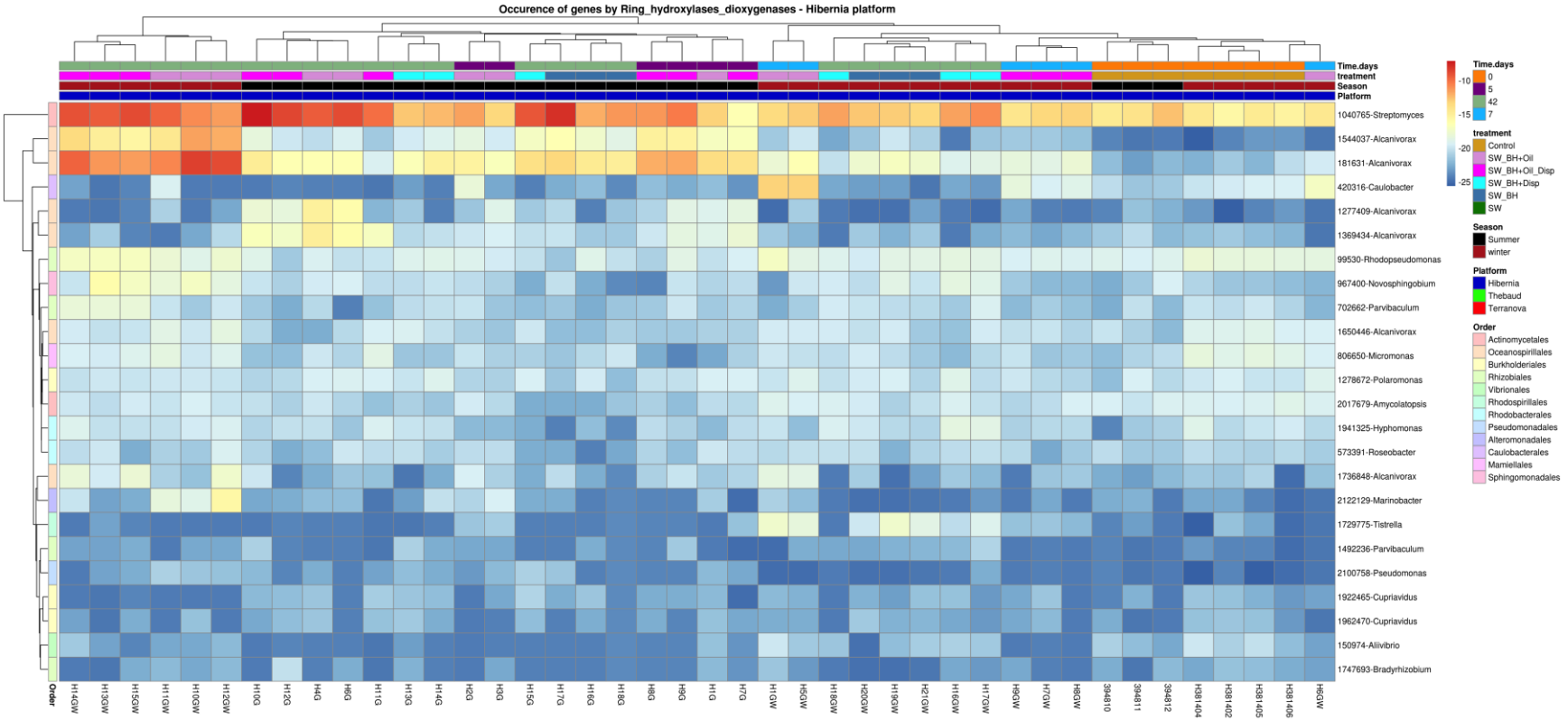

Figure 8-10: Metatranscriptomic analysis of the Hibernia site showing up-regulation of ring-hydroxylases/dioxygenases in comparison to time zero. The colored horizontal bars along the top of the heatmap provide a color-key for the site (lowest bar), followed by sampling season, then microcosm treatment and finally time of microcosm sacrificing (days), as presented on the right side of the heatmap. The identities/producers of the individual ring hydroxylases/dioxygenases is shown on the right y-axis, while sample identities are shown on the x-axis. Results have been trimmed to show only the most up-regulated pathways (log fold-change ≥ 3). Cell color intensity represents log_2 transformed gene expression values to enhance visual contrast.

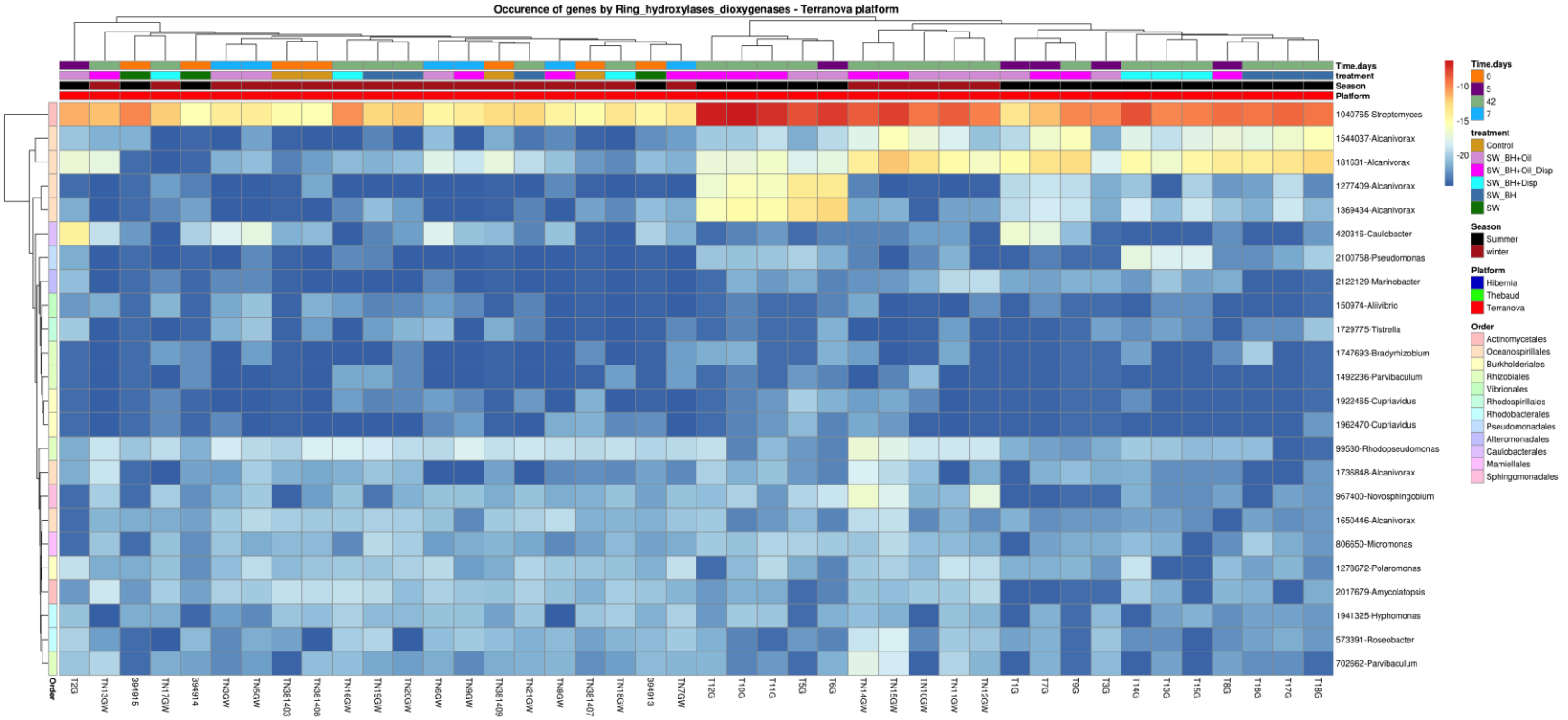

Figure 8-11: Metatranscriptomic analysis of the Terra Nova site showing up-regulation of ring-hydroxylases/dioxygenases in comparison to time zero. The colored horizontal bars along the top of the heatmap provide a color-key for the site (lowest bar), followed by sampling season, then microcosm treatment and finally time of microcosm sacrificing (days), as presented on the right side of the heatmap. The identities/producers of the individual ring hydroxylases/dioxygenases is shown on the right y-axis, while sample identities are shown on the x-axis. Results have been trimmed to show only the most up-regulated pathways (log fold-change ≥ 3). Cell color intensity represents log_2 transformed gene expression values to enhance visual contrast.

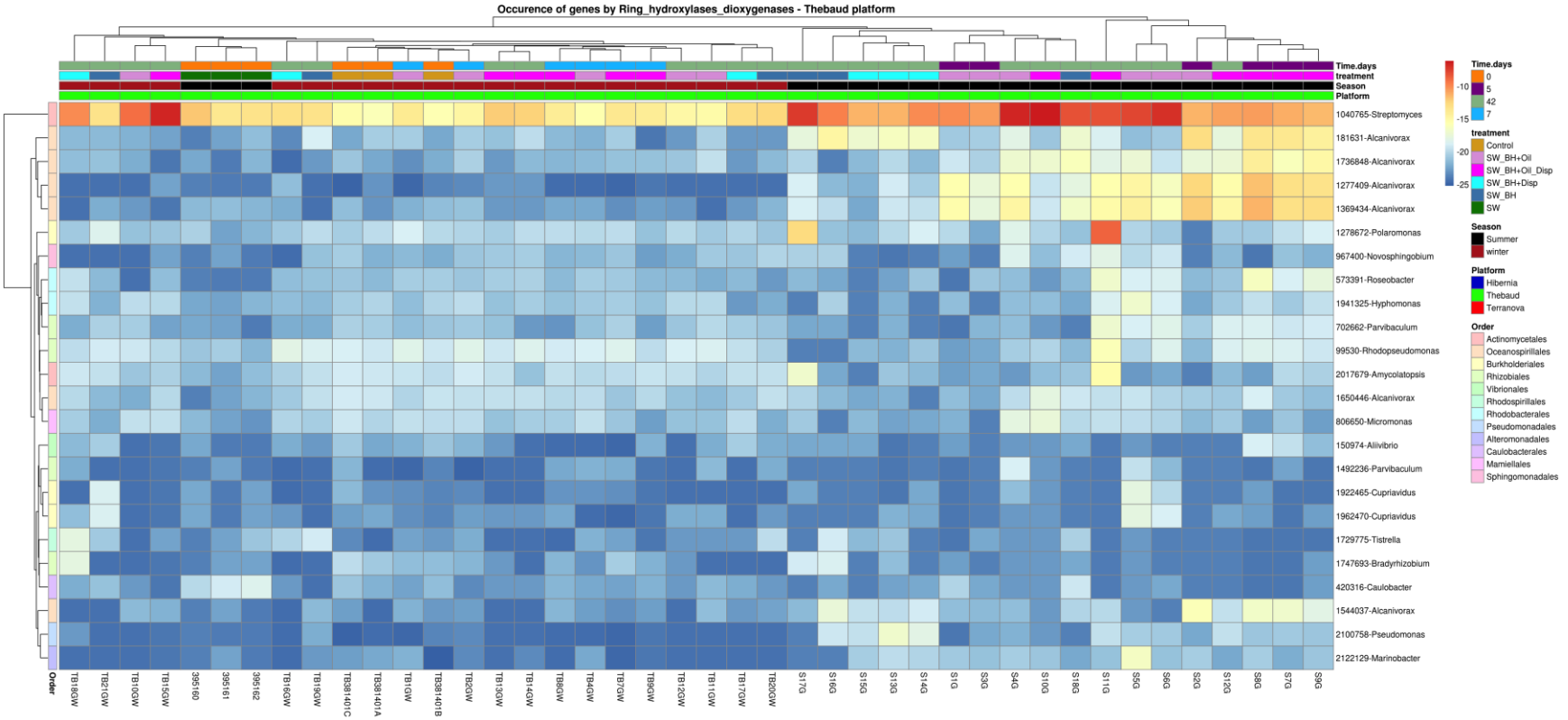

Figure 8-12: Metatranscriptomic analysis of the Thebaud (Sable) site showing up-regulation of ring-hydroxylases/dioxygenases in comparison to time zero. The colored horizontal bars along the top of the heatmap provide a color-key for the site (lowest bar), followed by sampling season, then microcosm treatment and finally time of microcosm sacrificing (days), as presented on the right side of the heatmap. The identities/producers of the individual ring hydroxylases/dioxygenases is shown on the right y-axis, while sample identities are shown on the x-axis. Results have been trimmed to show only the most up-regulated pathways (log fold-change ≥ 3). Cell color intensity represents log_2 transformed gene expression values to enhance visual contrast.